การกำจัดแมงกานีส เหล็ก และแคดเมียม ในน้ำบาดาลสังเคราะห์ ด้วยโปแทสเซียม
เปอร์แมงกาเนต และการแยกตะกอนที่เกิดขึ้นด้วยไมโครฟิลเทรชัน

นายเพียว ผาใต้

REMOVAL OF MANGANESE, IRON AND CADMIUM IN SYNTHETIC GROUNDWATER USING POTASSIUM PERMANGANATE AND SEPARATION OF RESULTING PRECIPITATES BY MICROFILTRATION

Piaw Phatai

A Thesis Submitted in Partial Fulfillment of the Requirements for the

Degree of Doctor of Philosophy in Chemistry

Suranaree University of Technology

Academic Year 2011

REMOVAL OF MANGANESE, IRON AND CADMIUM IN SYNTHETIC GROUNDWATER USING POTASSIUM PERMANGANATE AND SEPARATION OF RESULTING PRECIPITATES BY MICROFILTRATION

Suranaree University of Technology has approved this thesis submitted in partial fulfillment of the requirements for the Degree of Doctor of Philosophy.

Thesis Examining Committee

_____

(Asst. Prof. Dr. Kunwadee Rangsriwatananon)

Chairperson

_____

(Assoc. Prof. Dr. Jatuporn Wittayakun)

Member (Thesis Advisor)

_____

(Asst. Prof. Dr. Sanchai Prayoonpokarach)

Member

_____

(Assoc. Prof. Dr. Nurak Grisdanurak)

Member

_____

(Assoc. Prof. Dr. Albert Schulte)

Member

_____   _____

(Prof. Dr. Sukit Limpijumnong)   (Assoc. Prof. Dr. Prapun Manyum)

Vice Rector for Academic Affairs   Dean of Institute of Science

เพียว ผาใต้ : การกำจัดแมงกานีส เหล็ก และแคดเมียม ในน้ำบาดาลสังเคราะห์ ด้วยโปแทสเซียม
เปอร์แมงกาเนต และการแยกตะกอนที่เกิดขึ้นด้วยไมโครฟิลเทรชัน (REMOVAL OF
MANGANESE, IRON AND CADMIUM IN SYNTHETIC GROUNDWATER USING
POTASSIUM PERMANGANATE AND SEPARATION OF RESULTING PRECIPITATES
BY MICROFILTRATION) อาจารย์ที่ปรึกษา : รองศาสตราจารย์ ดร.จตุพร วิทยาคุณ, 143 หน้า.

วิทยานิพนธ์นี้มุ่งเน้นการกำจัดไอออนแมงกานีส เหล็ก และแคดเมียมในน้ำบาดาลสังเคราะห์โดย
ปฏิกิริยาออกซิเดชันด้วยอากาศและโปแทสเซียมเปอร์แมงกาเนต เพื่อทำให้ความเข้มข้นของไอออนต่ำกว่า
ระดับการปนเปื้อนสูงสุดที่อนุญาต (MCL) กระบวนการประกอบด้วยการเติมอากาศระดับต่ำและเติม
โปแทสเซียมเปอร์แมงกาเนตในระบบ Jar test ความเข้มข้นของแมงกานีส เหล็ก และแคดเมียม คือ 0.50
0.50 และ 0.01 มิลลิกรัมต่อลิตร ซึ่งเหมือนกับความเข้มข้นในน้ำบาดาลธรรมชาติ การกำจัดไอออนศึกษา
ในระบบที่มีองค์ประกอบไอออนที่แตกต่างกัน 3 ระบบ ได้แก่ แมงกานีสเชิงเดี่ยว แมงกานีสและเหล็กเชิงคู่
และแมงกานีส เหล็ก และแคดเมียม

ในระบบการกำจัดไอออนแมงกานีสเชิงเดี่ยว พารามิเตอร์ที่ศึกษาได้แก่ การเติมอากาศ พีเอช
ปริมาณตัวออกซิไดส์ และความเร็วการกวน พบว่าการเติมอากาศอย่างเดียวไม่เพียงพอสำหรับการกำจัด
ไอออนแมงกานีสถึงแม้เพิ่มพีเอชของสารละลาย เมื่อใช้โปแทสเซียมเปอร์แมงกาเนตด้วยปริมาณสัมพันธ์
(0.96 มิลลิกรัมต่อลิตร) ไอออนแมงกานีสถูกกำจัดอย่างสมบูรณ์ในเวลา 15 นาที พีเอชที่ 8.0 เมื่อเพิ่ม
ปริมาณโปแทสเซียมเปอร์แมงกาเนตเป็นสองเท่า ประสิทธิภาพการกำจัดลดลง นอกจากนี้การกำจัดไอออน
แมงกานีสเกิดขึ้นอย่างสมบูรณ์ที่พีเอช 9.0 โดยใช้ปริมาณโปแทสเซียมเปอร์แมงกาเนต 0.48 มิลลิกรัมต่อ
ลิตร การวิเคราะห์ลักษณะอนุภาคแมงกานีสไดออกไซด์ที่เกิดขึ้นใช้กล้องจุลทรรศน์อิเล็กตรอนแบบส่อง
กราด-การกระจายพลังงานของรังสีเอ็กซ์ (SEM-EDX)

ในระบบการกำจัดไอออนแมงกานีสและเหล็กเชิงคู่ พารามิเตอร์ที่ศึกษาได้แก่ ปริมาณตัวออกซิ
ไดส์ การมีไอออนแคลเซียมและแมกนีเซียมร่วมอยู่ และการเติมสารส้มหลังจากการออกซิเดชัน การศึกษา
พบว่าไอออนแมงกานีสถูกกำจัดบางส่วนโดยการเติมอากาศทั้งระบบการออกซิเดชันเชิงเดี่ยวและเชิงคู่ ด้วย
การกำจัดสูงสุดร้อยละ 30.6 และ 37.2 ตามลำดับ ไอออนเหล็กช่วยเพิ่มการกำจัดไอออนแมงกานีสด้วยการ
ก่อตัวเป็นแมงกานีส-เหล็กออกไซด์ซึ่งยืนยันองค์ประกอบโดยกล้องจุลทรรศน์แบบดิจิทัล และการกระจาย
พลังงานของรังสีเอกซ์ นอกจากนี้ยังพบว่า ปริมาณตัวออกซิไดส์ 0.603 มิลลิกรัมต่อลิตร เป็นปริมาณต่ำ
ที่สุดที่ลดความเข้มข้นของไอออนแมงกานีสสู่ระดับที่ต่ำกว่า MCL การมีไอออนแคลเซียมและแมกนีเซียม
จะรบกวนการกำจัดไอออนแมงกานีสเล็กน้อยและความเข้มข้นสุดท้ายยังคงต่ำกว่าระดับที่ยอมรับได้ การ
เติมสารส้มหลังปฏิกิริยาออกซิเดชันส่งผลทางลบต่อการกำจัดไอออนแมงกานีส กลไกการกำจัดไอออน
แมงกานีสและเหล็ก ที่เป็นไปได้ทั้งในสภาวะที่มีและ ไม่มีไอออนปรากฏ ซึ่งศึกษาโดยการวัดการ
เปลี่ยนแปลงพีเอช ประกอบด้วยการดูดซับไอออนโลหะที่ละลายบนออกไซด์

ในการกำจัดไอออนแมงกานีส เหล็กและแคดเมียม พารามิเตอร์ที่ศึกษาได้แก่ พีเอช 8.0 ปริมาณตัว ออกซิไดส์ ความเข้มข้นเริ่มต้นของแคดเมียม และการมีไอออนแคลเซียมและแมกนีเซียมร่วมอยู่ การศึกษา พบว่าการเติมอากาศสามารถกำจัดไอออนแมงกานีส เหล็กและแคดเมียมได้ร้อยละ 14.2 88.4 และ10.0 ตามลำดับ โปแทสเซียมเปอร์แมงกาเนต 0.824 มิลลิกรัมต่อลิตร เป็นปริมาณที่ดีที่สุดสำหรับการกำจัด ไอออนสู่ระดับที่ต่ำกว่าระดับ MCL การมีไอออนแคลเซียมและแมกนีเซียมร่วมอยู่ จะไม่รบกวนการกำจัด ไอออนแมงกานีสและแคดเมียม   มากกว่านั้นกลไกการกำจัดแคดเมียมที่เสนอประกอบด้วยการดูดซับบน แมงกานีส-เหล็กออกไซด์ที่มีน้ำเป็นองค์ประกอบ ความเข้มข้นเริ่มต้นของแคดเมียม 0.025 มิลลิกรัมต่อลิตร เป็นความจุสูงสุดของการดูดซับบนออกไซด์

ตะกอนที่เกิดขึ้นของแมงกานีส-เหล็กจากการกำจัดไอออนแมงกานีส   เหล็กและแคดเมียมถูกแยก โดยใช้ไมโครฟิลเทรชันด้วยเยื่อ พอลิไวนิลลิดีน ฟลูออรีน (PVDF) ที่มีขนาดรูพรุน 0.30 ไมครอน การศึกษาพบว่าชนิดของการอุดตันเยื่อคือ การอุดตันรวมโดยมีกลไกหลักคือ การอุดตันแบบเค้ก เมื่อล้าง อนุภาคแมงกานีส-เหล็กออกไซด์ที่สะสมตัวอยู่บนเยื่อด้วยวิธีต่างๆ ได้แก่ การล้างแบบย้อนกลับ การล้าง ด้วยคลื่นเหนือเสียง และการล้างด้วยการรวมกันของทั้งสองวิธี การศึกษาพบว่า การล้างด้วยคลื่นเหนือเสียง 1 นาที ให้ประสิทธิภาพดีที่สุดโดยใช้ค่าการย้อนกลับของฟลักซ์สูงสุดประมาณร้อยละ 92 แต่ประสิทธิภาพ การล้างลดลงตามจำนวนรอบการล้างด้วยคลื่นเหนือเสียง   การล้างด้วยการรวมทั้งสองวิธีไม่ช่วยเพิ่มการ ย้อนกลับของ ฟลักซ์

สาขาวิชาเคมี   ลายมือชื่อศึกษา_____

ปีการศึกษา 2554   ลายมือชื่ออาจารย์ที่ปรึกษา_____

PIAW PHATAI : REMOVAL OF MANGANESE, IRON AND CADMIUM IN

SYNTHETIC GROUNDWATER USING POTASSIUM PERMANGANATE AND

SEPARATION OF RESULTING PRECIPITATES BY MICROFILTRATION.

THESIS ADVISOR : ASSOC. PROF. JATUPORN WITTAYAKUN, Ph.D.

143 PP.

DIVALENT IONS/MANGANESE/IRON/CADMIUM/SYNTHETIC

GROUNDWATER/POTASSIUM PERMANGANATE/MICROFILTRATION

This thesis focuses on removal of Mn^{2+}, Fe^{2+} and Cd^{2+} from synthetic groundwater by oxidation using combined aeration and $KMnO_4$ to make their concentrations below the maximum contaminant level (MCL). The process included aeration and addition of $KMnO_4$ in a Jar test system. The concentration of Mn^{2+}, Fe^{2+} and Cd^{2+} was 0.50, 0.50 and 0.01 mg/L, similar to that of natural groundwater. The removal was performed in three systems including single Mn^{2+}; dual Mn^{2+} and Fe^{2+}; and triple Mn^{2+}, Fe^{2+} and Cd^{2+}.

For the single removal of Mn^{2+} ions, parameters such as aeration, pH, oxidant and stirring speed were studied. Aeration alone was not sufficient to remove Mn^{2+} ions completely although the pH was increased to 9.0. When a stoichiometric amount of $KMnO_4$ (0.96 mg/L) was used, a complete removal was achieved within 15 min at an optimum pH of 8.0. When the amount of $KMnO_4$ was doubled, the removal efficiency was lower. Besides, the removal of Mn^{2+} ions was complete at pH 9.0 using an oxidant dose of 0.48 mg/L. The MnO_2 particles were characterized by SEM-EDX.

For the dual removal of Mn^{2+} and Fe^{2+} ions, various parameters including oxidant, coexisting Ca^{2+} and Mg^{2+} ions and alum addition after the oxidation were investigated. Mn^{2+} was partially removed by aeration in both single and dual oxidation with the maximum removal of 30.6 and 37.2%, respectively. The presence of Fe^{2+} improved the removal of

Mn^{2+} ion forming hydrous manganese-iron oxide which was confirmed by digital microscopy and EDX. The oxidant dose of 0.603 mg/L $KMnO_4$ was a minimum amount to reduce the Mn^{2+} concentration to the level below the MCL. The presence of Ca^{2+} or Mg^{2+} slightly disturbed the elimination of Mn^{2+}, but the concentration was still lower than the permitted level. Alum addition after the oxidation had a negative effect on the Mn^{2+} removal. Possible mechanisms of the removal of Mn^{2+} and Fe^{2+} ions with and without the coexisting ions proposed by monitoring the pH variations involved sorption of the dissolved metal ions on the hydrous oxide.

For the triple removal of Mn^{2+}, Fe^{2+} and Cd^{2+} ions, the studied conditions included pH of 8.0 and various oxidant doses, initial Cd^{2+} concentrations, and coexisting Ca^{2+} and Mg^{2+} ions. The percent removal of Mn^{2+}, Fe^{2+} and Cd^{2+} ions by aeration were 14.2, 88.4 and 10.0%, respectively. The $KMnO_4$ dose of 0.824 mg/L was optimum to eliminate those metal ions to the concentration level below the MCL. The coexisting Ca^{2+} and/ or Mg^{2+} did not disturb the elimination of Mn^{2+} and Cd^{2+}. Furthermore, the proposed removal mechanism of Cd^{2+} involved sorption on the hydrous Mn-Fe oxide with the initial Cd^{2+} concentration of 0.025 mg/L as a maximum sorption capacity.

The resulting Mn-Fe precipitates from the triple system were separated using microfiltration (MF) by polyvinylidene fluorine (PVDF) membrane with a nominal pore size of 0.30 μm. The type of membrane fouling could be a mixed pore-blocking mechanism with the predominance of cake filtration. The Mn-Fe oxide particles accumulated on the membrane were cleaned by several methods including backwashing, ultrasound and their combined methods. Ultrasonic cleaning for 1 min was the most effective giving a maximum flux recovery of about 92% but its efficiency decreased with ultrasonic cleaning cycle. The combined methods did not improve the flux recovery.

School of Chemistry   Student,s Signature_____

Academic Year 2011   Advisor,s Signature_____

ACKNOWLEDGMENTS

CONTENTS

CONTENTS (Continued)

CONTENTS (Continued)

CONTENTS (Continued)

CONTENTS (Continued)

CONTENTS (Continued)

LIST OF TABLES

LIST OF TABLES (Continued)

LIST OF FIGURES

LIST OF FIGURES (Continued)

LIST OF FIGURES (Continued)

LIST OF FIGURES (Continued)

LIST OF FIGURES (Continued)

LIST OF FIGURES (Continued)

LIST OF FIGURES (Continued)

LIST OF ABBREVIATIONS

BW   Backwashing

CF   Cake filtration

CPB   Complete pore blocking

EDX   Energy dispersive X-ray analysis

GAC   Granular activated carbon

ICP-OES   Inductively coupled plasma-optical emission spectrometry

IPB   Intermediate pore blocking

MCL   Maximum contaminant level

MF   Microfiltration

NF   Nano-filtration

NOMs   Natural organic matters

ORP   Oxidation reduction potential

PVDF   Polyvinylidene fluorine

PZC   Points of zero charge

RO   Reverse osmosis

SEM   Scanning electron microscope

SPB   Standard pore blocking

TEM   Transmission electron microscope

THMs   Trihalomethanes

UF   Ultra-filtration

US   Ultrasound

USEPA   The United States Environmental Protection Agency

CHAPTER I

INTRODUCTION

1.1 Significance of the study

Groundwater is an important source of drinking water in developing countries. There has been a growing concern about the presence of heavy metals in groundwater including manganese (Mn), iron (Fe), arsenic (As), zinc (Zn), copper (Cu) and cadmium (Cd) (Bhattacharjee, Chakravarty, Maity, Dureja, and Gupta, 2005; Rajmohan and Elango, 2005; Mondal, Majumder, and Mohanty, 2008; Akoteyon, Mbata, and Olalude, 2011). Among those, Mn^{2+} and Fe^{2+} are mainly found in natural groundwater as a result of dissolution from clay minerals under anaerobic conditions. Besides, they can be released from agricultural and industrial activities. The distribution of Mn^{2+}, Fe^{2+} and other metal ions in groundwater is documented in many countries.

Based on an annual report on quality of groundwater in Taichung, Taiwan (2008), concentrations of Mn^{2+}, Fe^{2+} and Cd^{2+} are 0.50, 0.50 and 0.01 mg/L, respectively. These values are higher than the maximum contaminant level (MCL) allowed in drinking water which are 0.05, 0.30 and 0.005 mg/L, respectively (Lingireddy, 2002). Moreover, Ca^{2+} and Mg^{2+} are found in wide concentration ranges, namely, 12-200 and 3-40 mg/L, respectively. The groundwater with excessive concentration of Mn^{2+}, Fe^{2+} and Cd^{2+} ions is not suitable to use or consume and can impact on environment and health.

The impact of excessive amount of Mn^{2+} and Fe^{2+} ions in groundwater may become serious when they expose to air or oxygenic substances because they can form $MnO(OH)_2$ and $Fe(OH)_3$ that can stain household utensils, clothes and cause undesirable taste to the

water. Cd^{2+} and its compounds are extremely toxic even in low concentrations causing immediate poisoning and damage of liver and kidney. Therefore, suitable treatment methods of groundwater are essential for the purpose of producing drinking water with safe quality.

This thesis was conducted mainly in Taiwan as part of a collaboration with Department of Environmental Engineering and Science, Chia Nan University of Pharmacy and Science (CNU) with a project incorporated with Taiwan Water Cooperation. The incorporation emphasizes on determination of proper conditions of water pollutant ions including Mn^{2+}, Fe^{2+} and Cd^{2+} by oxidation using combined air and potassium permanganate ($KMnO_4$). The resulting precipitates were separated by microfiltration (MF) instead of using sand filtration which is currently predominantly used in water treatment plant in Taichung, Taiwan. The entire lab-scale results were expected to be applicable in the plant.

1.2 Outline of the thesis

Overall procedures are summarized in Figure 1.1. There are mainly two sections including removal of Mn^{2+}, Fe^{2+} and Cd^{2+} ions from synthetic groundwater and separation of resulting precipitates using MF.

In the first section, three compositions of synthetic groundwater including single Mn^{2+}; dual Mn^{2+} and Fe^{2+}; and Mn^{2+}, Fe^{2+} and Cd^{2+} ions were investigated. Single removal of Mn^{2+} ions is discussed in Chapter III. Various parameters including pH, oxidant dose and stirring speed were studied to obtain the optimum conditions which could reduce the concentrations of Mn^{2+}, Fe^{2+} and Cd^{2+} ions to the level below the MCL. The MnO_2 particles were characterized by scanning electron microscopy coupled with energy dispersive X-ray analysis (SEM-EDX). The optimum condition obtained from Chapter III was employed further in dual removal of Mn^{2+} and Fe^{2+} ions as presented in Chapter IV. Various parameters including oxidant dose, coexisting Ca^{2+} and Mg^{2+} ions and alum addition after the oxidation were investigated. The surface charge of the hydrous manganese-iron oxide

was analyzed by zeta potentiometry. The formation of the oxide was confirmed by digital microscopy and EDX. The removal mechanism of Mn^{2+} and Fe^{2+} was also discussed. The joint removal of Mn^{2+}, Fe^{2+} and Cd^{2+} ions was addressed in Chapter V. The studied conditions included pH of 8.0 and various oxidant doses, initial Cd^{2+} concentrations, and coexisting Ca^{2+} and Mg^{2+} ions. The removal mechanism of Cd^{2+} was also discussed.

In the second section, the separation of the resulting Mn-Fe precipitates using MF is of concern in Chapter VI. A dead-end PVDF microfiltration with pressures of 20, 35 and 50 kPa was employed. Theoretical models were used to fit the flux obtained to propose the possible membrane fouling mechanisms. The Mn-Fe oxide particles accumulated on the membrane were removed by several cleaning methods including backwashing (BW), ultrasound (US) and their combined methods with different sequences, namely, BW-US and US-BW. Final conclusions and recommendation for future work are presented in Chapter VII.
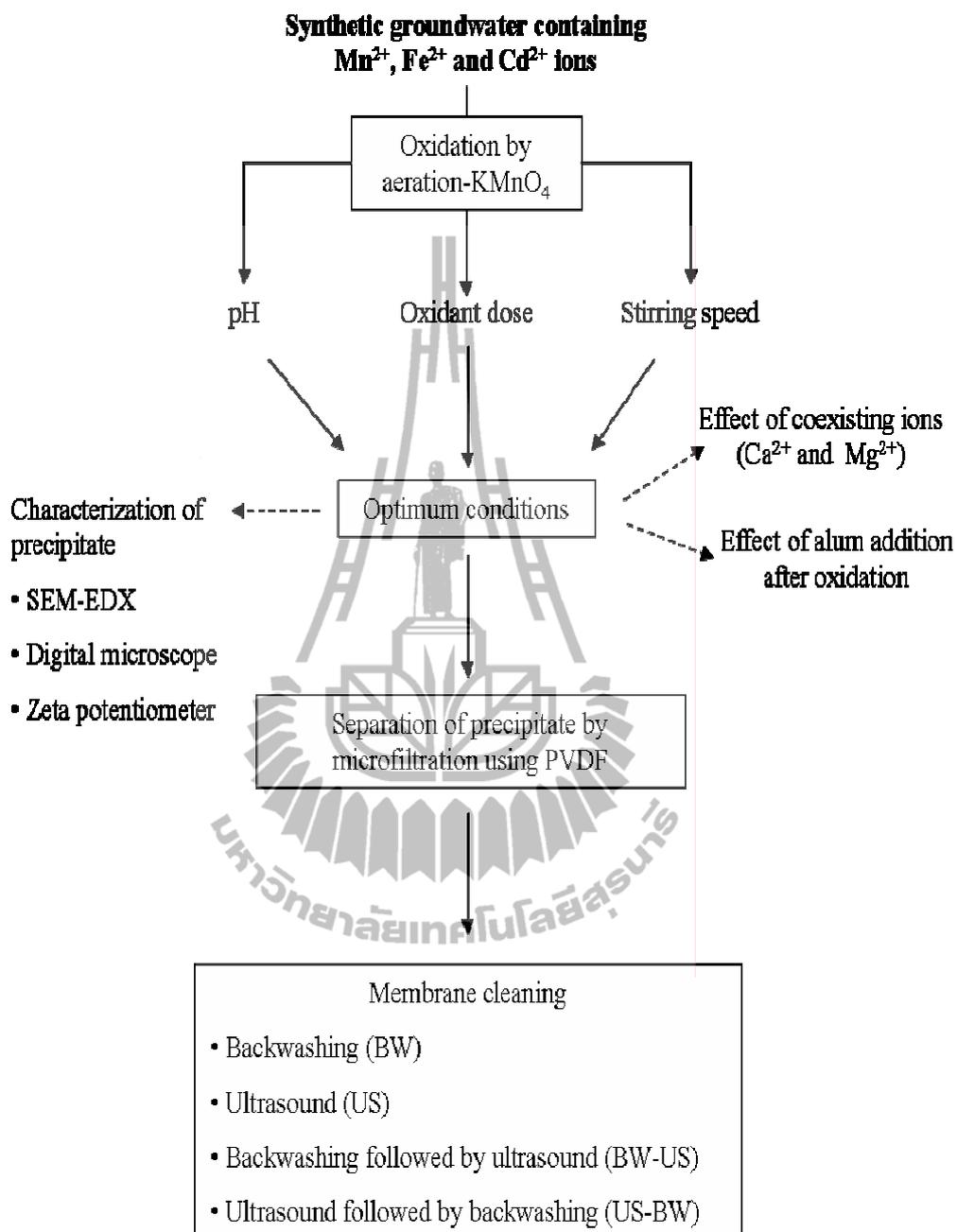
Figure 1.1 The schematic of overall experimental procedures.

1.3 Research objectives

1.3.1 To determine the conditions for an effective removal of Mn^{2+}, Fe^{2+} and Cd^{2+} from synthetic groundwater by oxidation using aeration and $KMnO_4$.

1.3.2 To propose possible mechanisms of the removal of Mn^{2+}, Fe^{2+} and Cd^{2+} ions from solutions with and without Ca^{2+} and Mg^{2+} ions.

1.3.3 To study the properties of the precipitated manganese-iron oxide using SEM-EDX, digital microscope and zeta potentiometer.

1.3.4 To investigate membrane fouling mechanisms comparing to several pore block models.

1.3.5 To study membrane cleaning efficiency of different methods including BW, US and their combined techniques.

1.3.6 To study the morphology of fouled and cleaned membranes obtained from different cleaning methods by a digital microscope.

1.4 Scope and limitations of the study

The concentrations of Mn^{2+}, Fe^{2+} and Cd^{2+} ions in the synthetic groundwater were 0.5, 0.5 and 0.01 mg/L, respectively, similar to those in the natural groundwater in Changhua water treatment plant, Taichung, Taiwan. The synthetic groundwater was employed to avoid any interference in the natural groundwater.

Oxidants used were air and $KMnO_4$. Aeration was used because it was expected to partially oxidize Mn^{2+} ions and decrease a consumption of $KMnO_4$ needed for the oxidation. $KMnO_4$ is an attractive oxidant because it is very effective in treating the wastewater contaminated by both volatile and non-volatile compounds, not toxic and easy to handle.

Polyvinylidiene fluoride (PVDF) with a nominal pore size of 0.30 μm was used as a membrane filter in MF system because of its interesting properties such as moderate hydrophobicity, excellent durability, chemical and biological resistance (Li, Fane, Winston

Ho, and Matuura, 2008). Membrane filtration was conducted in unstirred dead-end filtration which is generally used for slightly turbid water. A membrane permeate flux was monitored using an electronic balance connected with a personal computer.

1.5 References

Akoteyon, I. S., Mbata, U. A. and Olalude, G. A. (2011). Investigation of heavy metal concentration in groundwater around landfill site in a typical sub-urban settlement in Alimisho, Lagos-Nigeria. **Journal of Applied Science in Environmental Sanitation**. 6: 155-163.

Annual report of groundwater quality in Changhua Water Treatment Plant, Taichung, Taiwan, 2008.

Bhattacharjee, S., Chakravarty, S., Maity, S., Dureja, V. and Gupta, K. K. (2005). Metal contents in the groundwater of Sahebgunj district, Jharkhand, India, with special reference to arsenic. **Chemosphere**. 58: 1203-1217.

Lingireddy, S. (2002). **Control of microorganisms in drinking water**. American Society of Civil Engineers. Water Supply Engineering Technical Committee. U.S.A. p. 149.

Li, N. N., Fane, A. G., Winston Ho, W. S. and Matuura, T. (2008). **Advanced membrane technology and applications**, New Jersey: U.S.A.: John Wiley and Sons. p. 218.

Mondal, P., Majumder, C. B. and Mohanty, B. (2008). Effect of adsorbent dose, its particle size and initial arsenic concentration on the removal of arsenic, iron and manganese from simulated groundwater by Fe^{3+} impregnated activated carbon. **Journal of Hazardous Materials**. 150: 695-702.

Rajmohan, N. and Elango, L. (2005). Distribution of iron, manganese, zinc and atrazine in groundwater in parts of Palar and Cheyyar river basins, south India. **Environmental Monitoring and Assessment**. 107: 115-131.

CHAPTER II

LITERATURE REVIEW

2.1 Removal of Mn^{2+} and Fe^{2+} ions in groundwater

Several methods have been used to treat manganese-iron contaminated groundwater including biological (Lingireddy, 2002; Stembal, Markic, Ribicic, Briski, and Sipos, 2005), physical (Okoniewska, Lach, Kacorzak, and Neczaj, 2008) and chemical processes (El Araby, Hawash, and El Diwani, 2009).

Biological treatment includes activated sludge, anaerobic digestion, aerated surface impoundments and tricking filters. Among those, the tricking filters are widely employed that take advantages in their oxidation abilities of certain bacteria to remove Mn^{2+}. The process involved oxidation phenomena in which the oxidized manganese is deposited as MnO_2 layer and further acts as a catalyst for oxidation of the residual Mn^{2+} ions by dissolved oxygen (Stembal Markic, Ribicic, Briski, and Sipos, 2004; Pacini, Ingallinella, and Sanguinetti, 2005; Tekerlekopoulou and Vayenas, 2007; Burger, Mercer, Shupe, and Gagnon, 2008; Tekerlekopoulou and Vayenas, 2008). Katsoyiannis and Zouboilis (2004) studied removal of Mn^{2+} and Fe^{2+} using biological oxidation in upflow filtration. The process was mediated by specific bacteria, namely the *Leptothix ochracea and Gallionella ferruginea. L. ochracea* produced a mixed amorphous oxide of Mn^{3+}/Mn^{4+} which were concentrated on the bacteria surface. Subsequently, Mn^{2+} and Fe^{2+} were removed to the level below the MCL with the

presence of manganese oxidizing bacteria. However, the slow formation of MnO_2 and biofilm is considered as a major disadvantage (Stembal et al., 2005).

Physical treatment includes density separation, filtration, reverse osmosis, air and steam stripping, incineration and adsorption. Among those, adsorption of Mn^{2+} and Fe^{2+} in groundwater on absorbent materials such as clay, zeolite, sand and granular activated carbon (GAC) has been commonly studied (Jusoh, Cheng, Low, Nora, and Megat, 2005; Okoniewska et al., 2008; Mondal, Majumder, and Mohanty, 2008) because this method is low operation cost and easy handling. The adsorption phenomenon involves the separation of a substance from one phase accompanied by its concentration on surface of another. Okoniewska et al. (2008) reported that adsorption of Mn^{2+} and Fe^{2+} is a complex process which depends on initial concentration of the ions, pH and filtration speed. The simultaneous removal was difficult because of a competition of the ions onto the adsorbent. Moreover, this method usually needs a frequent regeneration of the adsorbents to maintain high efficiency (Senior, 1995).

Chemical treatment includes precipitation, neutralization, ion exchange and oxidation/reduction. Among those, chemical oxidation is a common process which is very effective in treating wastewater contaminated by both volatile and non-volatile compounds. For the purpose of producing safe drinking water quality, it is important to select appropriate chemical oxidants in the treatment process. Indeed, environmental consideration was addressed when chlorine dioxide (ClO_2) was employed as an oxidant because it could react with some organic compounds to generate toxic trihalomethanes (THMs). El Araby et al. (2009) used ozone (O_3) for

removal of Mn^{2+} and Fe^{2+} in synthetic water and reported that at pH 9.0-10.0, the oxidant (3.0 mg/L) was effective due to decomposition of O_3 into hydroxyl radicals (OH·). The increase of O_3 dose led to an increase of the removal efficiency of Mn^{2+} while an overdose (3.5 mg/L) decreased the removal efficiency. However, the oxidant could not reduce the concentration of Mn^{2+} to the level below the MCL. $KMnO_4$ as an oxidant was selected for manganese removal in some studies. The major consideration is due to its non-toxicity. This oxidant has no effect on organic compounds and does not produce any THMs (Crittenden, Trussell, Hand, Howe, and Tchobanoglous, 2005). Additionally, $KMnO_4$ removes undesirable tastes and odors from water and generates nontoxic by-products including CO_2, H_2O and MnO_2 (Wang, Hung, and Shammas, 2006). Thus, chemical oxidation using $KMnO_4$ was chosen in this study to remove mainly Mn^{2+} and Fe^{2+} ions contaminating groundwater. The oxidation of Mn^{2+} and Fe^{2+} by $KMnO_4$ is displayed in Eq. 2.1 and Eq. 2.2, respectively (Morgan and Stumm, 1964).

$$3Mn^{2+}_{(aq)} + 2\ KMnO_{4(aq)} + 2H_2O_{(l)} \rightarrow 5MnO_{2(s)} + 2K^+_{(aq)} + 4H^+_{(aq)} \qquad (2.1)$$

$$3Fe^{2+}_{(aq)} + KMnO_{4(aq)} + 7H_2O_{(l)} \rightarrow 3Fe(OH)_{3(s)} + K^+_{(aq)} + MnO_{2(s)} + 5H^+_{(aq)} \quad (2.2)$$

The produced precipitates, MnO_2 and $Fe(OH)_3$ obtained after the oxidation can be separated by membrane filtration in order to produce drinking water with safe quality.

2.2 Membrane filtration

Because filtration by sand is not effective to separate particles smaller than 0.45 µm, such particles still remain in the water and can cause clogging in the filtration and decrease filtration rate. Therefore, membrane filtration is an alternative method for use in a water treatment plant which can be employed for component separation based primarily on size differences and used further for the separation of dissolved solute in liquid streams.

Pressure-driven membranes are normally classified into four classes according to the pore size including microfiltration (MF), ultra-filtration (UF), nano-filtration (NF) and reverse osmosis (RO). High-pressure processes, NF and RO, principally eliminate constituents through chemical diffusion. In contrast, low-pressure processes, MF and UF, mainly remove constituents through physical sieving. In this study, MF was chosen to remove precipitates of manganese-iron oxides after the chemical oxidation.

2.2.1 Types of microfiltration process

Membrane separation process includes dead-end and cross-flow filtrations. Their schematic representations are shown in Figure 2.1.

In dead-end filtration, all of the feed solution is forced through the membrane by an applied pressure. Retained particles are collected on or in the membrane. The feed flow direction is perpendicular to surface of the filtration membrane. The permeate direction through the membrane is identical with the feed flow. The retained particles in the feed solution will adhere to the surface of membrane and limit the filter lifetime. Most type of filters can not be cleaned for reuse. In cross-flow filtration, the fluid to be filtered is pumped across the membrane

parallel to its surface. Cross-flow filtration produces two solutions including a clear filtrate or permeate and a retentate that contains most of the retained particles in the solution.
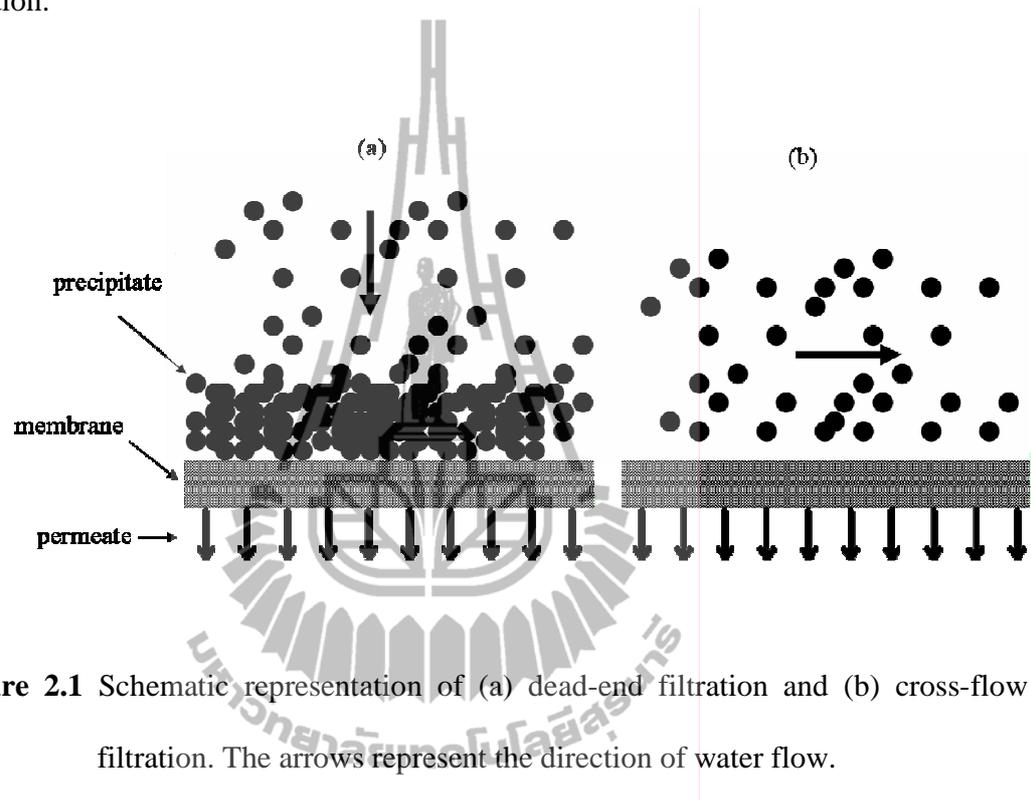
Figure 2.1 Schematic representation of (a) dead-end filtration and (b) cross-flow filtration. The arrows represent the direction of water flow.

The dead-end flow is most common in membrane filtration, while cross-flow filtration is more complicated and not suitable for groundwater treatment because the facilities are built with high capacity to circulate a large fraction of feed water in the system. Moreover, the electricity costs of cross flow pumping can triple the operating costs over dead-end operation (Glucina, Laine, and Durand-Bourlier, 1998).

Based on above considerations, unstirred dead-end filtration was utilized in this study. It was applied for the separation of the Mn-Fe precipitates after oxidation. The suspended solution was conveyed through a membrane with a specific pressure. However, membrane fouling caused by the accumulation of Mn-Fe oxide on

the membrane surface is a significant problem and may impede the efficient operation of membrane filtration in this kind of operation process.

2.2.2 Membrane cleaning

Various cleaning methods have been proposed for re-establishing permeate flux including chemical, biological and physical treatments.

Chemical methods are the most widely employed to act on membrane fouling using various cleaning agents such as alkali, acids, surfactants and disinfactants (Zhang and Liu, 2003). For example, Puspitasari, Granville, Le-Clech, and Chen (2010) investigated cleaning of a PVDF membrane (nominal pore size of 0.22 µm) fouled by alginate/bovine serum albumin using sodium hypocholite (NaOCl) as a cleaning agent. 1% of NaOCl provided 95% cleaning efficiency in a single cleaning step and its efficiency decreased with increase of cleaning cycle. This was because of the dense of the foulant and difficult to remove. Some drawbacks of this method include generation of new waste solutions, higher costs and operational aspects of chemical supply and handling problems, especially, in ships or remote places.

Biological methods employ bioactive agents such as enzymes to enhance cleaning effectiveness. For instance, Arguello, Alvarez, Riera, and Alverez (2003) studied cleaning of inorganic membrane fouled by whey protein solution using proteolytic enzymes. High cleaning efficiency of almost 100% was obtained in 20 min. However, membrane cleaning had to be carried out under strong pH (9.5-10.0) and 30% of enzymatic activity was lost during cleaning cycle.

Physical methods depend on mechanical forces to remove foulants from surface of a membrane and enhance cleaning effectiveness. The mechanical cleanings include forward and reverse flushing (Wang, Chen, Hung, and Shammas, 2010), ultrasonication (Matsumoto, Miwa, Nakao, and Kimura, 1996) and backwashing (Levesley and Hoare, 1999). Among those, ultrasound is an effective technique for cleaning a variety of membrane surfaces. It has been reported by several researchers (Lamminen, Walker, and Weavers, 2004). All of these studies demonstrated the effectiveness of ultrasound in controlling membrane fouling and enhancing permeates flux using both polymeric and ceramic membranes. Lim and Bai (2003) studied cleaning of a PVDF membrane (nominal pore size of 0.10 µm) fouled by activated sludge by sonication. The use of sonication alone was not effective in flux recovery, while a combination of clean water backwashing, sonication and chemical cleaning with alkali and acid could achieve almost complete flux recovery. Based on literature review, there has been no report on using ultrasound and backwashing in cleaning of PVDF membrane fouled by manganese-iron oxide particles. They were expected to be effective for a reduction of membrane fouling and thus practical for use in actual water treatment plants.

2.3 References

Arguello, M. A., Alvarez, S., Riera, F. A. and Alverez, R. (2003). Enzymatic cleaning of inorganic ultrafiltration membranes used for whey protein fractionation. **Journal of Membrane Science**. 216: 121-134.

Burger, M. S., Mercer, S. S., Shupe, G. D. and Gagnon, G. A. (2008). Manganese removal during bench-scale biofiltration. **Water Research**. 42: 4733-4742.

Crittenden, J. C., Trussell, R. R., Hand, D. W., Howe, K. J. and Tchobanoglous, G. (2005). **Water Treatment Principles and Design** (2nd ed.). U.S.A.: John Wiley and Sons. pp. 556-557.

El Araby, R., Hawash, S. and El Diwani, G. (2009). Treatment of iron and manganese in simulated groundwater via ozone technology. **Desalination**. 249: 1345-1349.

Glucina, K., Laine, J. M. and Durand-Bourlier, L. (1998). Assessment of filtration mode for the ultrafiltration membrane process. **Desalination**. 118: 205-221.

Jusoh, A. B., Cheng, W. H., Low, W. M., Nora's aini, A. and Megat Mohd Noor, M. J. (2005). Study on the removal of iron and manganese in groundwater by granular activated carbon. **Desalination**. 182: 347-353.

Katsoyiannis, I. A. and Zouboilis, A. I. (2004). Biological treatment of Mn^{2+} and Fe^{2+} containing groundwater: kinetic considerations and product characterization. **Water Research**. 38: 1922-1932.

Lamminen, M. O., Walker, H. W. and Weavers, L. K. (2004). Mechanisms and factors influencing the ultrasonic cleaning of particle-fouled ceramic membranes. **Journal of Membrane Science**. 237: 213-223.

Levesley, J. A. and Hoare, M. (1999). The effect of high frequency backflushing on the microfiltration of yeast homogenate suspensions for the recovery of solutes protein. **Journal of Membrane Science**. 158: 29-39.

Lim, A. L. and Bai, R. (2003) Membrane fouling and cleaning in microfiltration of activated sludge wastewater. **Journal of Membrane Science**. 216: 279-290.

Lingireddy, S. (2002). Control of microorganisms in drinking water. American Society of Civil Engineers. Water Supply Engineering Technical Committee. **Technology and Engineering**. p. 149.

Matsumoto, Y., Miwa, T., Nakao, S. and Kimura, S. (1996). Improvement of membrane permeation performance by ultrasonic microfiltration. **Journal of Chemical Engineering of Japan**. 29: 561-567.

Mondal, P., Majumder, C. B. and Mohanty, B. (2008). Effect of adsorbent dose, its particle size and initial arsenic concentration on the removal of arsenic, iron and manganese from simulated groundwater by Fe^{3+} impregnated activated carbon. **Journal of Hazardous Materials**. 150: 695-702.

Morgan, J. J. and Stumm, W. (1964). Colloid-chemical properties of manganese dioxide. **Journal of Colloid and Science**. 19: 347-359.

Okoniewska, E., Lach, J., Kacorzak, M. and Neczaj, E. (2008). The removal of manganese, iron and ammonium nitrogen on impregnated activated carbon. **Desalination**. 206: 251-258.

Pacini, V. A., Ingallinella, A. M. and Sanguinetti, G. (2005). Removal of iron and manganese using biological roughing up flow filtration technology. **Water Research**. 39: 4463-4475.

Puspitasari, V., Granville, A., Le-Clech, P. and Chen, V. (2010). Cleaning and aging effect of sodium hypochlorite on polyvinylidene fluoride (PVDF) membrane. **Separation and Purification Technology**. 72: 301-308.

Senior, E. (1995). **Microbiology of landfill sites, Pietermaritzburg, Republic of South Africa** (2nd ed.). U.S.A.: CRC Press. p. 141.

Stembal, T., Markic, M., Ribicic, N., Briski, F. and Sipos, L. (2004). Rapid start-up of biofilters for removal of ammonia, iron and manganese from groundwater. **Journal of Water Supply: Research and Technology-AQUA**. 57: 509-518.

Stembal, T., Markic, M., Ribicic, N., Briski, F. and Sipos, L. (2005). Removal of ammonia, iron and manganese from groundwater of northern Croatia-pilot plant studies. **Process Biochemistry**. 40: 327-335.

Tekerlekopoulou, A. G. and Vayenas, D. V. (2007). Ammonia, iron and manganese removal from potable water using trickling filters. **Desalination**. 210: 225-235.

Tekerlekopoulou, A. G. and Vayenas, D. V. (2008). Ammonia, iron and manganese removal from potable water using trickling filters. **Biochemical Engineering Journal**. 39: 215-220.

Wang, L. K., Chen, J. P., Hung, Y-T. and Shammas, N. K. (2010). **Handbook of Environmental Engineering 13: Membrane and desalination technologies**. U.S.A.: Humana Press. p. 590.

Wang, L. K., Hung, Y-T. and Shammas, N. (2006). **Handbook of Environmental Engineering: Advanced physicochemical treatment**. New York, U.S.A.: Humana Press. pp. 493-499.

Zhang, G. and Liu, Z. (2003). Membrane fouling and cleaning in ultrafiltration of wastewater form banknote printing works. **Journal of Membrane Science**. 211: 235-249.

CHAPTER III

REMOVAL OF MANGANESE IONS FROM SYNTHETIC GROUNDWATER BY OXIDATION USING POTASSIUM PERMANGANATE

Abstract

The purpose of this study was to determine optimum conditions for the removal of manganese ions from synthetic groundwater by oxidation using $KMnO_4$ as an oxidant to keep the concentration below the allowed level (0.05 mg/L). The process included low-level aeration and addition of $KMnO_4$ in a Jar test system with Mn^{2+} concentration of 0.50 mg/L, similar to that of natural groundwater in Taiwan. Parameters such as aeration-pH, oxidant dose and stirring speed were studied. Aeration alone was not sufficient to remove Mn^{2+} ions completely even when the pH was increased. When a stoichiometric amount of $KMnO_4$ (0.96 mg/L) was used, a complete removal was achieved within 15 min at an optimum pH of 8.0. When the amount of $KMnO_4$ was doubled, lower removal efficiency was obtained because the oxidant also generated manganese ions. In addition, the removal of Mn^{2+} ions was complete at pH 9.0 using an oxidant dose of 0.48 mg/L because Mn^{2+} could be sorbed onto MnO_2 particles resulted from the oxidation. Finally, The MnO_2 particles were characterized by SEM-EDX.

3.1 Introduction

Divalent manganese ions (Mn^{2+}) are found particularly in deep wells (groundwater), which contain little oxygen and in areas where the groundwater flows through organic-rich soil (Berbenni, Pollice, Canziani, Stabile, and Nobili, 2000). Indeed, problems have been global issue caused by Mn^{2+} ions in groundwater environments (Overnel, 2002; Buschmann, Berg, Stengel, and Sampson, 2007). Although human ingestion of Mn^{2+} ions above 0.50 mg/L has no harmful health effects (Kohl and Medlar, 2006), the presence in drinking water at concentrations above 0.10 mg/L is not suitable for public consumers. The United States Environmental Protection Agency (USEPA) has recommended the limitation levels for Mn^{2+} ions in drinking water at 0.05 mg/L (Lee and Lin, 2007). An impact of excessive amount of Mn^{2+} ions in groundwater may become serious when they expose to air or oxygenic substances and may form MnO_2 precipitates that can stain household utensils and clothes, or cause undesirable taste in drinking water. Moreover, Mn^{2+} ions cause membrane fouling in reverse osmosis and nanofiltration systems (Kohl and Medlar, 2006).

Several methods have been applied to treat manganese-contaminated groundwater including biological, physical and chemical processes. Biological treatment is fundamentally a filtration process that takes advantages of oxidation abilities of certain bacteria to assimilate the manganese ions. The process involves oxidation phenomena that the oxidized manganese is deposited as MnO_2 layer which further acts as a catalyst for oxidation of Mn^{2+} ions by dissolved oxygen (Stembal, Markic, Ribicic, Briski, and Sipos, 2004; Pacini, Ingallinella, and Sanguinetti, 2005; Tekerlekopoulou and Vayenas, 2007; Burger, Mercer, Shupe, and Gagnon, 2008;

Tekerlekopoulou and Vayenas, 2008). However, a long formation of MnO_2 and biofilm is considered as a major disadvantage (Stembal, Markic, Ribicic, Briski, and Sipos, 2005). Physical treatment is mainly an adsorption for example by using granular activated carbon (GAC) (Jusoh, Cheng, Low, Nora aini, and Megat Mohd Noor, 2005; Okoniewska, Lach, Kacorzak, and Neczaj, 2008; Mondal, Majumder, and Mohanty, 2008). This operation usually needs a frequent regeneration of the active carbon or a replacement of the carbon column to maintain high efficiency (Senior, 1995). Chemical oxidation is another common method which is very effective in treating the wastewater contaminated by both volatile and non-volatile compounds. For the purpose of producing safe drinking water, it is essential to select suitable chemical oxidants. Indeed, an environmental consideration was addressed when ClO_2 was used as an oxidant because it could react with some organic compounds to generate THMs. $KMnO_4$ was selected in some studies because it is not toxic, and easy to handle, has no effect to organic compounds and does not produce THMs (Crittenden, Trussell, Hand, Howe, and Tchobanoglous, 2005). In addition, $KMnO_4$ assists elimination of undesirable tastes and odors from water. Only nontoxic by-products including CO_2, H_2O and MnO_2 are produced (Wang, Hung, and Shammas, 2006).

The oxidation of Mn^{2+} by $KMnO_4$ is displayed in Eq. 2.1 (Hendricks, 2010). The $KMnO_4$ itself undergoes reduction under an acidic condition as shown in Eq. 3.1. Thus, a primary control parameter is the solution pH.

$$KMnO_{4(aq)} + 8H^+_{(aq)} + 5e^-_{(aq)} \leftrightarrow Mn^{2+}_{(aq)} + K^+_{(aq)} + 4H_2O_{(l)}, \quad E^0 = +1.51 \text{ V} \qquad (3.1)$$
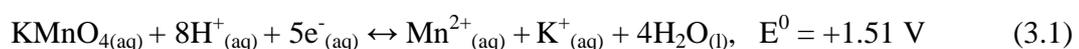
Under neutral, weakly acidic or basic conditions, the reduction half-reaction can be written as:

$$KMnO_{4(aq)} + 2H_2O_{(l)} + 3e^-_{(aq)} \leftrightarrow MnO_{2(s)} + K^+_{(aq)} + 4OH^-_{(aq)}, E^0 = +0.59 \text{ V} \quad (3.2)$$

Based on Eq. 2.1, 1.92 mg or 1.21×10^{-5} mol of $KMnO_4$ is needed to oxidize 1 mg or 1.82×10^{-5} mol of Mn^{2+}. The reaction is further enhanced by the formation of hydrous manganese dioxide flocs (MnO_2) which act as a catalyst for further oxidation (Roccaro, Barone, Mancini, and Vagliasindi, 2007; Buamah, Petrusevski, and Schippers, 2008; Crimi and Ko, 2009). The shape of the active oxide flocs depends on the pH and oxidation reduction potential (ORP). In general, the overall redox potential in aqueous solution increases when pH decreases (Takeno, 2005). Therefore, the control of pH throughout the manganese oxidation is necessary.

This study focused on the removal of Mn^{2+} ions in synthetic groundwater using $KMnO_4$. The synthetic groundwater was used to avoid any interference in the natural groundwater. This investigation utilized a combined system of low-level aeration and $KMnO_4$ to determine the optimum conditions to make the Mn^{2+} concentration below the permitted level (0.05 mg/L). The synthetic groundwater was prepared to contain Mn^{2+} concentration at 0.50 mg/L. Parameters studied were aeration-pH, oxidant dose and stirring speed.

Size distributions of the MnO_2 particles were determined to obtain the information for further studies on membrane filtration. SEM-EDX was used to examine the morphology and determine compositions of the oxides. The results would be useful for natural groundwater treatment.

3.2 Experimental

3.2.1 Chemicals

Deionized (DI) water with a resistivity of 18.90 MΩ produced by Ruda Ultrapure Water system was used in the preparation of all samples and standards. Chemicals included manganese chloride tetrahydrate ($MnCl_2 \cdot 4H_2O$), sodium hydrogen carbonate ($NaHCO_3$), sodium sulfate (Na_2SO_4), nitric acid (HNO_3), hydrochloric acid (HCl), potassium chloride (KCl) and sodium hydroxide (NaOH) and all were obtained from Merck, Germany. $KMnO_4$ was obtained from J. T. Baker, U.S.A. and sodium chloride (NaCl) was obtained from Taiyen Biotech, Taiwan.

3.2.2 Experimental methods

The synthetic groundwater used in this study was self-prepared to simulate natural groundwater in Taiwan. A 0.50 mg/L solution of $NaHCO_3$ was used to adjust alkalinity to 200 mg/L as $CaCO_3$. Solutions of Na_2SO_4, NaCl and KCl with the concentration of 250, 480 and 500 mg/L, respectively, were used to regulate the solution salinity. A stock solution containing 1000 mg/L of Mn^{2+} was prepared using $MnCl_2 \cdot 4H_2O$ and stored in high density polypropylene bottles at 4°C. A solution of $KMnO_4$ with concentration of 1000 mg/L was used as an oxidant. The solution pH was adjusted to desired values (if necessary) using 0.1 M and 1.0 M of HCl and NaOH. A solution of HNO_3 with concentration at 1:50 ratio (volume of acid and sample) was used to dissolve any manganese oxide suspension before the elemental analysis.

3.2.3 Batch Study

Experiments were carried out using a standard Jar test system with a dimension of $11.5 \times 11.5 \times 21.0$ cm (Figure 3.1). The system was equipped with an electrically-controlled agitator, timer, pH meter and ORP meter.
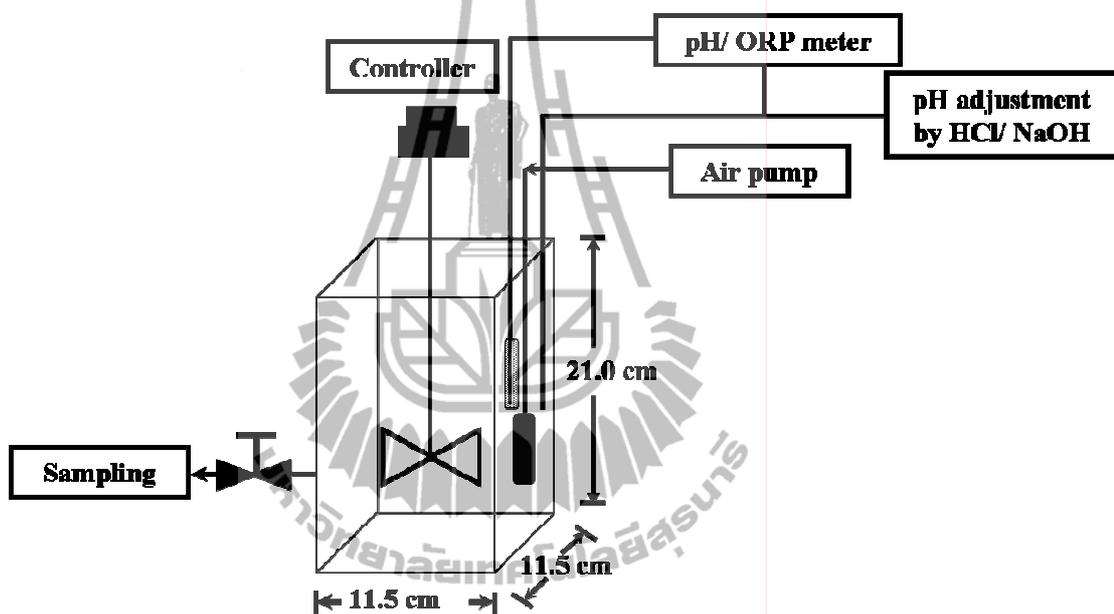
Figure 3.1 Configuration of a Jar test system.

The synthetic groundwater volume was adjusted to 2 L and it was aerated for 20 min using an air pump (Elite 802, China) to partially oxidize Mn^{2+} (except in the study on effect of aeration which was done for 60 min). This procedure was performed to minimize a consumption of $KMnO_4$ when the process is used continuously with a large flow (Schafer and Prokop, 1995). After that the solution pH was controlled to an acceptable range ($\pm$ 0.1 pH unit) and the stock solution of $KMnO_4$ was added to the solution. The reaction was investigated for total retention

time of 60 min. The mixture was sampled every 15 min and separated by filtration with a 0.45 μm cellulose membrane filter. HNO_3 solution was dropped into the filtrate obtained prior to the elemental analysis. Each experiment was repeated three times and their results were averaged.

Control parameters included aeration-pH (6.0, 7.0, 8.0 and 9.0), oxidant dose (0.48, 0.96 and 1.92 mg/L) and stirring speed (50, 120 and 200 rpm). The pH values were ranged similarly to natural groundwater. The oxidant doses applied were calculated from stoichiometic amount from Eq. 2.1. The stirring speeds studied were considered from general operation in water treatment plant.

3.2.4 Characterization

The residual Mn^{2+} concentration was determined using inductively coupled plasma-optical emission spectrometry (ICP-OES, Perkin Elmer DV 2000). The concentrate HNO_3 was added to the filtrate to ensure the solubility of all manganese particles. A blank solution was prepared from the synthetic groundwater and Mn^{2+} ions were not detected in the blank. A calibration curve was obtained from measuring standard solutions of Mn^{2+} ions with the concentrations of 0.1, 0.3, 0.5, 0.7 and 1.0 mg/L. The correlation coefficient (R^2) was ranged in acceptable values (higher than 0.95). The remaining concentration of Mn^{2+} ions was averaged.

An oxidation reduction potentiometer (ORP, 5041, Rocker) was used to measure intensity of oxidation-reduction process and tendency of manganese species formed in water during the oxidation. The ORP probe was dipped into the water as shown in Figure 3.1 and the ORP value was recorded at the same time with the water sampling.

The particle size of precipitates produced during the oxidation was analyzed by N5 Submicron Particle Size Analyzer Beckman Coulter. The water was sampled, filled into glass cuvettes and the particle size was measured immediately.

The morphology and composition of the precipitates were analyzed by SEM (Hitashi S-4800) coupled with EDX (Horiba Emax 400). The precipitates were collected by filtration through a 0.45 μm cellulose membrane filter, dried at room temperature and kept in a desiccator before the analysis. The membrane containing the precipitates was cut and mounted with carbon tape on a specimen stub prior to coating with gold. The SEM image was recorded at an accelerating voltage of 15 kV and a magnification of 10,000.

3.3 Results and discussion

3.3.1 Effect of aeration-pH

Aeration of the synthetic groundwater was initially investigated to study partial removal of Mn^{2+} ions. The average removal and ORP at various reaction pH and time are shown in Figure 3.2 and Figure 3.3, respectively. The removal efficiency increased with the increasing pH values and the highest was observed at pH 9.0 (Figure 3.2). Although the ORP values were more than 400 mV at pH 6.0 and 7.0 (Figure 3.3), the removal efficiencies were not as high as that at pH 9.0. This result indicated that the formation of MnO_2 particles was favorable with increasing pH rather than the ORP values. However, the residual concentration of Mn^{2+} was still higher than the permitted level allowed in drinking water. This result was in agreement with Kaya, Karadurmus, and Alicilar (2005) that the oxidation of Mn^{2+} by air reached only about 70% even at pH 11.0, when the initial concentration was 25

mg/L. Therefore, to reach the high removal efficiency, an additional oxidant is necessary. As mentioned previously, KMnO$_4$ was selected and its efficiency was investigated under various conditions.
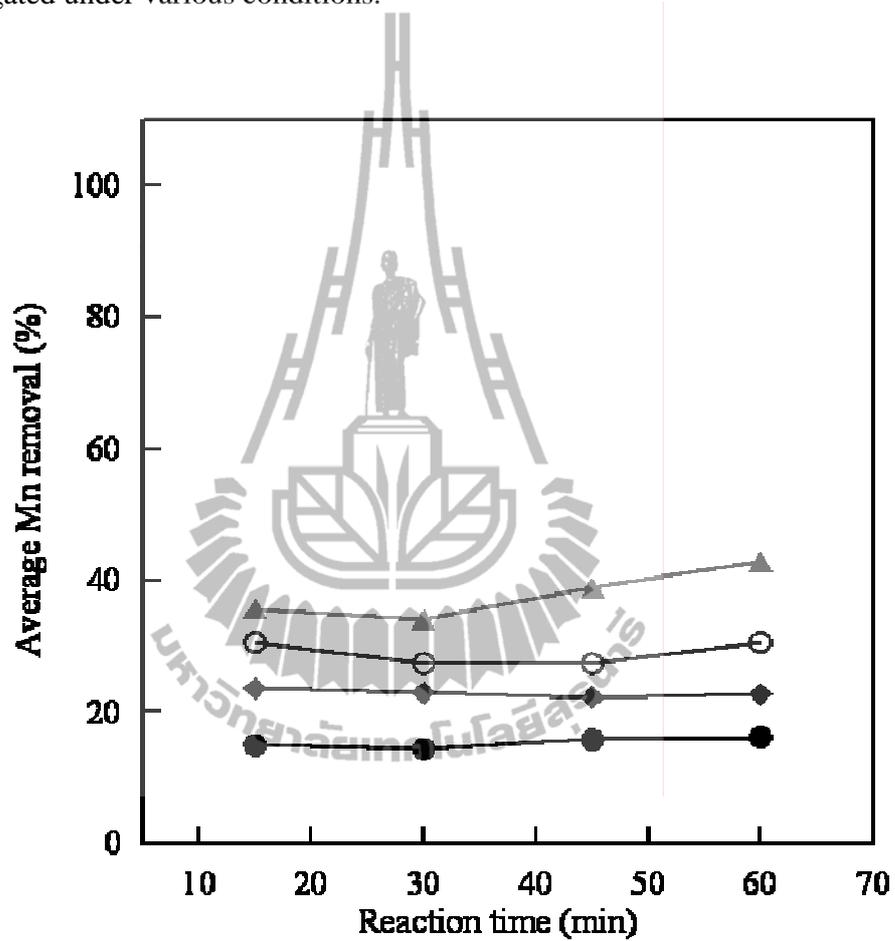
Figure 3.2 Removal efficiency of Mn^{2+} by aeration at different pH; (●) pH 6.0, (♦) pH 7.0, (○) pH 8.0, (▲) pH 9.0; stirring speed 120 rpm.
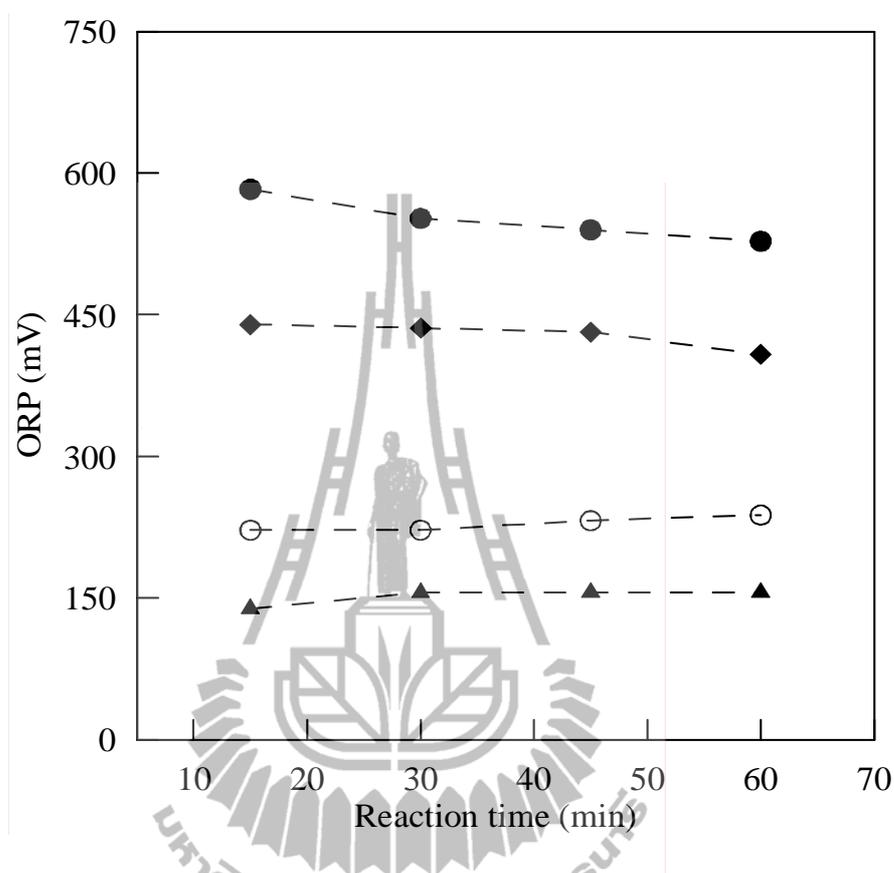
Figure 3.3 ORP values from the oxidation of Mn^{2+} by aeration at different pH; ($\bullet$) pH 6.0, ($\blacklozenge$) pH 7.0, ($\circ$) pH 8.0, ($\blacktriangle$) pH 9.0; stirring speed 120 rpm.

The stoichiometric amount of $KMnO_4$, 0.96 mg/L was added to the synthetic groundwater at pH 6.0 to 9.0. The removal efficiency and ORP are presented in Figure 3.4 and Figure 3.5, respectively. The removal efficiency at pH 6.0 was 85% after 15 min but the residual Mn^{2+} concentration was still higher than the MCL (0.05 mg/L). This result indicated that the oxidation of Mn^{2+} is not favorable under an acidic condition because the reverse reaction based on Eq. 3.1 could occur. The ORP value reached the highest level at pH 6.0 (Figure 3.5). Such value was not favorable for the formation of MnO_2. At the higher pH, the ORP values decreased and the complete

removal efficiencies were achieved. Takeno (2005) indicated that the ORP at pH 6.0

had to be in the range between 800 and 1020 mV to form MnO_2.
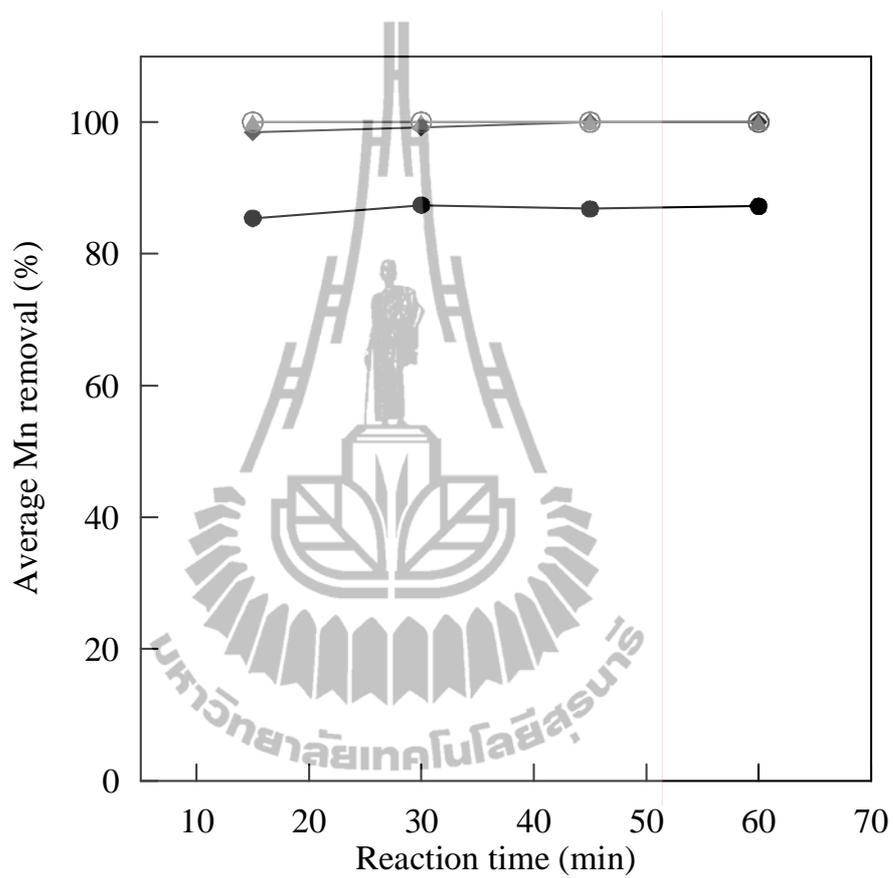
Figure 3.4 Removal efficiency of Mn^{2+} by $KMnO_4$ at different pH; (●) pH 6.0, (♦) pH

7.0, (○) pH 8.0, (▲) pH 9.0; 0.96 mg/L $KMnO_4$; stirring speed 120 rpm.
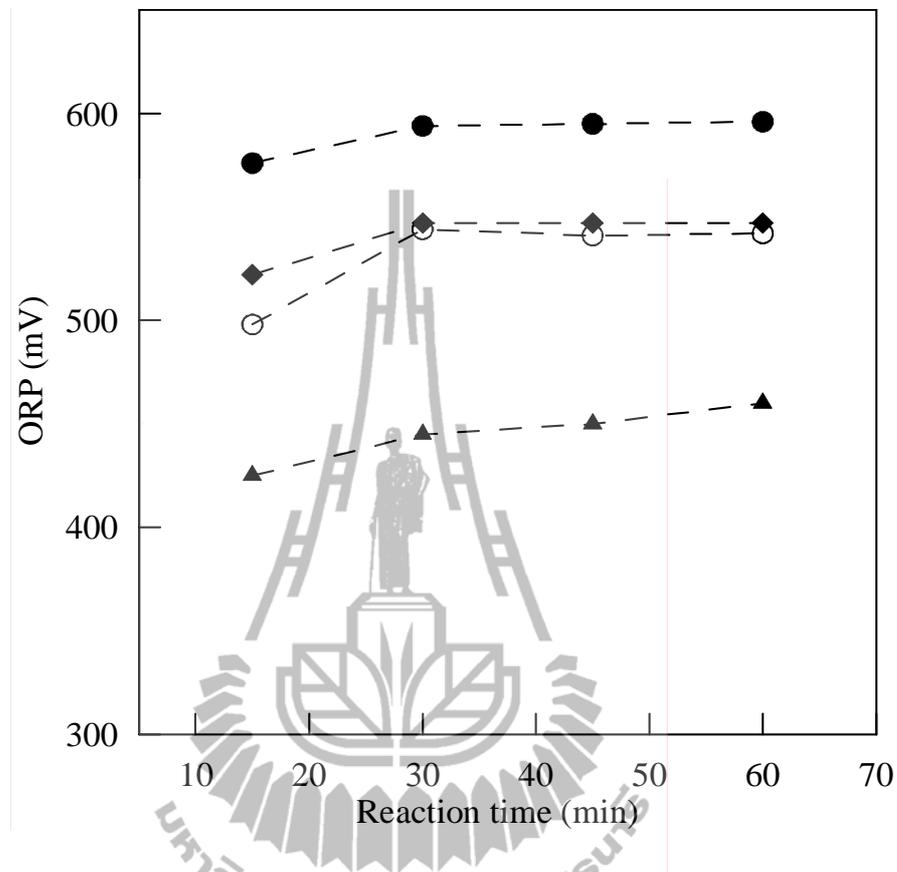
Figure 3.5 ORP values from the oxidation of Mn^{2+} by $KMnO_4$ at different pH; (●) pH
6.0, (♦) pH 7.0, (○) pH 8.0, (▲) pH 9.0; 0.96 mg/L $KMnO_4$; stirring speed
120 rpm.

The particle size distributions of MnO_2 precipitates after the oxidation
using 0.96 mg/L $KMnO_4$ under various pH values are shown in Figure 3.6. Increasing
pH values from 6.0 to 9.0 generated larger sizes of particles from 1.0 to 500 µm. This
led to higher efficiency of Mn^{2+} ions removal at higher pH values.
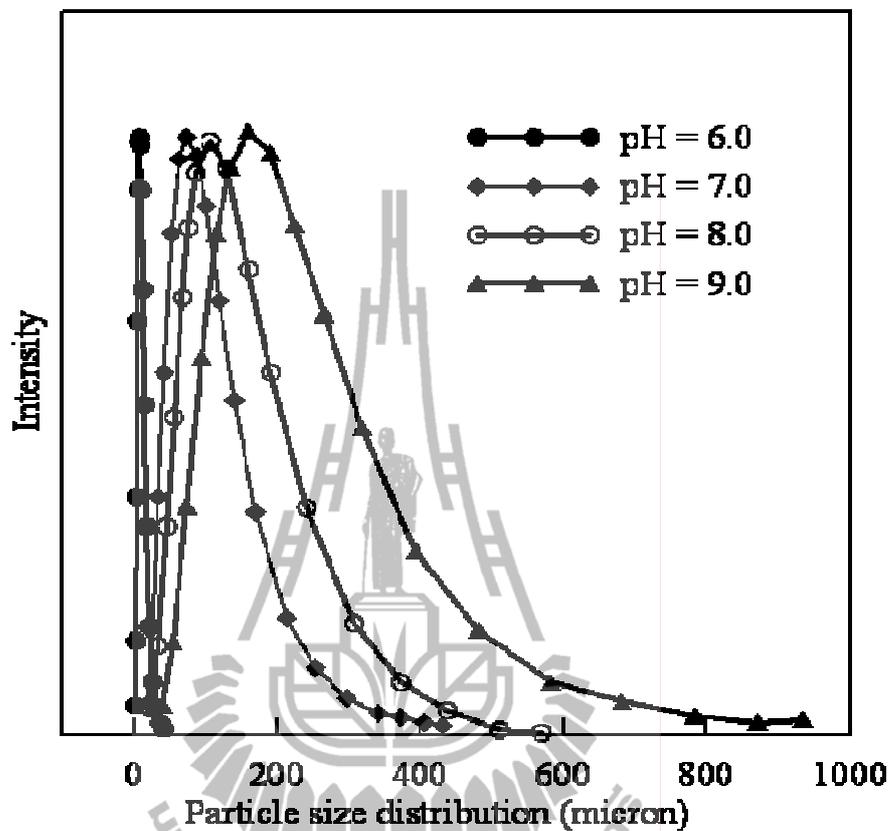
Figure 3.6 Particle size distribution of precipitates from oxidation of Mn^{2+} with 0.96

mg/L $KMnO_4$ at different pH (●) pH 6.0, (♦) pH 7.0, (○) pH 8.0, (▲) pH

9.0; stirring speed 120 rpm.

3.3.2 Effects of oxidant dose

According to the average pH values of groundwater in Taiwan, the effect

of oxidant dose was only investigated at pH 8.0 and 9.0. The removal efficiencies and

ORP with $KMnO_4$ doses of 0.48, 0.96 and 1.92 mg/L at pH 8.0 are shown in Figure

3.7 and Figure 3.8, respectively. The removal efficiency reached 80% at the dose of

0.48 mg/L, which was higher than from that by aeration alone with about 30%.

Moreover, the removal efficiency increased only slightly after 15 min with the slow

increase of ORP (Figure 3.8). The results indicated that at 0.48 mg/L the oxidant was consumed within 15 min and further removal was from the continuous aeration and catalytic oxidation of MnO_2 precipitate which also caused an increase of ORP. However, the residual Mn^{2+} concentration was still higher than the MCL (0.05 mg/L) implying that a higher oxidant dose was needed.

When the $KMnO_4$ dose was 0.96 mg/L, a complete removal of Mn^{2+} was accomplished after 15 min. The ORP ranged from 500 mV to 540 mV at 30 min and became constant. The constant ORP implied that there was no further oxidation.

When 1.92 mg/L of $KMnO_4$ was used, the average manganese removal at 15 min dropped to 86% because the excess amount of permanganate could generate additional Mn^{2+} ions resulting in the residual Mn^{2+} in the solution. The generated residual Mn^{2+} was then removed by permanganate and aeration to the final species, MnO_2 (Vigneswaran and Visvanathan, 1995). The ORP increased continuously indicating an ongoing oxidation throughout the 60 min study period.
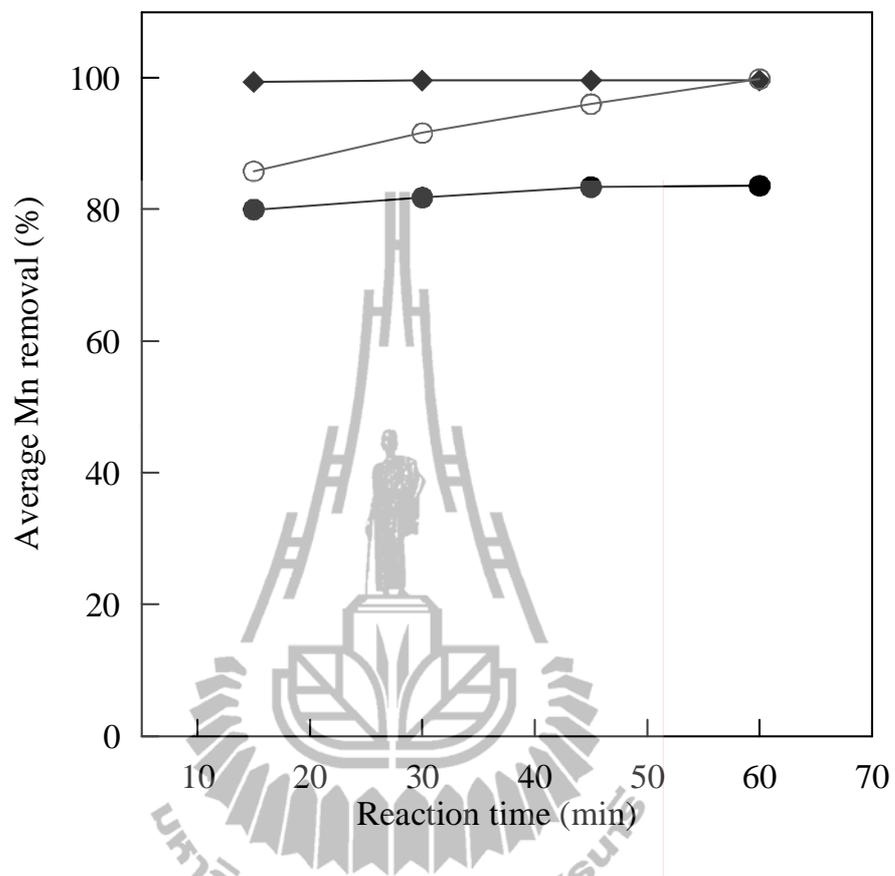
Figure 3.7 Removal efficiency of Mn^{2+} by KMnO$_4$ with different oxidant doses; (●) 0.48 mg/L, (♦) 0.96 mg/L, (○) 1.92 mg/L; pH 8.0, stirring speed 120 rpm.
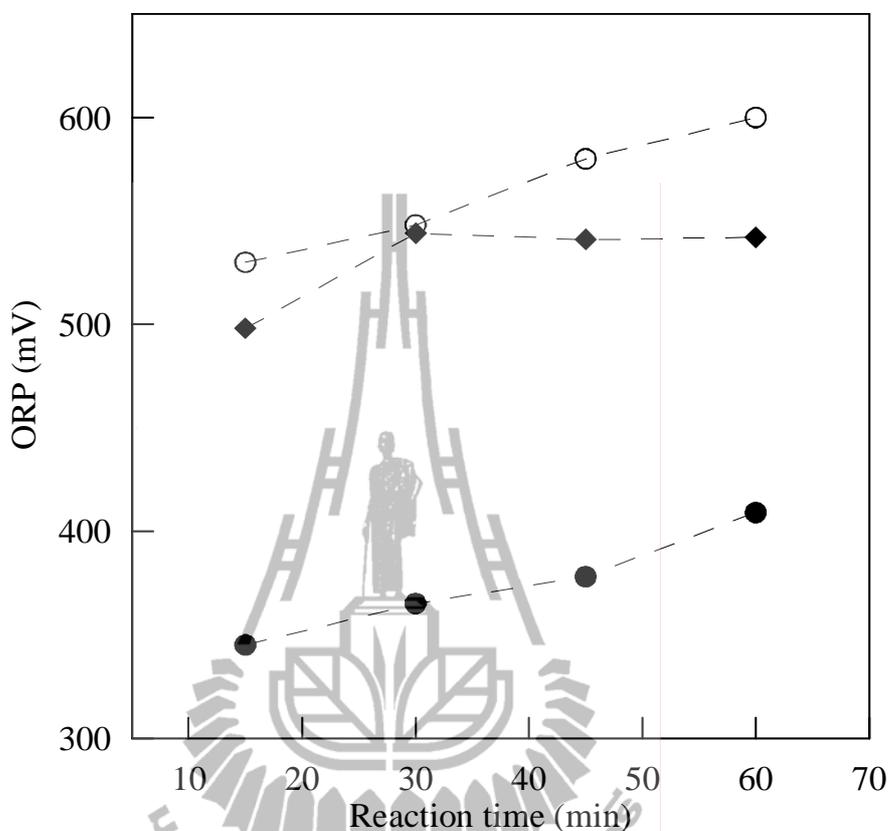
Figure 3.8 ORP values from the oxidation of Mn^{2+} by $KMnO_4$ with different oxidant

doses; (●) 0.48 mg/L, (♦) 0.96 mg/L, (○) 1.92 mg/L; pH 8.0, stirring

speed 120 rpm.

Similar studies were conducted at pH 9.0 and the results are shown in

Figure 3.9. The removal of Mn^{2+} was almost complete with 0.48 mg/L of $KMnO_4$ in

15 min. Under this pH condition, it was reported that the MnO_2 layer consisting of

black deposits and colloidal particles executed the catalytic effects on Mn^{2+} ions

removal (Sahabi, Takeda, Suzuki, and Koizumi, 2009). At this dose, all the MnO_4^-

was used up completely for the oxidation and converted to MnO_2 particle. Any

remaining Mn^{2+} could adsorb on the particle surface. The sorption rates of Mn^{2+} onto

the MnO_2 particles depend on the growth rates of MnO_2 particles. Because there was electrons transfer in this adsorption process, the ORP values increased (Figure 3.10). The result was similar to that of the oxidation with 0.96 mg/L $KMnO_4$.
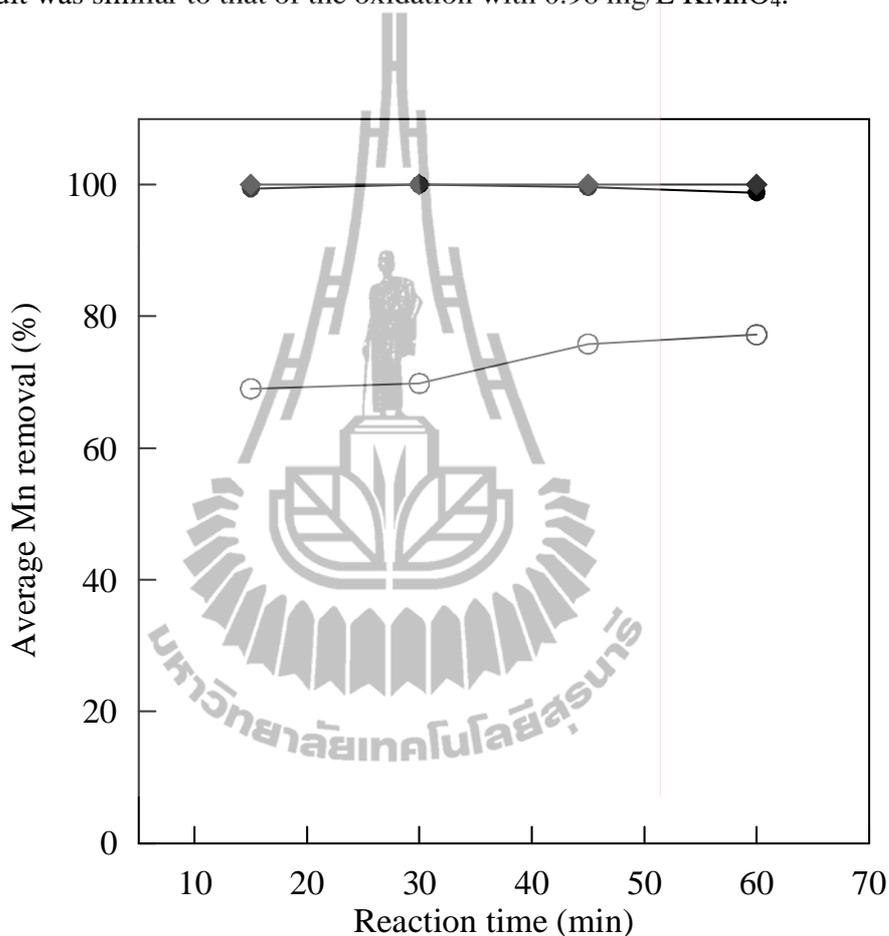
Figure 3.9 Removal efficiency of Mn^{2+} by $KMnO_4$ with different $KMnO_4$ doses; (●) 0.48 mg/L, (♦) 0.96 mg/L, (○) 1.92 mg/L; pH 9.0; stirring speed 120 rpm.

As illustrated in Figure 3.7, similar result was confirmed in Figure 3.9 by using increasing amounts of $KMnO_4$ that could induce the formation of residual Mn^{2+} ions. The increasing amounts of Mn^{2+} ions could disturb the adsorption on the MnO_2 surface (Vigneswaran and Visvanathan, 1995). The nearly constant ORP at 250 mV suggested that there was no electron transfer (Figure 3.10). Thus, the $KMnO_4$ dose of

1.92 mg/L gave low removal efficiency and was not sufficient to remove Mn^{2+} ions to the level below the MCL.
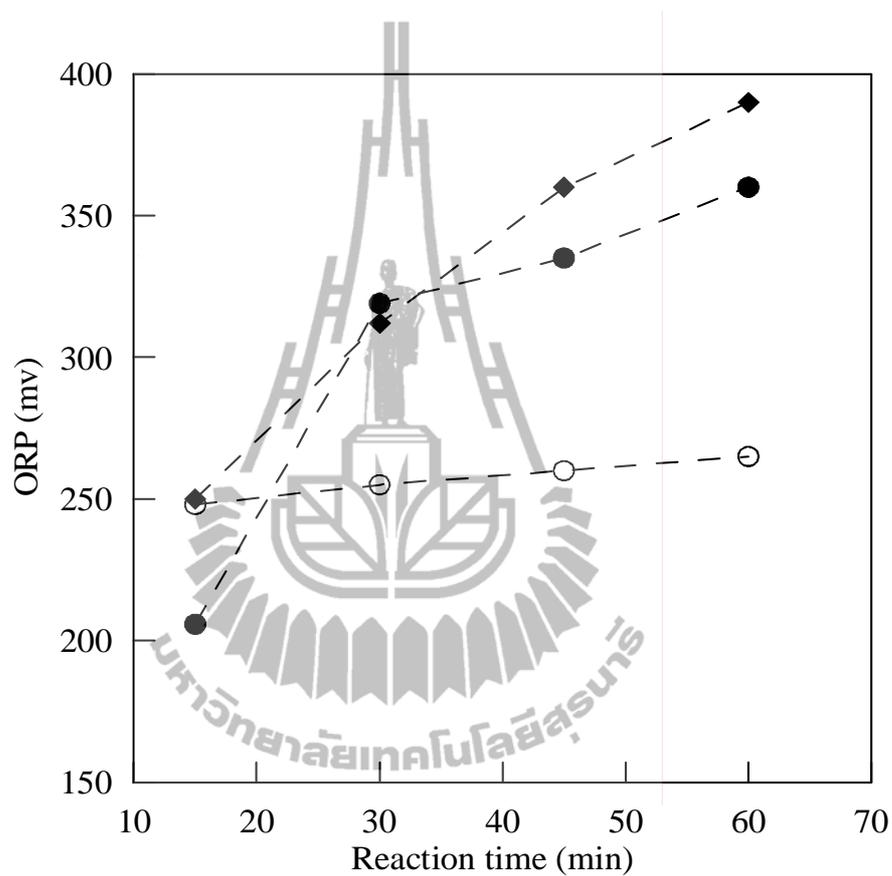
Figure 3.10 ORP values from the oxidation of Mn^{2+} by $KMnO_4$ with different oxidant doses; (●) 0.48 mg/L, (♦) 0.96 mg/L, (○) 1.92 mg/L; pH 9.0; stirring speed 120 rpm.

3.3.3 Effects of stirring speed

The oxidation of Mn^{2+} ions using $KMnO_4$ as oxidant combined with aeration could be influenced by the stirring speed which affects the diffusion of oxygen in aqueous phase (Guisnet et al., 1991). The effect of the stirring speed was

investigated by using the rate at 50, 120 and 200 rpm under the optimal removal condition, 0.96 mg/L of $KMnO_4$ at pH 8.0. The removal efficiency and ORP are shown in Figure 3.11 and Figure 3.12, respectively.
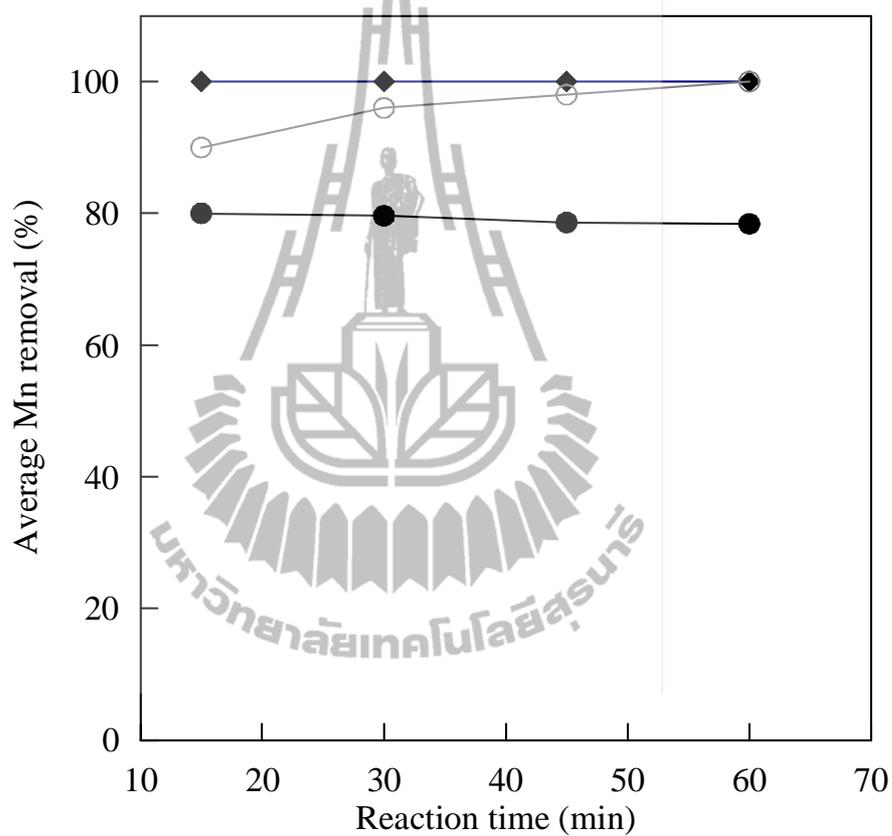
Figure 3.11 Removal efficiency of Mn^{2+} by $KMnO_4$ at different stirring speeds; (○) 50 rpm, (♦) 120 rpm, (●) 200 rpm; pH 8.0; 0.96 mg/L $KMnO_4$.
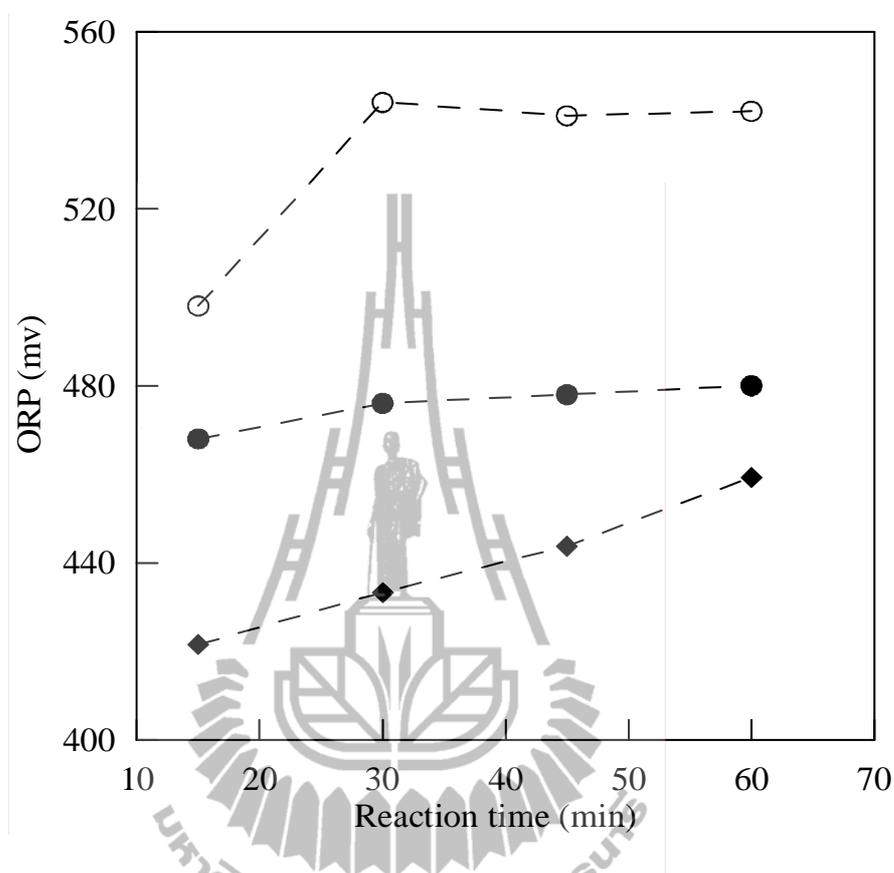
Figure 3.12 ORP from the oxidation of Mn^{2+} by $KMnO_4$ at different stirring speeds; (○) 50 rpm, (♦) 120 rpm, (●) 200 rpm; pH 8.0; 0.96 mg/L $KMnO_4$.

At 50 rpm, the removal efficiency of Mn^{2+} ions gradually increased and reached 100% in 60 min. ORP values increased from 500 to 550 mV in 30 min and became constant. The result was due to the gradual oxidation of Mn^{2+} to form MnO_2 particles. The low stirring speed resulted in less oxygen transfer in the oxidation and low removal efficiency. Besides, some MnO_2 particles were at the bottom due to gravity, causing a decrease in adsorption of Mn^{2+} (Harmankaya and Gunduz, 1998).

The complete removal efficiency of Mn^{2+} ions was observed at 120 rpm in 15 min (Figure 3.11). The ORP values ranged from 400 to 450 mV (Figure 3.12) indicating that the oxygen transfer gradually increased at a longer contact time.

At 200 rpm, the removal of Mn^{2+} was constant at 80% which illustrated the lower removal efficiency in three different stirring speeds. The ORP value ranged from 460 to 480 mV. The result indicated that the oxidation of Mn^{2+} took place only slightly. It was possibly because the higher stirring speed disturbed the growth of MnO_2 particles where the Mn^{2+} ions in the solution were adsorbed to enhance catalytic effects on Mn^{2+} ions removal. It was suggested that the amount of MnO_2 particles could affect removal of contaminants in water such as cadmium and manganese (Crimi, 2002).

Similar result was reported by Tian, Guo, Yi, and Li (2010) who studied effect of stirring speed on precipitation of cobalt (Co) using ozone as a precipitant. The Co^{2+} concentration in solution decreased more quickly with an increase of stirring speed from 400 to 1200 rpm. With a faster agitation, the ozone diffusion rate was accelerated and the reaction time decreased. However, at high stirring speed the cobalt concentration became steady because ozone diffusion was limited.

Based on all experimental results, the optimum condition for the removal of Mn^{2+} ions in synthetic groundwater to the level below the MCL in 15 min was as follows: pH 8.0, stirring speed 120 rpm and $KMnO_4$ dose 0.96 mg/L. This set of parameters was in good accordance with the one valid for the water treatment plant (Crittenden et al., 2005). Although the Mn^{2+} removal was also achieved at pH 9.0 with half stoichiometric dose of 0.48 mg/L $KMnO_4$, the high pH value is not preferable in drinking water (Dietrich, 2006). The oxidation of Mn^{2+} by $KMnO_4$ with a subsequent flocculation, sedimentation and filtration was investigated previously with an initial Mn^{2+} concentration of 1.81 mg/L (Roccaro et al., 2007). The Mn^{2+} ion could be eliminated below the MCL level in 90 min with the half stoichiometric dose of 1.74

mg/L KMnO$_4$ and pH value at 8.5. However, in the study, polyelectrolyte, flocculation and filtration processes were used to removal Mn^{2+} ions.

3.3.4 Characterization of the precipitate

Figure 3.13 illustrates the SEM images of the precipitates obtained throughout the removal study to confirm the formation of MnO$_2$ which is crucial for the removal of Mn^{2+} ions. The MnO$_2$ particles were observed on the membrane surface compared to the pure membrane. The small particles indicated loose form, rough and porous surface morphology.

Figure 3.14 and Table 3.1 show the EDX spectra and elemental composition of the precipitates. The presence of Na and Cl with the amount of 0.32 and 0.45% by weight respectively was owing to the precipitation of the electrolytes composed in the synthetic groundwater. The presence of C with the amount of 69.26% by weight was resulted from compositions of cellulose acetate membrane. The existence of O with the amount of 28.48% by weight showed that the precipitates were oxide form with the 1.49% by weight of Mn.
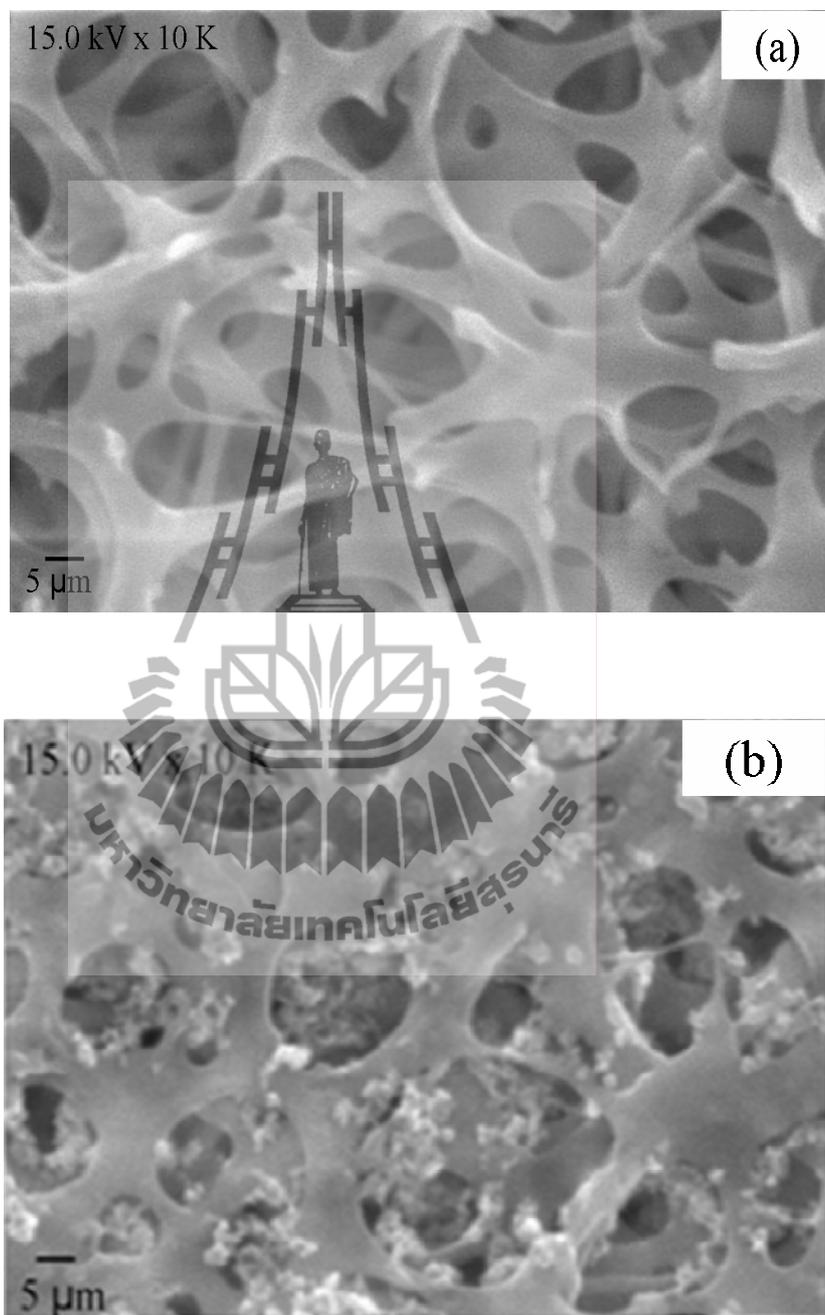
Figure 3.13 SEM images of (a) pure and (b) filtered membrane; pH 8.0, stirring speed

120 rpm; 0.96 mg/L KMnO$_4$; reaction time 60 min.
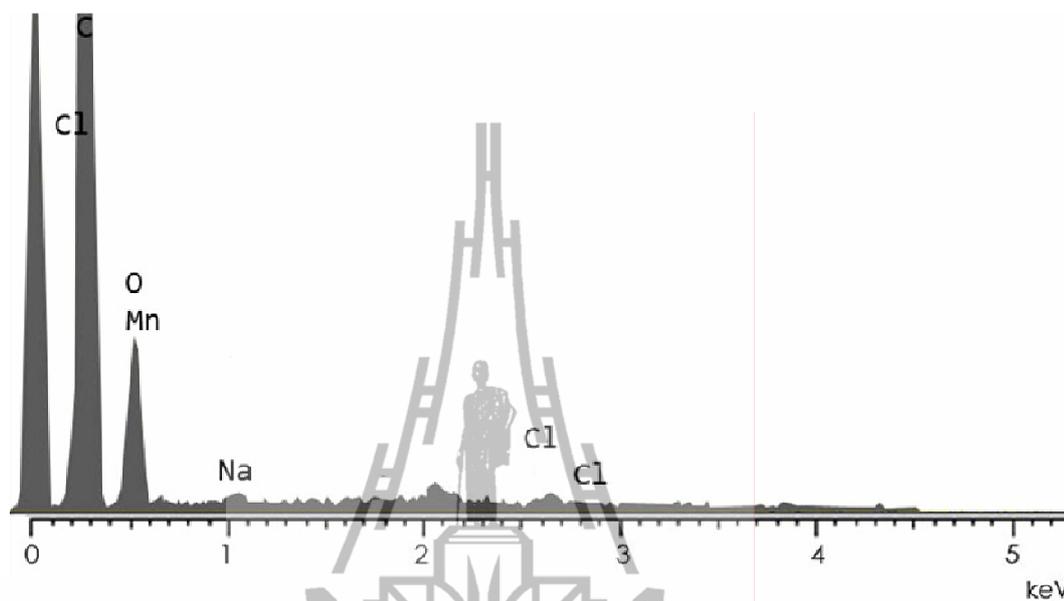
Figure 3.14 EDX spectra of the filtered membrane surface; pH 8.0, stirring speed 120 rpm; 0.96 mg/L $KMnO_4$; reaction time 60 min.

Table 3.1 Elemental composition of the filtered membrane surface obtained from EDX; pH 8.0, stirring speed 120 rpm; 0.96 mg/L $KMnO_4$; reaction time 60 min.

Element	Weight%	Atomic%
C	69.26	75.87
O	28.48	23.42
Na	0.32	0.19
Cl	0.45	0.17
Mn	1.49	0.35
Total	**100.00**	**100.00**

3.4 Conclusions

The conditions on the removal of Mn^{2+} ions from synthetic groundwater via $KMnO_4$ oxidation were studied. The results showed that the aeration, pH, oxidant dose and stirring speed were important parameters on the removal of Mn^{2+}. The partial removal of Mn^{2+} just using aeration was observed with a maximum removal of 40% even at pH 9.0. However, when $KMnO_4$ was used to oxidation, the removal efficiency of Mn^{2+} was enhanced. The pH of 8.0 and stirring speed of 120 rpm with the oxidant dose of 0.96 mg/L $KMnO_4$ were the optimum condition for the synthetic groundwater. The main composition of the precipitates was MnO_2. These MnO_2 precipitates could offer the adsorption sites for the Mn^{2+}. At the pH 9.0, the active adsorption on MnO_2 particles still can take place even the $KMnO_4$ dose is insufficient.

3.5 References

Berbenni, P., Pollice, A., Canziani, R., Stabile, L. and Nobili, F. (2000). Removal of iron and manganese from hydrocarbon-contaminated groundwaters. **Bioresource Technology**. 74: 109-114.

Buamah, R., Petrusevski, B. and Schippers, J. C. (2008). Adsorptive removal of manganese (II) from the aqueous phase using iron oxide coated sand. **Journal of Water Supply: Research and Technology-AQUA**. 57: 1-11.

Burger, M. S., Mercer, S. S., Shupe, G. D. and Gagnon, G. A. (2008). Manganese removal during bench-scale biofiltration. **Water Research**. 42: 4733-4742.

Buschmann, J., Berg, M., Stengel, C. and Sampson, M. L. (2007). Arsenic and manganese contamination of drinking water resources in Cambodia: coincidence of risk areas with low relief topography. **Environmental Science and Technology**. 41: 2146-2152.

Crimi, M. (2002). Particle genesis and effects on metals in the sunsurface during in situ chemical oxidation using permanganate. **Ph.D. thesis**, Colorado School of Mines, Colorado, U.S.A.

Crimi, M. and Ko, M. (2009). Control of manganese dioxide particles resulting from in situ chemical oxidation using permanganate. **Chemosphere**. 74: 847-853.

Crittenden, J. C., Trussell, R. R., Hand, D. W., Howe, K. J. and Tchobanoglous, G. (2005). **Water Treatment Principles and Design** (2nd ed.). U.S.A.: John Wiley and Sons. pp. 556-557.

Dietrich, A. G. (2006). Aesthetic issues for drinking water. **Journal of Water Health**. 4: 11-16.

Guisnet, M., Barrault, J., Bouchoule, C., Duprez, D., Perot, G., Maurel, R. and Montassier, C. (1991). **Studies in Surface Science and Catalysis: Heterogeneous catalysis and fine chemicals II**. New York, U.S.A.: Elsevier Science. p. 385.

Harmankaya, M. and Gunduz, G. (1998). Catalytic oxidation of phenol in aqueous solution. **Journal of Engineering and Environmental Sciences**. 22: 9-15.

Hendricks, D. W. (2010). **Fundamentals of Water Treatment Unit Processes: Physical, chemical and biological**. U.S.A.: CRC Press. p. 650.

Jusoh, A. B., Cheng, W. H., Low, W. M., Nora's aini, A. and Megat Mohd Noor, M. J. (2005). Study on the removal of iron and manganese in groundwater by granular activated carbon. **Desalination**. 182: 347-353.

Kaya, N., Karadurmus, E. and Alicilar, A. (2005). Catalytic air oxidation of manganese in synthetic waters. **Central European Journal of Chemistry**. 3: 511-519.

Kohl, P. and Medlar, S. (2006). **Occurrence of Manganese in Drinking Water and Manganese Control**. AWWA research foundation. United States Environmental Protection Agency. pp. 16-45.

Lee, C. C. and Lin, S. D. (2007). **Handbook of Environmental Engineering Calculations** (2nd ed.). New York, U.S.A.: McGraw Hill., p. 331.

Mondal, P., Majumder, C. B. and Mohanty, B. (2008). Effect of adsorbent dose, its particle size and initial arsenic concentration on the removal of arsenic, iron and manganese from simulated ground water by Fe^{3+} impregnated activated carbon. **Journal of Hazardous Materials**. 150: 695-702.

Okoniewska, E., Lach, J., Kacorzak, M. and Neczaj, E. (2008). The removal of manganese, iron and ammonium nitrogen on impregnated activated carbon. **Desalination**. 206: 251-258.

Overnel, J. (2002). Manganese and iron profiles during early diagenesis in Loch Etive, Scotland. Application of two diagenetic models. **Estuarine Coastal and Shelf Science**. 54: 33-44.

Pacini, V. A., Ingallinella, A. M. and Sanguinetti, G. (2005). Removal of iron and manganese using biological roughing up flow filtration technology. **Water Research**. 39: 4463-4475.

Roccaro, P., Barone, C., Mancini, G. and Vagliasindi, F. G. A. (2007). Removal of manganese from water supplied intended for human consumption: a case study. **Desalination**. 210: 205-214.

Sahabi, D. Takeda, M., Suzuki, M., I. and Koizumi, J-I. (2009). Removal of Mn^{2+} from water by "aged" biofilter media: The role of catalytic oxides layers. **Journal of Bioscience and Bioengineering**. 107: 151-157.

Schafer, P. L. and Prokop, W. H. (1995). **Odor Control in Wastewater Treatment Plants**, WEF Manual of Practice No. 22, ASCE Manuals and Reports on Engineering Practice No. 82, Water Environment Federation, Alexandria, VA, and American Society of Civil Engineers. New York, U.S.A. p. 136.

Senior, E. (1995). **Microbiology of Landfill Sites**, Pietermaritzburg, Republic of South Africa (2nd ed.). U.S.A.: CRC Press. p. 141.

Stembal, T., Markic, M., Ribicic, N., Briski, F. and Sipos, L. (2004). Rapid start-up of biofilters for removal of ammonia, iron and manganese from ground water. **Journal of Water Supply: Research and Technology-AQUA**. 57: 509-518.

Stembal, T., Markic, M., Ribicic, N., Briski, F. and Sipos, L. (2005). Removal of ammonia, iron and manganese from groundwaters of northern Croatia-pilot plant studies. **Process Biochemistry**. 40: 327-335.

Takeno, N. (2005). **Atlas of Eh-pH diagrams. Intercomparison of thermodynamic databases**, Geological surveys of Japan open file report No. 419.

Tekerlekopoulou, A. G. and Vayenas, D. V. (2007). Ammonia, iron and manganese removal from potable water using trickling filters. **Desalination**. 210: 225-235.

Tekerlekopoulou, A. G. and Vayenas, D. V. (2008). Simultaneous biological removal of ammonia, iron and manganese from potable water using a trickling filters. **Biochemical Engineering Journal**. 39: 215-220.

Tian, Q-h., Guo, X-y., Yi, Y. and Li, Z-h. (2010). Kinetics of oxidation-precipitation of cobalt from solution by ozone. **Transactions of Nonferrous Metals Society of China**. 20:42-45.

Vigneswaran, S. and Visvanathan, C. (1995). **Water Treatment Processes: Simple operations**, p. 167.

Wang, L. K., Hung, Y-T. and Shammas, N. (2006). **Handbook of Environmental Engineering: Advanced physicochemical treatment**. U.S.A.: Humana Press, pp. 493-499.
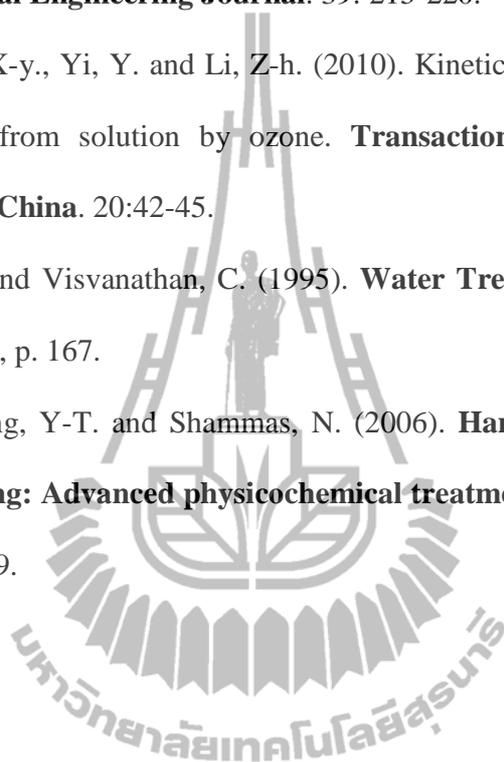
CHAPTER IV

REMOVAL OF MANGANESE AND IRON IONS FROM SYNTHETIC GROUNDWATER BY OXIDATION USING POTASSIUM PERMANGANATE

Abstract

The dual removal of Mn^{2+} and Fe^{2+} ions from synthetic groundwater by oxidation using $KMnO_4$ to keep their concentrations below the maximum contaminant level (MCL) was investigated. The batch experiments were performed in a Jar test at pH 8.0 to understand various parameters including oxidant dose, coexisting Ca^{2+} and Mg^{2+} ions and alum addition after the oxidation. Mn^{2+} was partially removed by aeration in both single and dual oxidation with the maximum removal of 30.6 and 37.2%, respectively. The presence of Fe^{2+} improved the removal of Mn^{2+} ion forming hydrous manganese-iron oxide which was confirmed by digital microscopy and EDX. The oxidant dose of 0.603 mg/L $KMnO_4$ was a minimum amount to reduce the Mn^{2+} concentration to the level below the MCL. The coexisting Ca^{2+} or Mg^{2+} slightly disturbed the elimination of Mn^{2+} but the concentration was still lower than the permitted level. Alum addition after oxidation had a negative effect for Mn^{2+} removal. Possible mechanisms of the removal of Mn^{2+} and Fe^{2+} ions with and without the coexisting ions were proposed by monitoring the pH variations. The removal

mechanisms could involve sorption between the hydrous oxide and the dissolved metal ions.

4.1 Introduction

In Chapter III, single removal of Mn^{2+} from synthetic groundwater by oxidation using aeration and $KMnO_4$ was investigated. Such method could remove Mn^{2+} to the level below MCL with the proper conditions including pH, oxidant dose and stirring speed. Mn^{2+} and Fe^{2+} are both naturally found in groundwater and the concentration of Fe^{2+} often exceeds that of Mn^{2+} (Buamah, Petrusevski, and Schippers, 2008). Thus, proper conditions for dual removal of Mn^{2+} and Fe^{2+} was were investigated in this Chapter.

Groundwater contaminated with Mn^{2+} and Fe^{2+} can be treated by several methods including biological, physical and chemical processes. The details of these methods were reported in Chapter III. Chemical oxidation by $KMnO_4$ was selected for the dual removal of Mn^{2+} and Fe^{2+} in this study because $KMnO_4$ is neither toxic nor expensive. It also helps to remove undesirable tastes and odors from manganese and iron bacteria, and hydrogen sulfide (H_2S) (Lehr, Hyman, Seevers, and Gass, 2002).

The concentration of $KMnO_4$ for the removal of Mn^{2+} and Fe^{2+} was calculated according to Eq. 2.1 and Eq. 2.2. A stoichiometric quantity of $KMnO_4$ to oxidize 1 mg of Mn^{2+} (1.82×10^{-5} mol) and Fe^{2+} (1.79×10^{-5} mol) is 1.92 mg (1.21×10^{-5} mol) and 0.94 mg (5.95×10^{-6} mol), respectively. An excess amount of $KMnO_4$ may obstruct the Mn^{2+} removal because MnO_4^- could also produce Mn^{2+} ions (Eq. 3.1). Therefore, an optimum amount of $KMnO_4$ is required to remove Mn^{2+} and Fe^{2+} to the level

below the MCL. By a method with combined aeration and oxidation, the $KMnO_4$ dose was determined according to the remaining amount of Mn^{2+} and Fe^{2+} after the aeration. The obtained optimum conditions, pH and stirring speed, from Mn^{2+} ions removal in Chapter III were still used.

The purpose of this chapter was to investigate dual removal of Mn^{2+} and Fe^{2+} from the synthetic groundwater by oxidation using combined aeration and $KMnO_4$ in a lab-scale to make their concentrations below the MCL levels. The oxidation by aeration was first investigated and the amount of oxidant, $KMnO_4$ for the remaining ions was determined. Single oxidation of water containing Mn^{2+} or Fe^{2+} and dual oxidation of water containing both Mn^{2+} and Fe^{2+} were studied to understand an influence of the coexisting Fe^{2+} ions on the oxidation of Mn^{2+} ions. The synthetic groundwater was prepared to contain similar concentration of Mn^{2+} and Fe^{2+} at 0.50 mg/L. Studied parameters included oxidant dose, effect of coexisting Ca^{2+} and Mg^{2+} ions, and alum addition after oxidation. The morphology and composition of the precipitates were analyzed by digital microscope and EDX, respectively. Particle charge was determined by zeta potentiometer.

4.2 Experimental

4.2.1 Chemicals

Deionized water (DI) with a resistivity of 18.9 MΩ was used in the preparation of all samples and standards. The chemicals employed were similar to those reported in Chapter III. Additional chemicals were iron sulfate heptahydrate ($FeSO_4 \cdot 7H_2O$) and calcium chloride tetrahydrate ($CaCl_2 \cdot 4H_2O$) which were obtained

from Merck, Germany and aluminum sulfate ($Al_2(SO_4)_3 \cdot 16\text{-}18H_2O$) was obtained from Nihon Shiyaku Reagent, Japan.

4.2.2 Experimental methods

The experimental procedures were done similarly to those in Chapter III. In addition, stock solutions of Mn^{2+} or Fe^{2+} with a concentration of 1000 mg/L were prepared from $MnCl_2 \cdot 4H_2O$ and $FeSO_4 \cdot 7H_2O$, respectively. A stock solution of alum with a concentration of 6000 mg/L was prepared from $Al_2(SO_4)_3 \cdot 16\text{-}18H_2O$. A stock solution of Ca^{2+} and Mg^{2+} with a concentration of 4000 mg/L (100 mM) and 2430 mg/L (100 mM) were prepared from $CaCl_2 \cdot 4H_2O$ and $MgCl_2 \cdot 4H_2O$, respectively.

4.2.3 Batch Study

The batch study was carried out with the method reported in Chapter III. The mixture was initially sampled after aeration for 20 min and this sample was referred to 0 min of reaction time. Then, $KMnO_4$ was added with studied concentration and the mixture was sampled every 15 min with the reaction time of 60 min, referred to 15, 30, 45 and 60 min.

4.2.4 Effect of coexisting ions

The concentrations of the coexisting ions were: Ca^{2+}, 4.0, 40.0 and 400.0 mg/L; Mg^{2+}, 2.4, 24.3 and 243.0 mg/L. The wide concentration range was selected since the amount of Ca^{2+} and Mg^{2+} normally fluctuates, which is caused by the changing conditions of natural groundwater.

4.2.5 Effect of alum addition after oxidation

Coagulation by alum at three concentrations, 10, 20 and 30 mg/L were studied. These chosen values are typically employed for inspecting low turbid water

(Lehr et al., 2002). The experiment was continuously done via the batch study as reported in 4.2.4. The stock solution of alum was added after 60 min of the oxidation, stirring speed was decreased to 50 rpm and the reaction time was expanded to 60 min. The samples were referred to 75, 90, 105 and 120 min of reaction time. To investigate the effect of alum, after initial aeration for 20 min, alum with the concentration of 30 mg/L was added into the water instead of $KMnO_4$. The stirring speed was 120 rpm for the first 60 min and then decreased to 50 rpm for the coagulation-flocculation processes. The sampling was done every 15 min during the reaction time of 120 min.

4.2.6 Characterization

The residual ions including Mn^{2+}, Fe^{2+}, Ca^{2+} and Mg^{2+} were analyzed by ICP-OES (Perkin Elmer DV 2000). A blank solution was prepared from the synthetic groundwater without those ions. The details of the analysis were reported in Chapter III.

The precipitates produced during the reaction were collected at 60 min after the reaction was carried out, dehydrated by freeze drying for 2 days to remove free water and finally kept in a desiccator before analyses by a digital microscope (Hirox, KH-7700) with a magnification of 700x and EDX (Hariba Emax 400).

The colloidal solution produced during the oxidation of dual Mn^{2+}-Fe^{2+} system at pH 6.0-9.0 was collected after 60 min of the oxidation before analyses by zeta potentiometer (Zetasizer Nano-ZS, Malvern instrument) to determine the surface charge of the precipitates.

4.3 Results and discussion

4.3.1 Effect of aeration in single and dual system

Aeration of the synthetic groundwater was first studied to investigate the removal of Mn^{2+} and Fe^{2+} ions. The average removal of the single and dual oxidation is presented in Figure 4.1 and Figure 4.2, respectively. By aeration in the single Mn^{2+} system (Figure 4.1), the removal efficiency became nearly constant after 15 min with the capacity of 30.6%. The remaining concentration of 0.347 mg/L was still higher than the MCL. The oxidation efficiency by aeration was low because the reaction requires an ORP higher than 400 mV (Takeno, 2005). In contrast, Fe^{2+} in the single system was eliminated more easily with a conversion of 90.0% and the remaining concentration was lower than the permitted level. The removal efficiency was higher because it could occur at a lower ORP, 0 mV (Takeno, 2005).

By aeration of the dual system consisting of Mn^{2+} and Fe^{2+} (Figure 4.2), the remaining concentration of both ions after 60 min were 0.314 mg/L (37.2% conversion) and 0.048 mg/L (90.4% conversion), respectively. The removal efficiency of Mn^{2+} increased 6.6% from that of the single oxidation possibly because of an assistance by the coexisting Fe^{2+} ions. Wolthoorn, Temminghoff, Weng, and Riemsdijk (2004) reported that Fe^{2+} was initially oxidized and $Fe(OH)_3$ was formed shortly after aeration. They suggested that the $Fe(OH)_3$ provided a surface for the autocatalyzed oxidation of Mn^{2+} and Fe^{2+} and could co-precipitate with other cations. However, the aeration of Fe^{2+} was less effective when Mn^{2+} was present in the groundwater (Wolthoorn et al., 2004). From this investigation, Fe^{2+} was still removed constantly with the coexisting Mn^{2+} after aeration, but the residual concentration of

Mn^{2+} was still higher than the MCL. Therefore, an additional oxidant is required to improve the removal efficiency of Mn^{2+} in both single and dual systems and the removal of Mn^{2+} would be focused on the rest of this chapter.
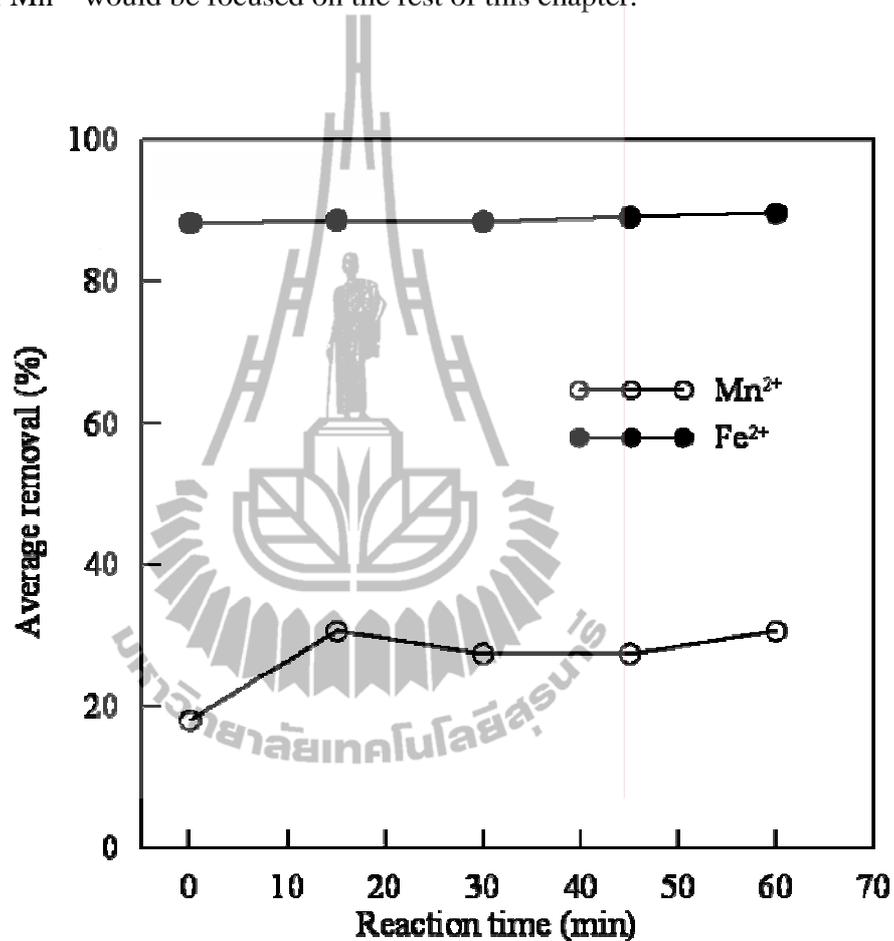
Figure 4.1 Removal efficiency of Mn^{2+} and Fe^{2+} by aeration in single oxidation. The

pH was 8.0 and stirring speed was 120 rpm.
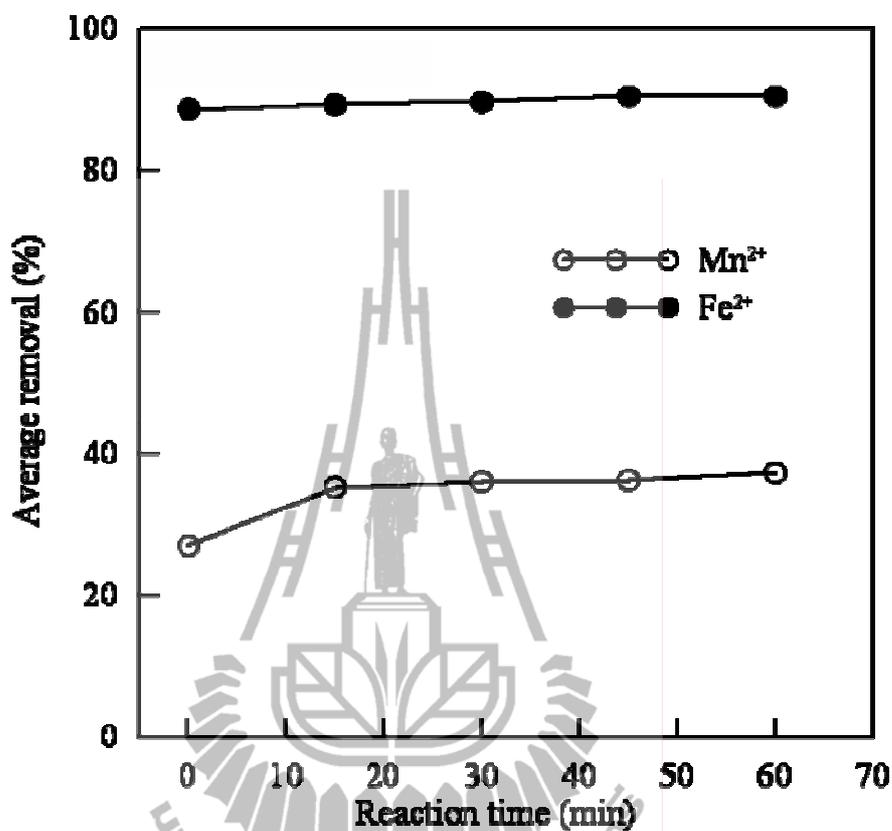
Figure 4.2 Removal efficiency of Mn^{2+} and Fe^{2+} by aeration in dual oxidation. The pH was 8.0 and stirring speed was 120 rpm.

4.3.2 Effect of oxidant dose in removal of Mn^{2+} in single and dual systems

Oxidation of the remaining Mn^{2+} by a minimum amount of $KMnO_4$ was investigated. The experiments were performed using low-level aeration combined with different doses of $KMnO_4$ in the synthetic groundwater. According to Eq. 2.1 and Eq. 2.2, the doses of $KMnO_4$ used in this study were 0.603 and 0.648 mg/L, according to the residual concentration after aeration of Mn^{2+} in the dual system (0.314 mg/L) and Fe^{2+} combined with Mn^{2+} in the dual system (0.048 and 0.314 mg/L), respectively.

The percent removal of Mn^{2+} ions in the single system and dual Mn^{2+}-Fe^{2+} system are demonstrated in Figure 4.3 and Figure 4.4, respectively. In the single Mn^{2+} system (Figure 4.3), the removal efficiency increased quickly in 15 min after adding $KMnO_4$. For the 0.603 mg/L dose (dash line), the efficiency was 84.6% and then increased slowly to 92.2% after 60 min where the remaining Mn^{2+} concentration was below the MCL. At 0.648 mg/L $KMnO_4$ (solid line), the percent removal reached the maximum at 92.2% after 15 min. The increase of oxidant dose raised the conversion of Mn^{2+} to MnO_2 precipitates which were also generated from the reduction of the oxidant itself. The remaining Mn^{2+} can be more sorbed on the produced oxide. They reported that the presence of MnO_2 may exert a catalytic effect on further precipitation of metal from liquid phase (Zaw and Chiswell, 1999; Berbenni, Pollice, Canziani, Stabile, and Nobili, 2000). A two-reaction mechanism has been proposed, where a relatively rapid adsorption is followed by a lower oxidation.

$$Mn^{2+}_{(aq)} + MnO_{2(s)} \rightarrow MnO_2Mn^{2+}_{(s)} \tag{4.1}$$

$$O_{2(g)} + MnO_2Mn^{2+}_{(s)} \rightarrow 2MnO_{2(s)} \tag{4.2}$$
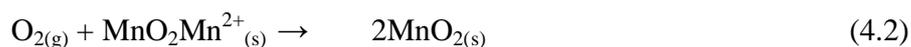
Therefore, Mn^{2+} can be removed by oxidation using $KMnO_4$ and by oxygen after adsorption on MnO_2. The single removal of Mn^{2+} was satisfactory with the minimum concentration of $KMnO_4$ (0.603 mg/L).
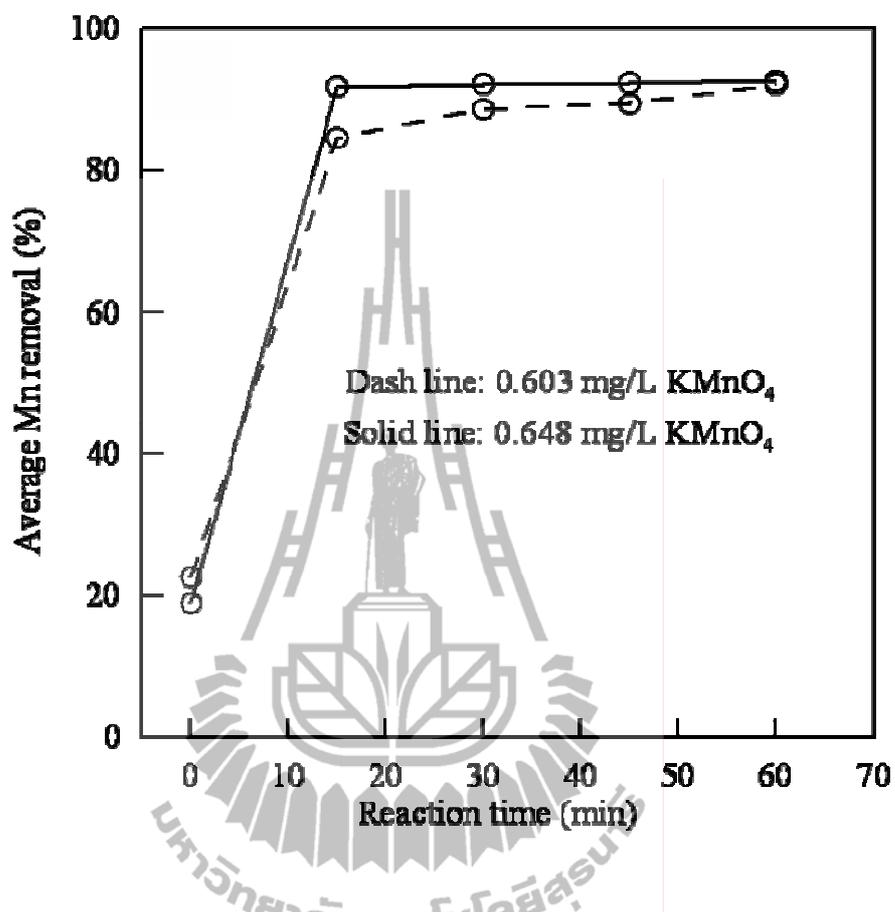
Figure 4.3 Removal efficiency of Mn^{2+} by KMnO$_4$ in single Mn^{2+} oxidation. The

oxidant doses were 0.603 (dash line) and 0.648 mg/L (solid line), pH was

8.0 and stirring speed was 120 rpm.
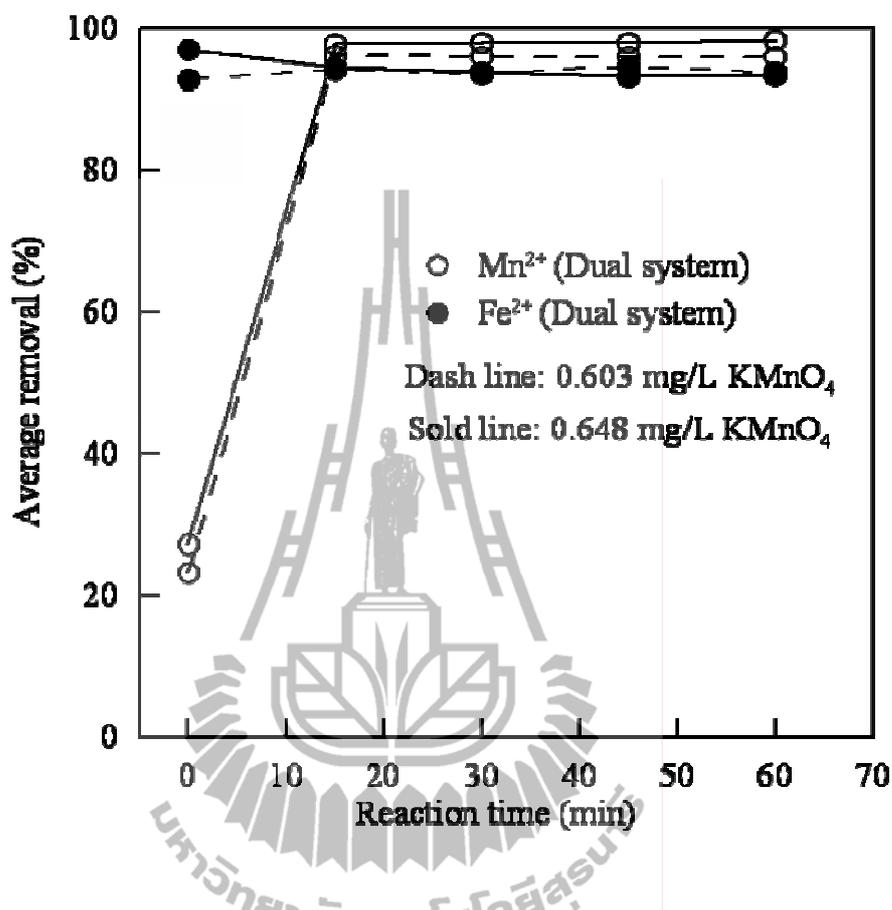
Figure 4.4 Removal efficiency of Mn^{2+} and Fe^{2+} by $KMnO_4$ in dual Mn^{2+} and Fe^{2+}

oxidation. The oxidant doses were 0.603 (dash line) and 0.648 mg/L

(solid line), pH was 8.0 and stirring speed was 120 rpm.

The removals of Mn^{2+} and Fe^{2+} in the dual system by both oxidant doses

(0.603 and 0.648 mg/L) shown in Figure 4.4 had a similar trend. Both doses gave the

Mn^{2+} level below the MCL within 15 min and the percent removal in the dual system

was higher than that in the single system. Throughout the studied time, the removal of

Fe^{2+} was above 94.0% which was about 4.0% higher than the result from aeration

alone and the removal was not affected by an increase of oxidant dose. The coexisting

Fe^{2+} could form Fe(OH)$_3$ which could incorporate with MnO$_2$ and enhance the sorption of Mn^{2+} ions. Zoller (1994) documented that oxides and hydroxides of Mn and Fe respectively showed a high capacity of reduction of heavy metals in an aqueous phase by means of sorption. Besides, the reduction of KMnO$_4$ forming MnO$_2$ could assist the sorption of Mn^{2+} ions (Berbenni et al., 2000; Crimi and Siegrist, 2004; Loomer, Al, Banks, Parker, and Mayer, 2006). The formation of MnO$_2$ and Mn-Fe oxides generated from the oxidation in this work was further confirmed in the characterization parts.

Because the removal of Mn^{2+} and Fe^{2+} ions in both single and dual systems by both oxidant doses were similar, the oxidant dose of 0.603 mg/L combined with aeration was sufficient and used as a minimum dose throughout the rest of the study.

4.3.3 Effect of Ca^{2+} and Mg^{2+} on removal of Mn^{2+} in dual system

The effect of coexisting Ca^{2+} and Mg^{2+} ions in the synthetic groundwater on the removal of the dual Mn^{2+} and Fe^{2+} system was investigated using the oxidant dose of 0.603 mg/L and pH 8.0. The average removals of Mn^{2+} with different concentrations of Ca^{2+} and Mg^{2+} are shown in Figure 4.5 and Figure 4.6, respectively.
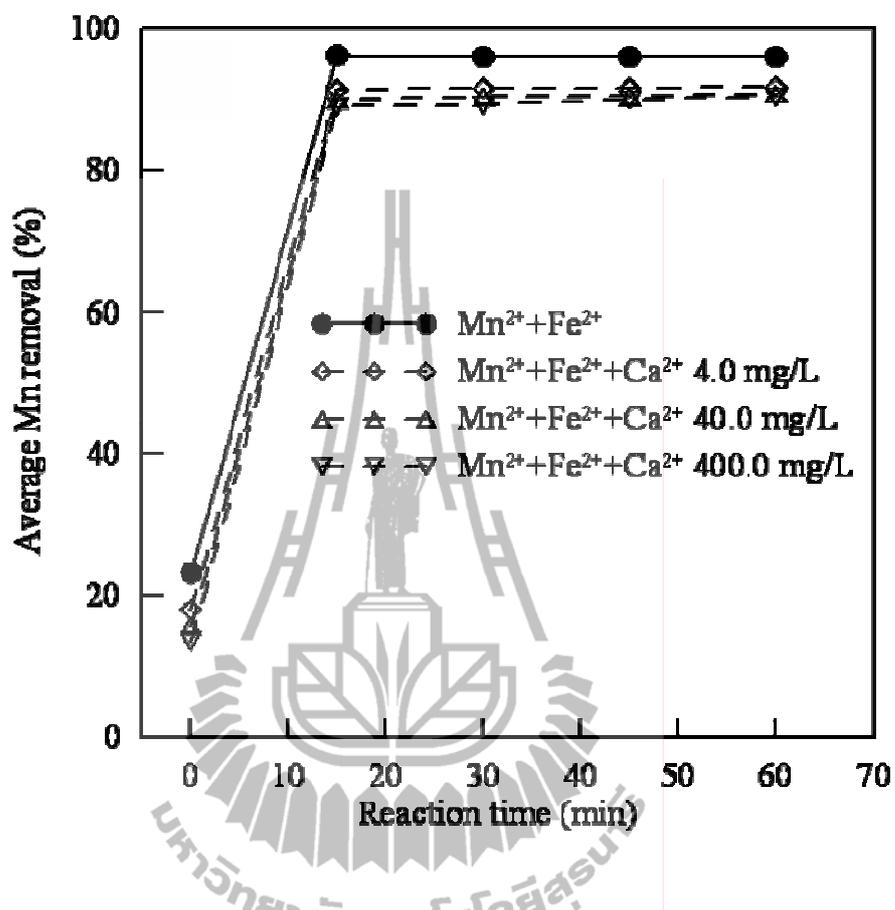
Figure 4.5 Removal efficiency of Mn^{2+} in dual Mn^{2+} and Fe^{2+} oxidation by $KMnO_4$

with the coexisting Ca^{2+}. The oxidant dose was 0.603 mg/L, pH was 8.0

and stirring speed was 120 rpm.
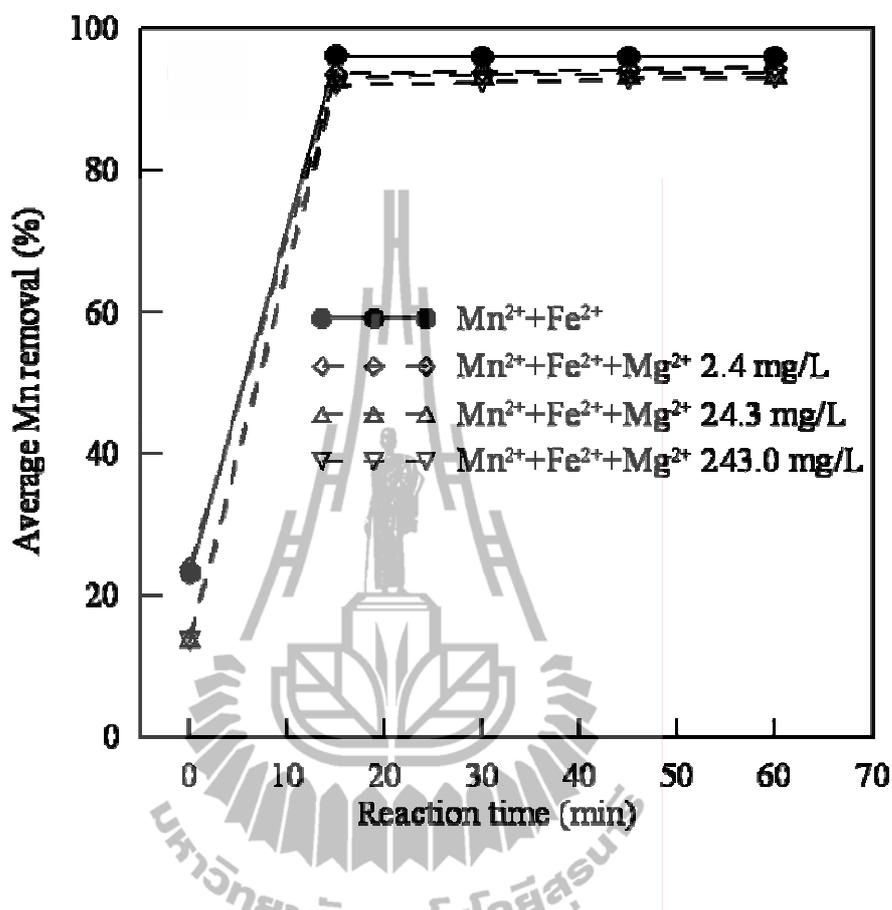
Figure 4.6 Removal efficiency of Mn^{2+} in dual Mn^{2+} and Fe^{2+} oxidation by $KMnO_4$

with the coexisting Mg^{2+}. The oxidant dose was 0.603 mg/L, pH was 8.0

and stirring speed was 120 rpm.

As shown in Figure 4.5, when the concentrations of the coexisting Ca^{2+}

ions were 4.0, 40.0 and 400.0 mg/L, the percent removal of Mn^{2+} decreased by 4.0,

6.0 and 6.0%, respectively, from that of the system without Ca^{2+}. However, the

remaining concentration of Mn^{2+} after oxidation was still lower than the MCL in all

cases. The results suggested that $KMnO_4$ was an effective oxidant for Mn^{2+} in the dual

Mn^{2+}-Fe^{2+} system with coexisting Ca^{2+} ions. The result can be explained in term of

surface charge of the Mn-Fe precipitates that can further interact with the remaining Mn^{2+} ions and other metal cations in water by sorption (Berbenni et al., 2000; Zogo, Bawa, Soclo, and Atchekpe, 2011).
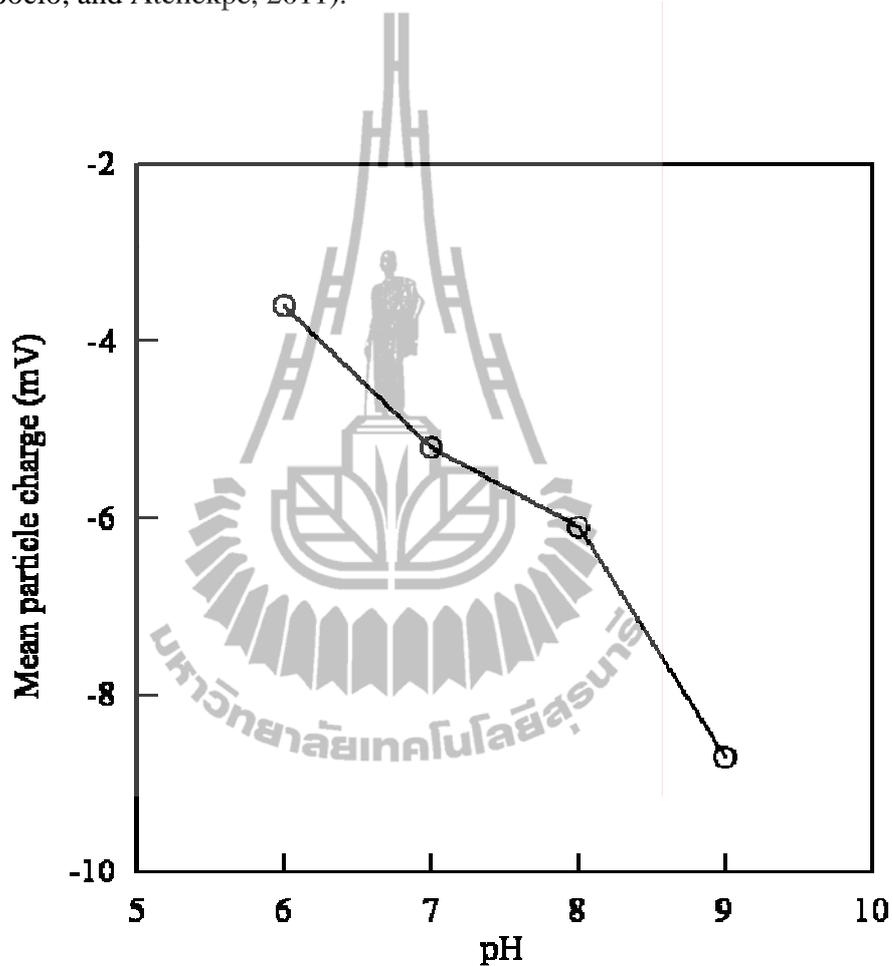
Figure 4.7 Mean particle charge of the forming precipitates after 60 min of dual Mn^{2+} and Fe^{2+} oxidation (without Ca^{2+} and/or Mn^{2+}). The oxidant dose was 0.603 mg/L, pH was 8.0 and stirring speed was 120 rpm.

Based on the oxidation of Mn^{2+} and Fe^{2+} ions in Eq. 2.1 and Eq. 2.2, the produced MnO_2 and $Fe(OH)_3$ have a surface charge which can be affected by pH.

Their points of zero charge (PZC), the pH at which the surface is uncharged, were about 3 and 8, respectively (Liu, Liu, Qiang, Qu, Li, and Wang, 2009). When the pH is less than pH_{PZC}, the surface charge is positive because of protonation and vice versa and the reactions are as follows (Davis and Leckie, 1978).

$$\equiv Mn\text{-}OH_{(s)} + H_2O_{(l)} \rightarrow \quad \equiv Mn\text{-}OH_2^+{}_{(s)} + OH^-{}_{(aq)} \ (pH < pH_{PZC}) \qquad (4.3)$$

$$\equiv Mn\text{-}OH_{(s)} + H_2O_{(l)} \rightarrow \quad \equiv Mn\text{-}O^-{}_{(s)} + H_3O^+{}_{(aq)} \ (pH > pH_{PZC}) \qquad (4.4)$$
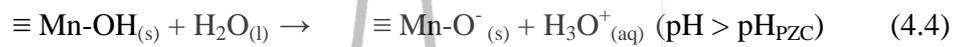
where $\equiv Mn\text{-}OH_2^+$, $\equiv Mn\text{-}OH$ and $\equiv Mn\text{-}O^-$ represent positively, neutral and negatively charged surface hydroxyl, respectively.

As presented in Figure 4.7, the net charge of Mn-Fe precipitates was negative at pH 6.0-9.0 and decreased with increase of pH. The net negative charge was mainly resulted from manganese oxides from the oxidation of Mn^{2+} and reduction of MnO_4^- under alkaline condition, pH > pH_{PZC}. This evidence was proved from surface functional group of $\delta\text{-}MnO_2$ (Liu et al., 2009). At pH 7.0, $\delta\text{-}MnO_2$ had surface charge as low as   -23.4 mV and increased to -12.4 mV at 8.0 mg/L Ca^{2+}. In our work, at pH 8.0, Mn-Fe precipitates had surface charge of -6.0 mV and increased to -1.54 mV at 4.0 mg/L Ca^{2+}. Because Ca^{2+} decreased the surface negative charge and obstructed the removal of remaining Mn^{2+} ions.

The effect of Mg^{2+} on the removal of Mn^{2+} is presented in Figure 4.6. The percent removal decreased about 2.0, 3.0 and 3.0% when the Mg^{2+} concentrations were 2.4, 24.3 and 243.0 mg/L, respectively from that of the system without Mg^{2+}. However, the concentration of Mn^{2+} was still below the MCL in all cases. This result can be explained by the mean surface charge of the precipitates consisted of Mn^{2+},

Fe^{2+} and Mg^{2+} ions (-9.33 mV) which was more negative than that in the condition without Mg^{2+}. As a result, the existing Mg^{2+} did not obstruct the removal of Mn^{2+}.

Based on the results, the presence of Ca^{2+} and Mg^{2+} slightly obstructed the removal of Mn^{2+} but it was still lower than the MCL. This may be due to the sufficient amount of KMnO$_4$ used in the oxidation step, which produced Mn-Fe precipitates to enhance the removal of Mn^{2+} and Fe^{2+}. In addition, Ca^{2+} and Mg^{2+} could precipitate to form calcium and magnesium carbonate, which could capture residual Mn^{2+} (Guan, Ma, Dong, and Jiang, 2009; Masue, Loeppert, and Kramer, 2007).

4.3.4 Effect of coagulation after oxidation

The further removal of Mn^{2+} was studied by addition of alum to the mixture after combined aeration and oxidation. The results are presented in Figure 4.8. Without KMnO$_4$, the coagulation by alum has no effect on removal of Mn^{2+} ions (dash line). The maximum Mn^{2+} removal was somewhat constant about at 30.0%, similar to the removal by aeration alone. Similar result was obtained by Montiel and Welte (1990) that a manganese elimination yield was 25 to 35% (initial concentration of 0.5 to 1.0 mg/L) during coagulation using ferric chloride at pH between 7.6-7.8. Therefore, the removal of Mn^{2+} using coagulant alone was not sufficient and the addition of KMnO$_4$ was further studied.

With the combination between aeration and 0.603 mg/L KMnO$_4$, the percent removal of Mn^{2+} slightly decreased at 87.0%, 88.0% and 91.2% as the dosage of alum added increased from 10, 20 to 30 mg/L, respectively. The negative effect on the Mn^{2+} removal is due to alum causing the pH to drop, converting MnO$_2$ back to Mn^{2+} (Loomer et al., 2011). However, the residual amount of Mn^{2+} was still below

the permitted level. A similar result was obtained by Zogo et al. (2011) who showed that the partial removal of Mn^{2+} and Fe^{2+} from the initial concentration of 0.1 and 8.0, respectively, was observed using 40 mg/L alum at pH 6.5. After the coagulation followed by adding 2.5 mg/L $KMnO_4$ at pH 8.5, Mn^{2+} and Fe^{2+} were eliminated to the level below the acceptable level. Other studies also showed that the oxidized forms of MnO_2 and $Fe(OH)_3$ are good adsorbents which might improve the efficiency of coagulation (Berbenni et al., 2000). El Araby, Hawash, and El Diwani (2010) studied the removal of Mn^{2+} and Fe^{2+} with initial concentration of 1.0 and 2.6 mg/L, respectively, by 3.0 mg/L O_3 combined with 30 mg/L alum and pH 8.0. The method was not successful because the residual concentration of Mn^{2+} and Fe^{2+} were 0.1 and 0.13 mg/L, respectively, still higher than the MCL level. The result inferred that the amount of O_3 could produce insufficient sorption sites of Mn-Fe oxide for the remaining Mn^{2+} ions even alum was added (El Araby et al., 2010).
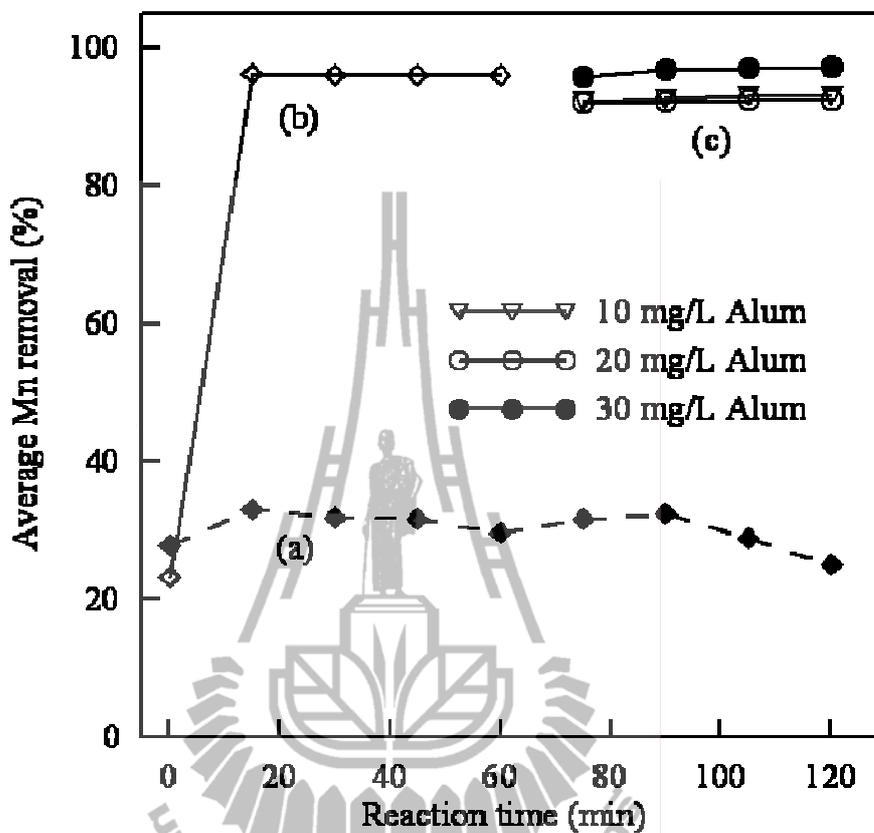
Figure 4.8 Removal efficiency of Mn^{2+} in dual Mn^{2+} and Fe^{2+} oxidation by $KMnO_4$;

(a) combined aeration and 30 mg/L alum, (b) combined aeration and

0.603 mg/L $KMnO_4$, (c) coagulation after 60 min of the oxidation. The

pH was 8.0 and stirring speed was 120 rpm.

4.3.5 Characterization of precipitates of the oxide

The morphology and composition of the precipitates obtained from single

and dual system were examined using the digital microscope and EDX. The results

are shown in Figure 4.9 to Figure 4.12.

In the single system, white particles were observed (Figure 4.9) due to the precipitation of the electrolytes composed in the synthetic groundwater. This was confirmed by EDX analysis revealing the presence of Na, Cl and K with the amount of 0.32, 0.48 and 0.35% by weight, respectively (Table 4.1). The presence of C with the amount of 72.41% by weight was resulted from compositions of cellulose acetate membrane. The existence of O with the amount of 35.60% by weight indicated that the light brown precipitates were oxide form with the 0.49% by weight of Mn. The formation of MnO_2 involved in the removal of Mn^{2+} and Fe^{2+}.

Figure 4.9 Image from a digital camera of the precipitates from single Mn^{2+} oxidation. The oxidant dose was 0.603 mg/L, pH was 8.0, stirring speed was 120 rpm and reaction time was 60 min.
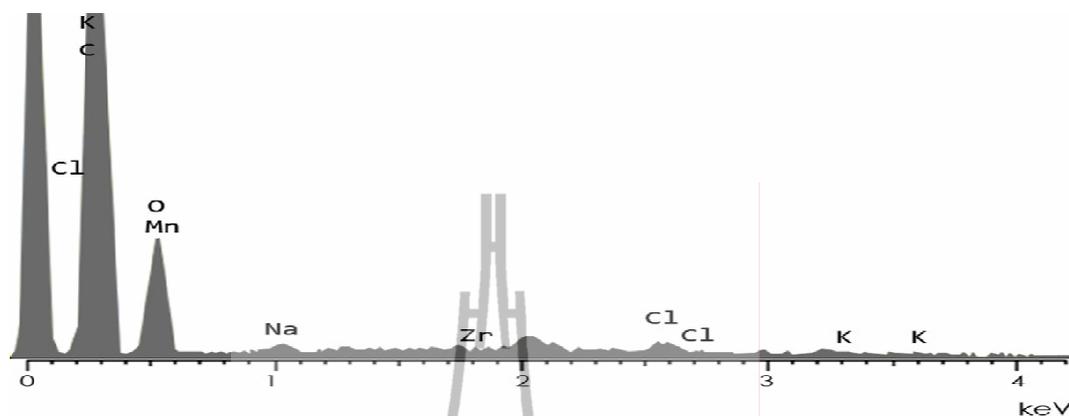
Figure 4.10 EDX spectra of the precipitates from single Mn^{2+} oxidation. The oxidant

dose was 0.603 mg/L, pH was 8.0, stirring speed was 120 rpm and

reaction time was 60 min.

Table 4.1 Elemental composition of the filtered membrane surface from single Mn^{2+}

oxidation; 0.603 mg/L $KMnO_4$; pH 8.0; stirring speed 120 rpm; reaction

time 60 min.

Element	Weight%	Atomic%
C	72.41	78.59
O	25.95	20.81
Na	0.32	0.18
Cl	0.48	0.18
K	0.35	0.12
Mn	0.49	0.12
Total	**100.00**	**100.00**

Considering the dual system, the white particles were still observed (Figure 4.11), similar to the single system. The particles were dark brown with the main compositions of manganese oxide (15.26% by weight) and iron oxide (16.40% by weight) (Table 4.2). The increase of manganese oxide in the dual system was due to the oxidation of Mn^{2+} as well as the reduction of MnO_4^-. The presence of these compositions during the oxidation led to the sorption of the dissolved metal ions in the water.

Figure 4.11 Image from a digital camera of the precipitates from dual Mn^{2+} and Fe^{2+} oxidation. The oxidant dose was 0.603 mg/L, pH was 8.0, stirring speed was 120 rpm and reaction time was 60 min.
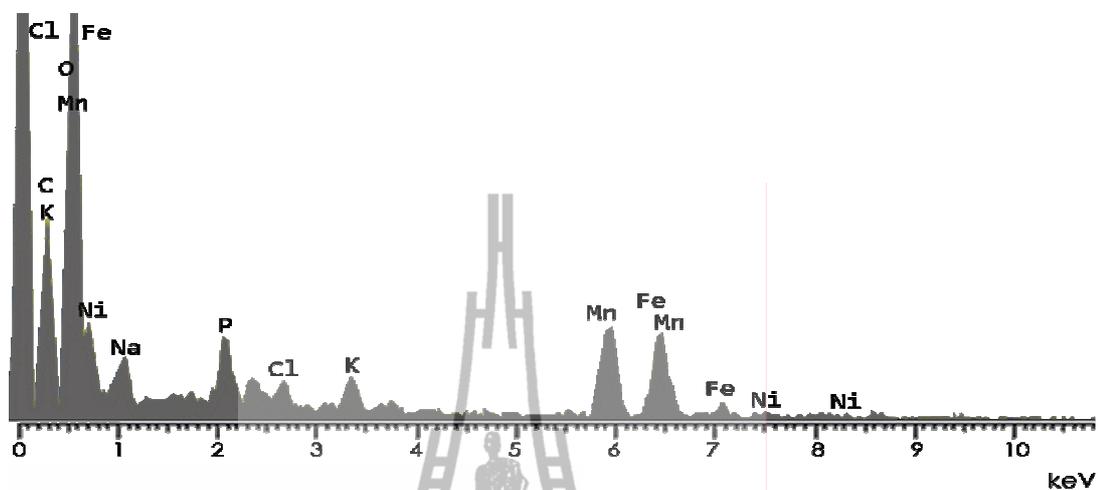
Figure 4.12 EDX spectra and elemental composition of the precipitates from dual

Mn^{2+} and Fe^{2+} oxidation. The oxidant dose was 0.603 mg/L, pH was 8.0,

stirring speed was 120 rpm and reaction time was 60 min.

Table 4.2 Elemental composition of the filtered membrane surface from dual Mn^{2+}

and Fe^{2+} oxidation; 0.603 mg/L $KMnO_4$; pH 8.0; stirring speed 120 rpm;

reaction time 60 min.

Element	Weight%	Atomic%
C	26.46	41.92
O	35.60	42.80
Na	1.84	1.57
P	1.89	1.57
Cl	1.07	0.59
K	1.48	0.74
Mn	15.26	5.44
Fe	16.40	5.75
Total	**100.00**	**100.00**

In conclusion, the optimum conditions for the removal of Mn^{2+} and Fe^{2+} in

the synthetic groundwater are as follows: pH value, 8.0; stirring speed, 120 rpm and

$KMnO_4$ dose, 0.603 mg/L. This use of set of parameter decreased the concentration of

both ions to the level below the MCL in 15 min. The coexisting Ca^{2+} and Mg^{2+}, and

coagulation by alum slightly affected the removal efficiency. The suitable

concentration of $KMnO_4$ employed and the formation of the Mn-Fe precipitates could

assist the removal of Mn^{2+} and Fe^{2+}. The possible mechanism of Mn^{2+} and Fe^{2+}

removal was further studied to develop a treatment method to increase the removal

efficiency of Mn^{2+}, Fe^{2+} contaminated in groundwater.

4.3.6 Possible mechanisms on removal of Mn^{2+} and Fe^{2+}

To study possible mechanisms on the elimination of Mn^{2+} and Fe^{2+} by 0.603 mg/L $KMnO_4$, the experiments were performed without pH adjustment with initial pH of 8.0. The experimental design was simulated the conditions existing during the remediation of contaminated water, where the pH control is either not necessary or difficult to be realized. Variations of solution pH and average removal of Mn^{2+} were recorded as shown in Figure 4.13 and Figure 4.14, respectively whereas the effect of coexisting ions is presented in Figure 4.15.

Without Ca^{2+} and Mg^{2+} ions, the pH of the synthetic groundwater containing free- Mn^{2+} and Fe^{2+} did not change after 60 min (Figure 4.13), indicating that oxidation did not take place in the system. However, the pH decreased swiftly within 1 min from 8.0 to 7.94 after adding $KMnO_4$ solution to the water containing Mn^{2+} and Fe^{2+}. They were obviously eradicated below the MCL within 1 min, even though pH decreased only slightly. The decrease of pH during adsorption was done by Corami, Mignardi, and Ferrini (2008).
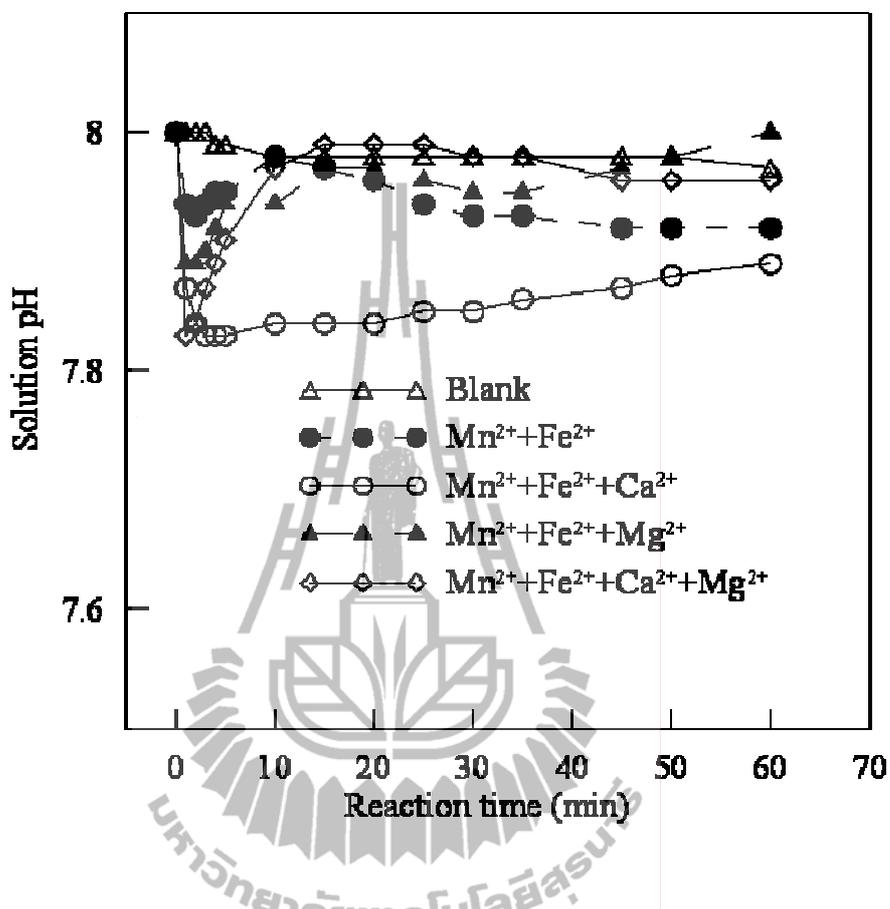
Figure 4.13 Removal efficiency of Mn^{2+} in dual Mn^{2+} and Fe^{2+} oxidation by $KMnO_4$

and solution pH in different compositions. The oxidant dose was 0.603

mg/L and stirring speed was 120 rpm.
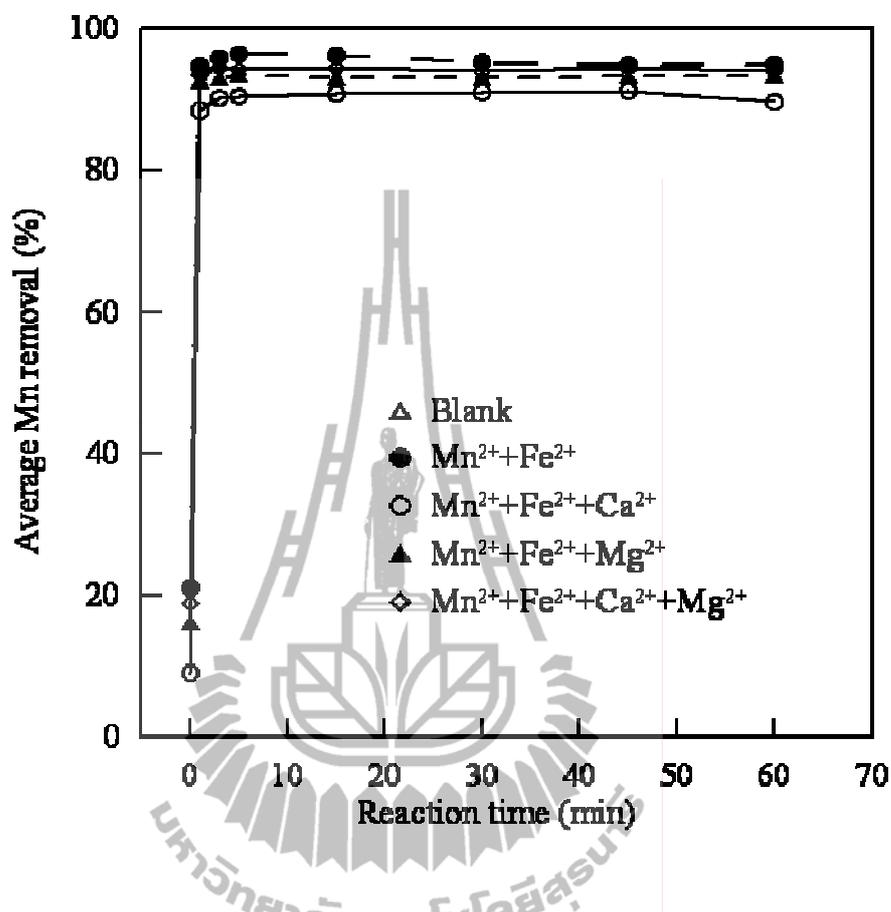
Figure 4.14 Removal efficiency of Mn^{2+} in dual Mn^{2+} and Fe^{2+} oxidation by $KMnO_4$

and solution pH in different compositions. The oxidant dose was 0.603

mg/L and stirring speed was 120 rpm.
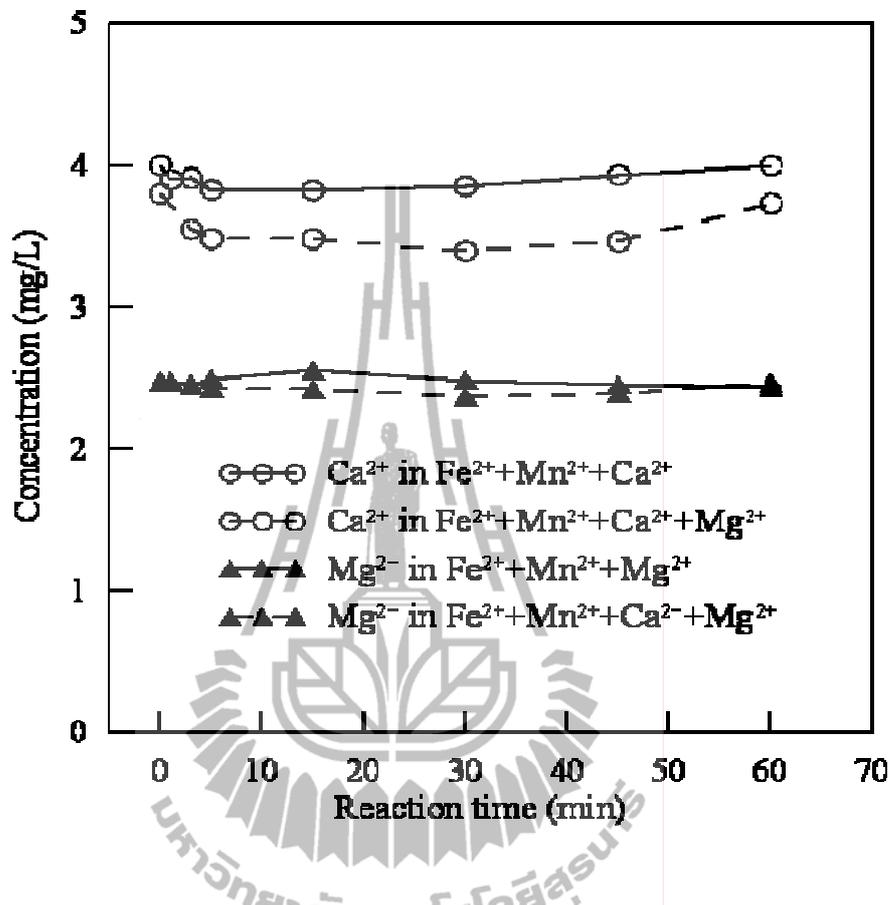
Figure 4.15 Concentration of Mg^{2+} and Ca^{2+} from dual Mn^{2+} and Fe^{2+} oxidation by

KMnO$_4$ in different compositions. The oxidant dose was 0.603 mg/L

and stirring speed was 120 rpm.

The possible mechanism includes oxidation of Mn^{2+} and Fe^{2+} (Eq. 2.1 and

Eq. 2.2) and sorption of the dissolved metal ions (Mn^{2+} and Fe^{2+}) by the hydrous

precipitates which is considered based on conventional reactions of surface hydroxyl

group (Zaw and Chiswell, 1999; Davranche and Bollinger, 2000, Davis and Leckie,

1978).

In the first mechanism, MnO_4^- reacts rapidly with Mn^{2+} and Fe^{2+}, and produces MnO_2, $Fe(OH)_3$ and H^+ to water (Eq. 2.1 and Eq. 2.2) causing the pH drop. The percent removal of Mn^{2+} increased quickly and reached 98% in 1 min and then became constant after 5 min. The result indicated that the oxidation using aeration and 0.603 mg/L $KMnO_4$ effectively removed Mn^{2+} to the level below the MCL in a shorter time and less concentration of $KMnO_4$ compared to other works. For example, Roccaro, Barone, Mancini, and Vagliasindi (2007) obtained a 95% removal of Mn^{2+} in 90 min after oxidation with $KMnO_4$ at pH 8.5 and an initial Mn concentration of about 1.80 mg/L. Zogo et al. (2011) obtained a complete removal of Mn^{2+} and Fe^{2+} which were monitored after 24 h sampling using alum dose of 40 mg/L at pH 6.5 and $KMnO_4$ dose of 2.5 mg/L at pH 8.5.

The second mechanism involves sorption of metal ions with hydrous metal oxide. A bond is initially formed between the Mn^{2+} and the surface oxygen atom of the hydrous Mn-Fe oxide, resulting in the release of protons and a drop in pH as shown in Eq. 4.5 (Buamah et al., 2008). In this study, the test was done in alkaline condition, the surface is predominantly negative charged according to the surface charge of Mn-Fe precipitates and then the surface becomes more attractive to cations (Buamah et al., 2008).

$$\equiv \text{(Mn-Fe)-OH} + M^{2+} + H_2O \quad \rightarrow \quad \equiv \text{(Mn-Fe)-O-M-O}^- + 3H^+ \tag{4.5}$$

where M is denoted as divalent ions, Mn^{2+}, Fe^{2+}, Ca^{2+} and Mg^{2+}

With coexisting Ca^{2+} and Mg^{2+} ions (Figure 4.14), the average Mn^{2+} removal have similar values in all system. However, solution pH was most basic in the absence of Ca^{2+} and Mg^{2+}. This indicates that either Ca^{2+} or Mg^{2+} could have

exchanged places with H^+ attached on Mn-Fe precipitate, releasing H^+ back into the solution. This result did not affect the removal of Mn^{2+} and Fe^{2+} as their concentrations were still below the MCL (Figure 4.14). The trend of pH decreases depended on the metal composition in the reaction. Solution pH of a solution with coexisting Ca^{2+} obviously decreased more than that with Mg^{2+}. This implied that the presence of Ca^{2+} increased surface charge of the precipitates and slightly disturbed the removal efficiency more than Mg^{2+}.

As presented in Figure 4.15, concentrations of Ca^{2+} and Mg^{2+} decreased immediately after adding $KMnO_4$ accompanied with the decreased solution pH. Finally, their concentration was slightly recovered within 60 min. These results validate that mechanism of sorption of Ca^{2+} and Mg^{2+} onto hydrous oxide in exchange with the bound H^+. However, Ca^{2+} and Mg^{2+} could be released back into the solution since they are weakly held by the oxygen groups of the oxide precipitate (Zoller, 1994). In addition, the result could be attributed to the reversible formation of $CaCO_3$ and $MgCO_3$ under these conditions.

However, these evidences on the possible mechanisms were not much clear that Mn^{2+} ions can be removed both oxidation by aeration-$KMnO_4$ and sorption on the hydrous oxide. The former pathway, oxidation reaction, would be a majority mechanism for the dual removal in this study. However, sorption of non-biodegradable metal like Cd^{2+} on the hydrous Mn-Fe oxide was further expected to investigate.

4.4 Conclusions

The dual removal of Mn^{2+} and Fe^{2+} from synthetic groundwater via oxidation using combined aeration and $KMnO_4$ was investigated under various studied parameters. The partial removal of Mn^{2+} using aeration was 30.6% and 37.2% for single and dual system, respectively. Aeration decreased the consumption of $KMnO_4$ needed for the dual oxidation. The minimum concentration of $KMnO_4$ was 0.603 mg/L, which can quickly oxidize Mn^{2+} below its MCL. The presence of Fe^{2+} improved the removal of Mn^{2+} due to the autocatalytic effect of hydrous Mn-Fe oxides. Characterization using digital microscope and EDX proved the formation of the oxides. The presence of Ca^{2+} and Mg^{2+} as well as alum addition slightly inhibited the removal of Mn^{2+}. The possible removal mechanism of Mn^{2+} and Fe^{2+} are oxidation and adsorption onto the oxide precipitate.

4.5 References

Berbenni, P., Pollice, A., Canziani, R., Stabile, L. and Nobili, F. (2000). Removal of iron and manganese from hydrocarbon-contaminated groundwaters. **Bioresource Technology**. 74: 109-114.

Buamah, R., Petrusevski, B. and Schippers, J. C. (2008). Adsorptive removal of manganese (II) from the aqueous phase using iron oxide coated sand. **Journal of Water Supply: Research and Technology-AQUA**. 57.1: 1-11.

Corami, A., Mignardi, S. and Ferrini, V. (2008). Cadmium removal from single- and multi-metal (Cd+Pb+Zn+Cu) solution by sorption on hydroxyapatite. **Journal of Colloid Interface Science**. 317: 402-408.

Crimi, M. L. and Siegrist, R. L. (2004). Association of cadmium with MnO_2 particles generated during permanganate oxidation. **Water Research**. 38: 887-894.

Davis, J. A. and Leckie, J. O. (1978). Surface ionization and complexation at the oxide/water interface II. Surface properties of amorphous iron oxyhydroxide and adsorption of metal ions. **Journal of Colloid and Interface Science**. 67: 90-107.

Davranche, M. and Bollinger, J-C. (2000). Heavy metals desorption from synthesized and natural iron and manganese oxyhydroxides: effect of reductive conditions. **Journal of Colloidal and Interface Science**. 227: 531-539.

El Araby, R., Hawash, S. and El Diwani, G. (2009). Treatment of iron and manganese in simulated groundwater via ozone technology. **Desalination**. 249: 1345-1349.

Guan, X., Ma, J., Dong, H. and Jiang, L. (2009). Removal of arsenic from water: Effect of calcium ions on As (III) removal in the $KMnO_4$-Fe (II) process. **Water Research**. 43: 5119-5128.

Lehr, J. H., Hyman, M., Seevers, W. J. and Gass, T. (2002). Handbook of complex environmental remediation problems. U.S.A.: McGraw-Hill. p. 101.

Liu, R., Liu, H., Qiang, Z., Qu, J., Li, G. and Wang, D. (2009). Effect of calcium ions on surface characteristics and adsorptive properties of hydrous dioxide. **Journal of Colloid and Interface Science**. 331: 275-280.

Loomer, D. B., Al, T. M., Banks, V. J., Parker, B. L. and Mayer, K. U. (2011). Manganese and trace-metal mobility under reducing conditions following in situ oxidation of TCE by $KMnO_4$: A laboratory column experiment. **Journal of Contaminant Hydrology**. 119: 13-24.

Masue, Y., Loeppert, R. H. and Kramer, T.A. (2007). Arsenate and arsenite adsorption and desorption behavior on co-precipitated aluminum: iron hydroxides. **Environmental Science and Technology**. 41: 837-842.

Montiel, A. and Welte, B. (1990). Manganese in water: Manganese removal by biological treatment. **Rev. Sci. Eau**. 3: 469-481.

Roccaro, P., Barone, C., Mancini, G. and Vagliasindi, F. G. A. (2007). Removal of manganese from water supplied intended for human consumption: a case study. **Desalination**. 210: 205-214.

Takeno, N. (2005). **Atlas of Eh-pH diagrams: Intercomparison of thermodynamic databases**. Geological surveys of Japan open file report No. 419.

Wolthoorn, A., Temminghoff, E. J. M., Weng, L. and Riemsdijk, W. H. V. (2004). Colloid formation in groundwater: effect of phosphate, manganese, silicate and dissolved organic matter on the dynamic heterogeneous oxidation of ferrous iron. **Applied Geochemistry**. 19: 611-622.

Zaw, M. and Chiswell, B. (1999). Iron and manganese dynamics in lake water. **Water Research**. 33: 1900-1910.

Zogo, D., Bawa, L. M., Soclo, H. H. and Atchekpe, D. (2011). Influence of pre-oxidation with potassium permanganate on the efficiency of iron and manganese removal from surface water by coagulation-flocculation using aluminium sulphate: case of the Okpara dam in the Republic of Benin. **International of Environmental Chemistry and Ecotoxicology**. 3: 1-8.

Zoller, URI. (1994). **Groundwater Contamination and Control**. New York, U.S.A.: Marcel Dekker. pp. 135, 246-247.
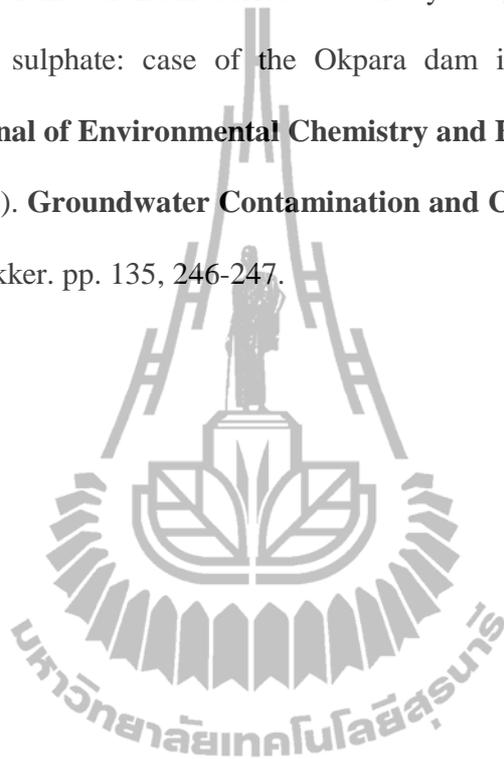
CHAPTER V

REMOVAL OF MANGANESE, IRON AND CADMIUM IONS FROM SYNTHETIC GROUNDWATER BY OXIDATION USING POTASSIUM PERMANGANATE

Abstract

Removal of triple Mn^{2+}, Fe^{2+} and Cd^{2+} ions from synthetic groundwater by oxidation using aeration and $KMnO_4$ to keep their concentrations to the level below the MCL was examined in batch experiments in a Jar test. The studied conditions included pH of 8.0 and various oxidant doses, initial Cd^{2+} concentrations, and coexisting Ca^{2+} and Mg^{2+} ions. The percent removal of Mn^{2+}, Fe^{2+} and Cd^{2+} ions by aeration were 14.2, 88.4 and 10.0%, respectively. The $KMnO_4$ dose of 0.824 mg/L was an optimum amount to eliminate those metal ions concentration to the level below the MCL. The initial Cd^{2+} concentration of 0.05 mg/L was a maximum adsorption capacity of the Mn-Fe oxide. The coexisting Ca^{2+} and/ or Mg^{2+} did not disturb the elimination of Mn^{2+} and Cd^{2+}. The removal mechanism of Cd^{2+} could involve sorption with the hydrous Mn-Fe oxide.

5.1 Introduction

In Chapter IV, dual removal of Mn^{2+} and Fe^{2+} from synthetic groundwater by oxidation using aeration and $KMnO_4$ was investigated. The result showed that the oxidation reaction using $KMnO_4$ is a major mechanism in the removal of Mn^{2+} and Fe^{2+}. The presence of Fe^{2+} improved the removal of Mn^{2+} due to the co-precipitation of Mn^{2+} onto hydrous manganese-iron oxide. However, the co-precipitation was still not clear that Mn^{2+} ions can be eliminated both oxidation by aeration-$KMnO_4$ and co-precipitation on the hydrous oxide. However, sorption of Cd^{2+} on the hydrous oxide was further investigated in this chapter.

Cadmium (Cd) is almost exclusively found as Cd^{2+} ion which is a highly toxic environmental pollutant. It enters into groundwater either by natural means or through anthropogenic activities such as residual sludge and manure, fertilizers, plating and galvanizing industries (Spring, 2010). Distribution of Cd^{2+} depends on the type of natural groundwater and conditions such as pH and ORP (Evanko and Dzombak, 1997; Takeno, 2005).

Concentration of Cd^{2+} in groundwater has been reported as shown in Table 5.1. Its concentration is higher than the MCL allowed in drinking water. Cd^{2+} and its compounds are extremely toxic even at low concentration causing immediate poisoning and liver damage (Pandey, Verma, Choubey, Pandey, and Chandrasekhar, 2008). Therefore, a suitable treatment method of groundwater is essential to produce safe drinking water.

A wide variety of methods such as ion exchange (Wang and Fthenakis, 2005), adsorption (Yadanaparthi, Graybill, and Wandruszka, 2009), precipitation and co-

precipitation (Mauchauffee, Meux, and Schneider, 2008) have been proposed for removal of Cd^{2+} from aqueous solution. Among those, co-precipitation on mixed oxides such as clay minerals, iron and manganese oxides, and calcite has been widely employed to remove Cd^{2+} ions. In addition replacement of Ca^{2+} in $CaCO_3$ by other elements can occur to co-precipitation. For example, Cd^{2+} can diffuse into $CaCO_3$ and form cadmium carbonate ($CdCO_3$) (Selinus et al., 2005).

Based on the oxidation of Mn^{2+} and Fe^{2+} (Eq. 2.1 and Eq. 2.2), the generated MnO_2 and $Fe(OH)_3$ precipitates promised good adsorptive activity owing to their high surface areas and the active surface hydroxyl groups (-OH) (Peacock and Sherman, 2004; Parida, Mallick, Mohapatra, and Misra, 2004). Crimi and Siegrist (2004) noted that MnO_2 particles could adsorb and immobilize Cd^{2+}, although the degree of adsorption depended on conditions of water. For example, the amount of Cd^{2+} sorption was higher at neutral pH than low pH because of competition between H^+ and Cd^{2+} for the available adsorption sites. Likewise, the presence of Ca^{2+} in solution also resulted in lower degrees of Cd^{2+} adsorption. In this chapter, the oxidation of Mn^{2+} and Fe^{2+} by $KMnO_4$ and consequent adsorption or co-precipitation of Cd^{2+} on the precipitate oxide was proposed.

The aim of this study was to investigate removal of Mn^{2+}, Fe^{2+} and Cd^{2+} in synthetic groundwater using $KMnO_4$ as an oxidant. The synthetic groundwater was prepared to contain Mn^{2+}, Fe^{2+} and Cd^{2+} concentrations at 0.50, 0.50 and 0.01 mg/L. The oxidation by aeration was first investigated and the amount of oxidant, $KMnO_4$, for the remaining ions was determined. An optimum dose of $KMnO_4$ was studied to minimize the obstruction from the excessive amount of the oxidant. Studied

parameters included oxidant dose, initial Cd^{2+} concentration and effect of coexisting Ca^{2+} and/or Mg^{2+}. The removal mechanisms of the removal of Cd^{2+} with and without the coexisting ions were proposed by monitoring the pH variations. Particle charge was investigated by zeta potentiometer.

Table 5.1 Reported concentration of cadmium in natural groundwater.

Groundwater sources	Concentration (mg/L)	References
Saudi Arabia	0.006-0.037	Sadiq and Alum, 1997
Yucatan, Mexico	0.001-0.015	Spring, 2010
Logos, Nigeria	0.001-0.098	Momodu and Anyakora, 2010

5.2 Experimental

5.2.1 Chemicals

Deionized water with resistivity of 18.90 MΩ was produced by Ruda Ultrapure Water system. The chemicals employed were similar to those reported in Chapter III and IV, except an additional chemical, cadmium nitrate tetrahydrtate $(Cd(NO_3)_2 \cdot 4H_2O)$ which was obtained from Merck, Germany.

5.2.2 Experimental Methods

The synthetic groundwater was prepared with the method reported in Chapter III. Stock solutions of Mn^{2+} and Fe^{2+} ions with a concentration of 1000 mg/L were prepared from $MnCl_2 \cdot 4H_2O$ and $FeSO_4 \cdot 7H_2O$. A stock solution of Cd^{2+} with the concentration of 200 mg/L was prepared from $Cd(NO_3)_2 \cdot 4H_2O$. For the study of coexisting Ca^{2+} and Mg^{2+} ions, stock solutions of Ca^{2+} and Mg^{2+} with a concentration

of 4000 (100 mM) and 2430 mg/L (100 mM) were prepared from $CaCl_2 \cdot 4H_2O$ and $MgCl_2 \cdot 4H_2O$, respectively.

5.2.3 Batch Study

The batch study was performed similarly to that in Chapter III. Control parameters included oxidant doses (0.603, 0.648, 0.824 and 0.878 mg/L), initial Cd^{2+} ion concentrations (0.01, 0.025, 0.05 and 0.10 mg/L) and existing of Ca^{2+} ion (4.0 mg/L), Mg^{2+} (2.43 mg/L) and combined Ca^{2+} and Mg^{2+}. The solution pH was controlled at 8.0±0.1 which was according to the average pH value of groundwater in Taiwan (Annual report in groundwater quality in Changhua Water Treatment Plant, Taichung, Taiwan, 2008). The initial concentrations of Cd^{2+}, Ca^{2+} and Mg^{2+} ion were added according to the typical amount found in the natural groundwater (Nishimura and Umetsu, 2001; Hui, 2006). The reaction was investigated with total retention time of 60 min. The mixture was sampled every 15 min and separated by filtration with a 0.45 μm membrane. Each experiment was repeated three times and the results were averaged.

5.2.4 Effect of oxidant dose

To study an optimum dose of $KMnO_4$ reducing the Mn^{2+}, Fe^{2+} and Cd^{2+} in the synthetic groundwater to the level below the MCL, the experiments were performed using different doses of $KMnO_4$, 0.603, 0.648, 0.824 and 0.878 mg/L. The oxidant doses of 0.603 and 0.648 mg/L were calculated according to the residual concentration of a single Mn^{2+} system (0.314 mg/L) and dual Mn^{2+} (0.314 mg/L) + Fe^{2+} (0.048 mg/L) ions, respectively, after dual oxidation of Mn^{2+} and Fe^{2+} by aeration. The doses of 0.824 and 0.878 mg/L were calculated according to the

remaining amount of Mn^{2+} alone (0.429 mg/L) and Mn^{2+} (0.429 mg/L) + Fe^{2+} (0.058 mg/L) ions, respectively, after the oxidation of Mn^{2+}, Fe^{2+} and Cd^{2+} by aeration.

5.2.5 Effect of initial Cd^{2+} concentration

As shown in Table 5.1, the concentration of Cd^{2+} in natural groundwater is fluctuated, thus sorption of Cd^{2+} with different initial concentrations, 0.010, 0.025, 0.050 and 0.100 mg/L was studied.

5.2.6 Effect of coexisting ions

The concentrations of the coexisting ions were: Ca^{2+}, 4.0, 40.0 and 400.0 mg/L; Mg^{2+}, 2.4, 24.3 and 243.0 mg/L. These wide concentration ranges were studied because the amount of Ca^{2+} and Mg^{2+} are normally fluctuated depending on conditions in natural groundwater (Orzepowski and Pulikowski, 2008; Cotruvo and Bartram, 2009).

5.2.7 Characterization

The residual metal ions in the synthetic groundwater including Mn^{2+}, Fe^{2+} and Cd^{2+} were determined using ICP-OES (Perkin Elmer DV 2000). The procedures of the analysis were done similarly to those in Chapter III. An ORP was recorded using an ORP meter (ORP 5041, Rocker).

To determine the surface charge of the precipitates, the colloidal solution produced during the reaction was collected after 60 min of the reaction and analyzed by Zeta potentiometer (Zetasizer Nano-ZS, Malvern Instrument).

5.3 Results and discussion

5.3.1 Effect of aeration

Aeration of synthetic groundwater containing Mn^{2+}, Fe^{2+} and Cd^{2+} ions was initially investigated and the results are presented in Figure 5.1. The removal of Mn^{2+} was consistently eradicated about 18% (0.429 mg/L remaining amount), while it was about 40% in dual Mn^{2+} and Fe^{2+} oxidation (see in Chapter IV). The removal of Fe^{2+} in the system containing Mn^{2+}, Fe^{2+} and Cd^{2+} was about 88% (0.058 mg/L remaining amount). This result indicated that Cd^{2+} ion could obstruct the removal of Mn^{2+} while its removal at 10% (0.009 mg/L remaining amount) was still above the MCL. Cd^{2+} could be eliminated by adsorption or co-precipitation during the aeration (Wolthoorn, Temminghoff, Weng, and Riemsdijk, 2004). However, active sites of the produced Mn-Fe precipitates were not suitable to efficiently remove Mn^{2+} and Cd^{2+} ions below the allowed level. Consequently, low-aeration combined with $KMnO_4$ is necessary to conduct to removal of Mn^{2+} and Cd^{2+}.
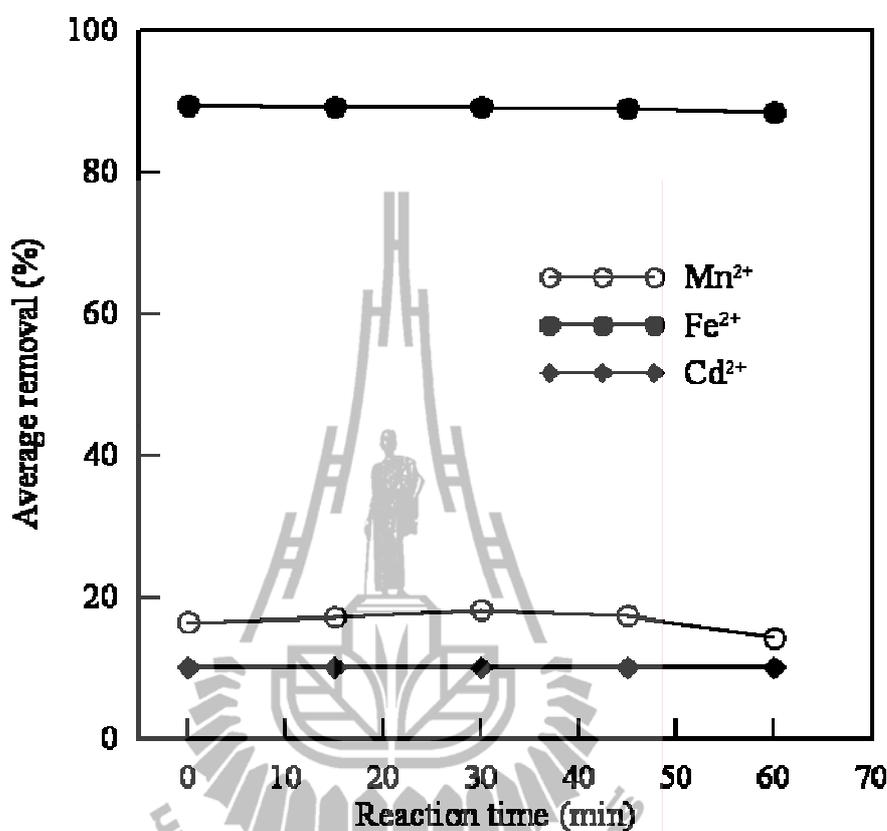
Figure 5.1 Average removal of Mn^{2+}, Fe^{2+} and Cd^{2+} from the synthetic groundwater

by aeration. The concentration of Mn^{2+}, Fe^{2+} and Cd^{2+} was 0.50, 0.05 and

0.01 mg/L, respectively; pH 8.0; stirring speed 120 rpm.

5.3.2 Effect of aeration-oxidant dose

Oxidation of the remaining Mn^{2+}, Fe^{2+} and Cd^{2+} ions by a minimum dose

of $KMnO_4$ was studied. The percent removal of Mn^{2+} and Cd^{2+} ions are reported in

Fig 5.2. At 0.603 mg/L $KMnO_4$ and 15 min, the remaining concentration of Mn^{2+}

(0.073 mg/L 85.4% conversion, Figure 5.2a) and Cd^{2+} (0.007 mg/L, 30% conversion,

Figure 5.2b) were still higher than the MCL values. The removal efficiencies of Mn^{2+}

and Cd^{2+} increased about 66 and 20%, respectively, from those of the oxidation by aeration. The result indicated that the oxidation by $KMnO_4$ effectively removed Mn^{2+} and Cd^{2+}. Considering only Mn^{2+} ion, the percent removal was lower than that of the dual Mn^{2+}-Fe^{2+} oxidation (see in Chapter IV), indicating that the existence of Cd^{2+} competed with the co-precipitation of Mn^{2+} ion by the forming oxides (Zaman, Mustafa, Khan, and Xing, 2009).

At 0.648 mg/L $KMnO_4$ after 15 min, the remaining concentration of Mn^{2+} (0.055 mg/L, 89% conversion, Figure 5.2a) and Cd^{2+} (0.006 mg/L, 40% conversion, Figure 5.2b) were still higher than the MCL. With increasing the oxidant doses, their removal efficiencies increased about 4 and 10%, respectively higher than those of the oxidation with 0.603 mg/L $KMnO_4$. The result could be ascribed to the different fractions of Mn and Fe oxidized by $KMnO_4$ and the properties of Mn-Fe precipitates formed in situ under different conditions. In this case, the increase of $KMnO_4$ dose increased the fraction of the Mn-Fe precipitates. As reported by Guan, Ma, Dong, and Jiang (2009), the increase of $KMnO_4$ doses enhanced the fraction of Fe in the precipitates produced during $KMnO_4$-Fe^{2+} oxidation which could further improve removal of As^{3+}.
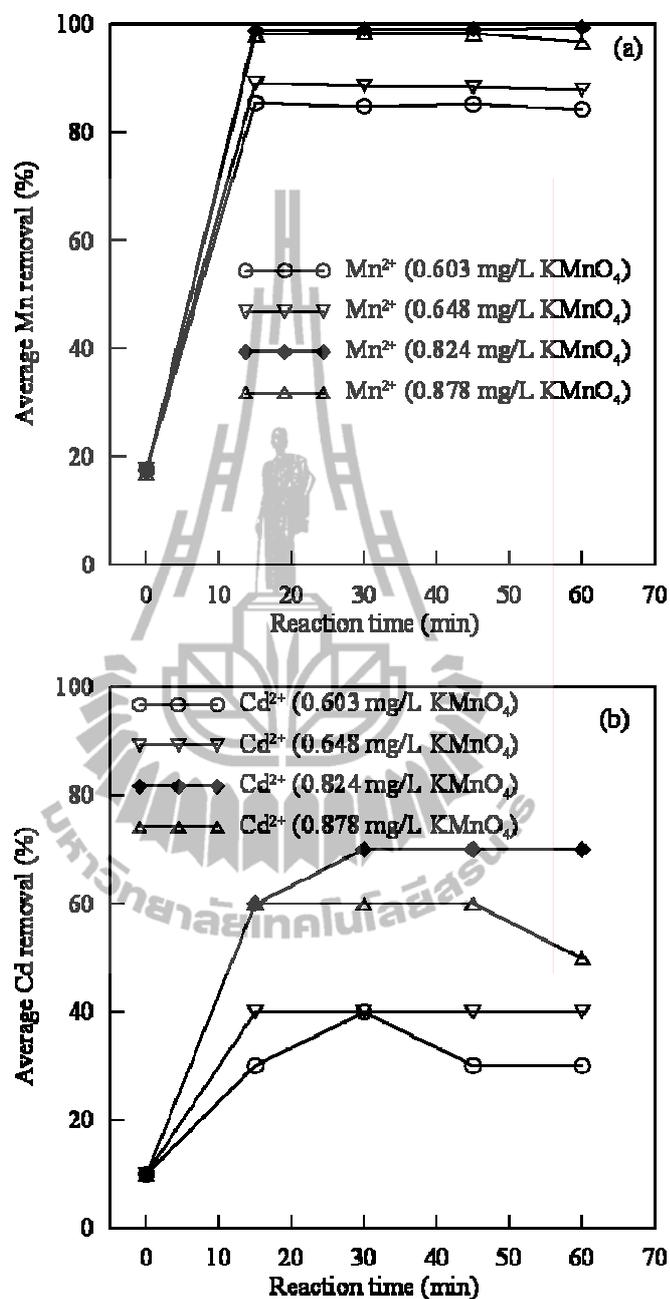
Figure 5.2 Average removal of (a) Mn^{2+} and (b) Cd^{2+} from the synthetic groundwater

by $KMnO_4$. The concentration of Mn^{2+}, Fe^{2+} and Cd^{2+} was 0.50, 0.05 and

0.01 mg/L, respectively; pH 8.0; stirring speed 120 rpm.

Because the doses of 0.603 and 0.648 mg/L $KMnO_4$ were insufficient to oxidize Mn^{2+} in these experimental conditions, the higher doses of $KMnO_4$ were applied to reduce Mn^{2+}, Fe^{2+} and Cd^{2+} ions concentration to the level below the MCL.

At 0.824 mg/L $KMnO_4$, the removal efficiencies of Mn^{2+} (99% conversion, Figure 5.2a) and Cd^{2+} (70% conversion, Figure 5.2b) reached the requirement of the MCL within 15 min where the remaining amount of those ions were 0.005 mg/L and 0.003 mg/, respectively.

At 0.878 mg/L $KMnO_4$, the removal efficiencies of Mn^{2+} (99% conversion, Figure 5.2a) and Cd^{2+} (60% conversion, Figure 5.2b) were achieved the MCL in 15 min where the remaining amount of those ions were 0.005 mg/L and 0.004 mg/L, respectively. After 45 min, removal efficiency of Cd^{2+} decreased about 10% from that in the 0.824 mg/L $KMnO_4$. The excess amount of permanganate probably disturbs the removal of Cd^{2+} ion. Also, Cd^{2+} had weak interaction with the oxide and it could be released back to the water (Czupyrna, Maclean, Levy, and Gold, 1989). However, the overloaded $KMnO_4$ did not interfere the removal efficiency of Mn^{2+} ion because it was completely eliminated.

From the results above, the optimum dose of $KMnO_4$ to eliminate Mn^{2+}, Fe^{2+} and Cd^{2+} ions to the levels below the allowed level was 0.824 mg/L. The sufficient oxidation of Mn^{2+} and Fe^{2+} by $KMnO_4$ led to the effective co-precipitation of Cd^{2+} onto the Mn-Fe oxide.

5.3.3 Effect of initial Cd^{2+} concentration

Based on the above results, the oxidation of Mn^{2+} and Fe^{2+} ions by 0.824 mg/L $KMnO_4$ produced Mn-Fe oxides which could sorb Cd^{2+} ion. To investigate the

maximum capacity of the oxides on the sorption of Cd^{2+} ion, its initial concentration was varied between 0.01 and 0.10 mg/L using 0.824 mg/L $KMnO_4$ and pH 8.0. The results are illustrated in Table 5.2. The complete removal of Mn^{2+} ion was observed in all cases. When the initial concentration was 0.01 and 0.025 mg/L, Cd^{2+} was removed to the level below the MCL. At 0.05 and 0.10 mg/L, the remaining concentration of Cd^{2+} was still higher than the permitted level. The results indicated that the surface saturation of the forming Mn-Fe oxides was dependent on the initial Cd^{2+} concentrations. At low concentrations, 0.01 and 0.025 mg/L, sorption sites took up the available Cd^{2+} more quickly. However, at higher concentrations, the sorption sites would be limited for Cd^{2+} due to the saturation of the Mn-Fe oxide. Similar result was reported by Xu, Yang, and Yang. (2010) who studied removal of Cd^{2+} in water by manganese coagulant prepared from $KMnO_4$ and $Na_2S_2O_3$. The removal increased with the increase of the initial concentration, less than 0.8 mg/L. With increase the concentration, the removal efficiency decreased because of the saturation of the binding sites.

From the result above, the maximum removal efficiency of Cd^{2+} was 92% with the initial concentration of 0.025 mg/L. The result supported the hypothesis that the sorption of Cd^{2+} on the Mn-Fe oxide took place.

Table 5.2 Remaining concentration and average removal of Mn^{2+} and Cd^{2+} with different initial concentrations of Cd^{2+}. The concentration of Mn^{2+} and Fe^{2+} was 0.50 and 0.50 mg/L, respectively; 0.824 mg/L $KMnO_4$; pH 8.0; stirring speed 120 rpm.

Initial Cd^{2+} concentration (mg/L)	Mn^{2+}		Cd^{2+}	
	Remaining concentration (mg/L)	Average removal (%)	Remaining concentration (mg/L)	Average removal (%)
0.01	0	100	0.003	70
0.025	0	100	0.002	92
0.05	0	100	0.005	90
0.10	0	100	0.009	91

5.3.4 Effect of coexisting Ca^{2+} and Mg^{2+}

The influence of Ca^{2+} and Mg^{2+} ions in the synthetic groundwater on the removal of Mn^{2+}, Fe^{2+} and Cd^{2+} was studied using the oxidant dose of 0.824 mg/L $KMnO_4$ and pH 8.0. As reported in Chapter VI, the coexisting ions slightly disturb the removal of Mn^{2+}. Thus, the minimum amount of Ca^{2+} (4.0 mg/L) and Mg^{2+} (2.43 mg/L) were employed. The average removals of Mn^{2+} and Cd^{2+} at 60 min are shown in Table 5.3.

Table 5.3 Remaining concentration and average removal of Mn^{2+} and Cd^{2+} with different coexisting ions. The concentration of Mn^{2+}, Fe^{2+}, Cd^{2+}, Ca^{2+} and Mg^{2+} was 0.50, 0.50, 0.01, 4.0 and 2.43 mg/L, respectively; 0.824 mg/L $KMnO_4$; pH 8.0; stirring speed 120 rpm.

Coexisting ions	Mn^{2+}		Cd^{2+}	
	Remaining concentration (mg/L)	Removal (%)	Remaining concentration (mg/L)	Removal (%)
Ca^{2+}	0	100	0.003	70
Mg^{2+}	0	100	0.002	80
$Ca^{2+}+ Mg^{2+}$	0	100	0.002	80

The result was similar to the dual Mn^{2+}-Fe^{2+} oxidation as reported in Chapter IV. Removal of Mn^{2+} was complete in 60 min with the coexisting Ca^{2+} and/ or Mg^{2+}, indicating that the coexisting ions did not obstruct to the removal of Mn^{2+}.

Removal of Cd^{2+} was 70%, similar to the condition without Ca^{2+}, meaning that the Ca^{2+} did not interfere the co-precipitation of Cd^{2+}. Besides, the removal was 80% for the conditions with coexisting Mg^{2+} and the both ions. The result can be explained that formation of calcium and/or magnesium carbonate precipitate in alkaline condition could entrap the residual ions such as As^{3+}, Mn^{2+} and Cd^{2+}.

In summary, the removal of Mn^{2+}, Fe^{2+} and Cd^{2+} by oxidation with 0.824 mg/L $KMnO_4$ could favorably produce Mn-Fe precipitates that could further sorb Cd^{2+} ion. They were removed even when Ca^{2+} and/or Mg^{2+} was co-existed.

5.3.5 Possible mechanisms of removal of Mn^{2+}, Fe^{2+} and Cd^{2+}

As proposed in Chapter IV on removal of Mn^{2+} and Fe^{2+} by aeration-$KMnO_4$, the predominant mechanism was the oxidation of Mn^{2+} and Fe^{2+}, while sorption of the remaining Mn^{2+} by the Mn-Fe oxides was not clear. Therefore, sorption between Cd^{2+} ion and the forming Mn-Fe oxides during the oxidation of Fe^{2+}, Mn^{2+} and Cd^{2+} by aeration-$KMnO_4$ was proven. The study was performed without pH adjustment with initial pH of 8.0 and 0.824 mg/L $KMnO_4$. For the coexisting ions, Ca^{2+} ion (4.0 mg/L) was selected because it behaved similarly to Mg^{2+} in this study. Variations of solution pH, ORP and average removal of each metal ion were recorded as shown in Figure 5.3.

Without Ca^{2+} (Figure 5.3a), the trend of pH after adding $KMnO_4$ was similar to dual Mn-Fe system. The possible mechanisms supported the dual removal of Mn^{2+} and Fe^{2+} as proposed in Chapter IV that the pathways included oxidation of Mn^{2+} and Fe^{2+} (Morgan and Stumm, 1964) and sorption of Cd^{2+} on the hydrous Mn-Fe precipitates (Zaw and Chiswell, 1999; Davis and Leckie, 1978). The details are as follows.

Firstly, permanganate reacted rapidly with Mn^{2+} and Fe^{2+} ions, and produced MnO_2, $Fe(OH)_3$ and H^+ (Eq. 2.1 and Eq. 2.2). These results were consistent with the decrease of Mn^{2+} and Fe^{2+} concentrations to the level below the MCL within 15 min and the increase of ORP from 254 mV to 300 mV. In addition, the pH of the

synthetic groundwater decreased rapidly after adding 0.824 mg/L $KMnO_4$. This result was reported by Corami, Mignardi, and Ferrini (2008) that the release of H^+ took place from the oxidation of Mn^{2+} and Fe^{2+} and the sorption between the $\equiv$ (Fe-Mn)-OH and Cd^{2+} according to Eq. 5.1.

$$\equiv \text{(Fe-Mn)-OH}_{(s)} + Cd^{2+}_{(aq)} + H_2O_{(l)} \leftrightarrow \equiv \text{(Fe-Mn)-O-Cd-O}^-_{(s)} + 3H^+_{(aq)} \qquad (5.1)$$

Secondly, the sorption of Cd^{2+} ion by the forming Mn-Fe precipitates could also occur, considering from the increased removal efficiency of Cd^{2+} and ORP values after adding $KMnO_4$. After 15 min, the oxidation of Mn^{2+} and Fe^{2+} was slow, which agreed the constant removal efficiencies of Mn^{2+} and Fe^{2+}, at the same time Cd^{2+} was constantly removed with 90% from 15 to 45 min and then dropped to 80%. This inferred that Cd^{2+} had weak interaction with the Mn-Fe oxide, similar to another report (Czupyrna et al., 1989). Besides, Selinus et al. (2005) reported that Cd^{2+} ions were not strongly retained on soil surfaces and they could be more readily available uptake by plants and is more easily leached down the soil than lead and copper.
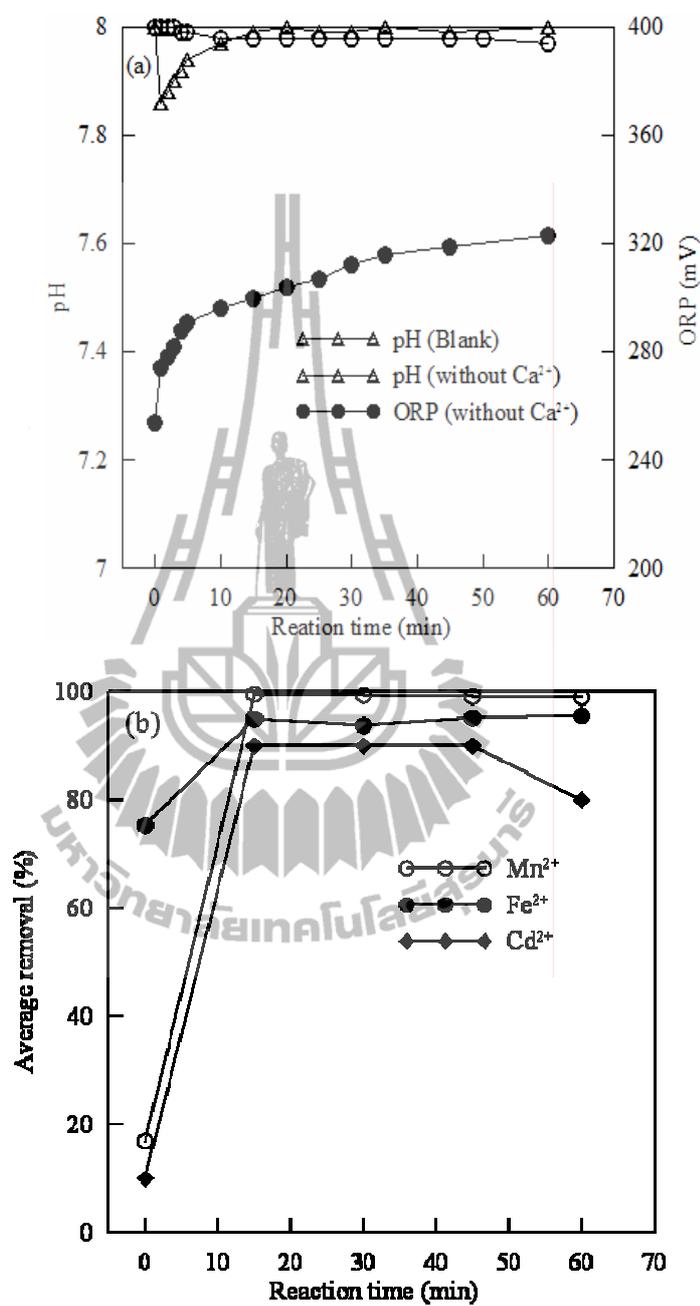
Figure 5.3 (a) Variations of pH and ORP, (b) average removal of Mn^{2+}, Fe^{2+} and Cd^{2+}

from the synthetic groundwater by 0.824 mg/L $KMnO_4$. The concentration of

Mn^{2+}, Fe^{2+} and Cd^{2+} was 0.50, 0.05 and 0.01 mg/L, respectively; pH 8.0;

stirring speed 120 rpm.

In the presence of coexisting Ca^{2+} (Figure 5.4), the average removals of Mn^{2+} and Cd^{2+} were similar to that without Ca^{2+}. A pH drop became lower than that in the condition without Ca^{2+} ion (Figure 5.4a). The results referred that ion exchange of Ca^{2+} ion and H^+ attached on the Mn-Fe oxide occurred, releasing additional H^+ ion to that from the oxidation (Buamah, Petrusevski, and Schippers, 2008). The ORP values increased from 340 to 370 mV. This result did not impede the removal efficiencies of Fe^{2+}, Mn^{2+} and Cd^{2+} (Figure 5.4b). For Ca^{2+} concentration, it gradually decreased, and then became constant within 15 min. This result indicated that few Ca^{2+} ions can bind with the precipitate without any displacement through the solution considering from the constant amount of Ca^{2+} and Cd^{2+}. However, there was a report that percent binding of Ca^{2+} on hydrous ferric oxide was higher than Cd^{2+} under alkaline condition (Stumm, Sigg, and Sulzberger, 1992). Thus, Ca^{2+} trends to be firstly interacted with the OH, and then released H^+ (Eq. 5.1). At the same time, Cd^{2+} would substitute Ca^{2+} ion and then release Ca^{2+} ion through the water.
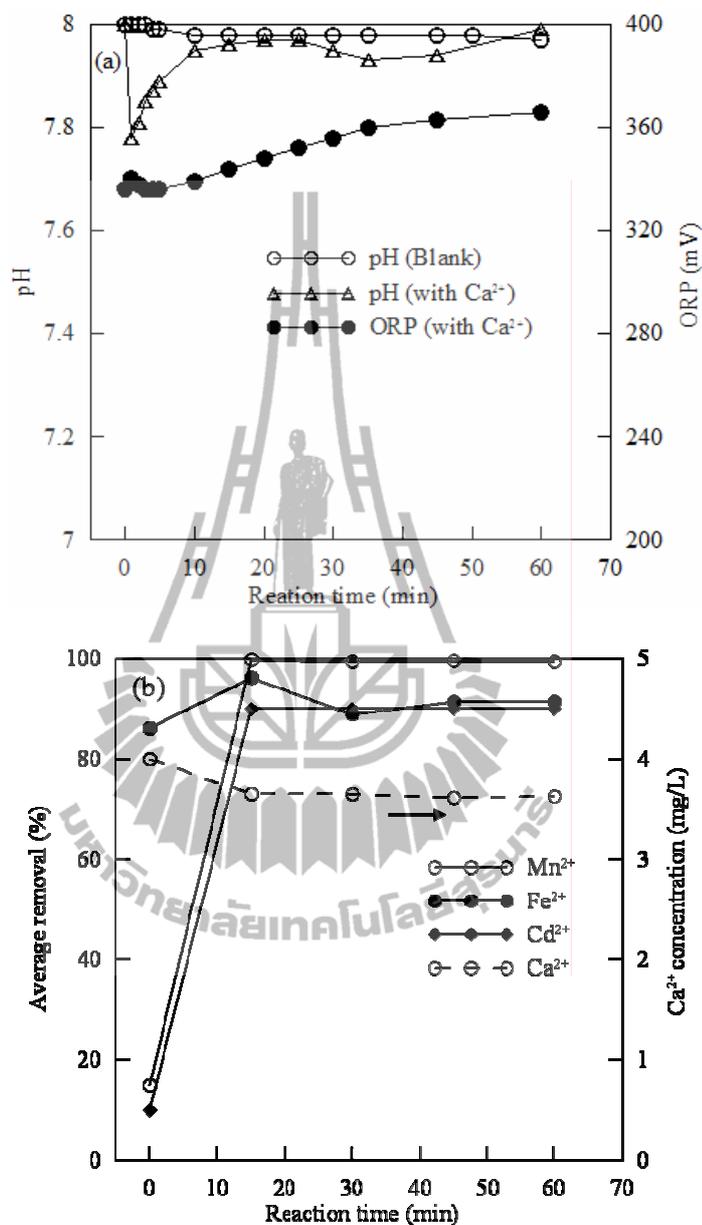
Figure 5.4 (a) Variations of pH and ORP, (b) average removal of Mn^{2+}, Fe^{2+} and Cd^{2+} from the synthetic groundwater by 0.824 mg/L $KMnO_4$. The concentration of Mn^{2+}, Fe^{2+} and Cd^{2+} was 0.50, 0.05 and 0.01 mg/L, respectively. The concentration of Ca^{2+} was 4.0 mg/L; pH 8.0; stirring speed 120 rpm.

The above results supported the proposed mechanisms on the removal of Mn^{2+} and Fe^{2+} ions in the dual system. Mn^{2+} and Fe^{2+} ions can be mainly eliminated by oxidation with $KMnO_4$ and Cd^{2+} ion was removed by sorption on the produced Mn-Fe precipitates.

5.4 Conclusions

The removal of Fe^{2+}, Mn^{2+} and Cd^{2+} from synthetic groundwater by combination of aeration and $KMnO_4$ was investigated. The removal by aeration alone was 18, 88 and 10%, respectively. The combination with $KMnO_4$ decreased their concentration to the level lower than the MCL. The contamination of Cd^{2+} resulted in higher $KMnO_4$ dose required. The Cd^{2+} concentration of 0.025 mg/L was the maximum sorption capacity for the Mn-Fe oxide. Our results supported a two step mechanism involved in the removal of Mn^{2+}, Fe^{2+} and Cd^{2+} by $KMnO_4$. Mn^{2+} and Fe^{2+} were mainly removed by oxidation reaction with $KMnO_4$, and Cd^{2+} could be eliminated by sorption of Cd^{2+} on the Mn-Fe oxides. The coexisting Ca^{2+} or Mg^{2+} did not disturb the elimination of the metal ions.

5.5 References

Alloway, B. (2005). Bioavailability of elements in soil. In Selinus, O., Alloway, B., Centeno, J. A., Finkelman, R. B, Fuge, R., Lindh, U., and Smedley, P. (2005). **Essentials of Medical Geology: Impact of the natural environment on public health**. U.S.A.: Elsevier. p.361.

Annual report of groundwater quality in Changhua Water Treatment Plant, Taichung, Taiwan, 2008.

Buamah, R., Petrusevski, B. and Schippers, J. C. (2008). Adsorptive removal of manganese (II) from the aqueous phase using iron oxide coated sand. **Journal of Water Supply: Research and Technology-AQUA**. 57.1: 1-11.

Corami, A., Mignardi, S. and Ferrini, V. (2008). Cadmium removal from single- and multi-metal (Cd+Pb+Zn+Cu) solution by sorption on hydroxyapatite. **Journal of Colloid Interface Science**. 317: 402-408.

Cotruvo, J. and Bartram, J. (2009). **Calcium and Manganese in Drinking Water: Public health significance**. Geneva, Switzerland: World Health Organization. pp. 37-56.

Crimi, M. L. and Siegrist. R. L. (2004). Association of cadmium with MnO2 particles generated during permanganate oxidation. **Water Research**. 38: 887-894.

Czupyrna, G., Maclean, A. I., Levy, R. D. and Gold, H. (1989). In situ immobilization of heavy-metal-contaminated soils. **Pollution Technology Review**. No. 173, p. 27.

Davis, J. A. and Leckie, J. O. (1978). Surface ionization and complexation at the oxide/water interface II. Surface properties of amorphous iron oxyhydroxide and adsorption of metal ions. **Journal of Colloid and Interface Science**. 67: 90-107.

Evanko, C. R. and Dzombak, D. (1997). Remediation of metals-contaminated soild and groundwater, **Technology Evaluation Report, TE-97-01**, Ground-water Remediation Technologies Analysis Center. U.S.A. pp. 9-10.

Guan, X., Ma, J., Dong, H. and Jiang, L. (2009). Removal of arsenic from water: effect of calcium ions on As (III) removal in the $KMnO_4$-Fe (II) process. **Water Research**. 43: 5119-5128.

Hui, Y. H. (2006). **Handbook of Food Science, Technology, and Engineering**. U.S.A.: CRC Press. p. 58.

Liu, R., Liu, H., Qiang, Z., Qu, J., Li, G. and Wang, D. (2009). Effect of calcium ions on surface characteristics and adsorptive properties of hydrous dioxide. **Journal of Colloid and Interface Science**. 331: 275-280.

Mauchauffee, S., Meux, E. and Schneider, M. (2008). Selective precipitation of cadmium from nickel cadmium sulphate solutions using sodium decanoate. **Separation and Purification Technology**. 62: 394-400.

Momodu, M. A. and Anyakora, C. A. (2010). Heavy metal concentration of groundwater: the Surulere case study. **Research Journal Environmental and Earth Sciences**. 2: 39-43.

Morgan, J. J. and Stumm, W. (1964). Colloid-chemical properties of manganese dioxide. **Journal of Colloid and Science**. 19: 347-359.

Nishimura, T. and Umetsu, Y. (2001). Oxidative precipitation of arsenic (III) with manganese (II) and iron (II) in dilute acidic solution by ozone. **Hydrometallurgy**. 62: 83-92.

Orzepowski, W. and Pulikowski, K. (2008). Magnesium, calcium, potassium and sodium content in groundwater and surface water in arable lands in the commune (Gmina) of Kata Wroclawskie. **Journal of Elementol**.13: 605-614.

Pandey, P. K., Verma, Y., Choubey, S., Pandey, M. and Chandrasekhar, K. (2008). Biosorptive removal of cadmium from contaminated groundwater and industrial effluents. **Bioresource Technology**. 99: 4420-4427.

Parida, K. M., Mallick, S., Mohapatra, B. K. and Misra, V. N. (2004). Studies on manganese-nodule leached residues 1. Physicochemical characterization and its adsorption behavior toward Ni^{2+} in aqueous system. **Journal of Colloid and Science**. 277: 48-54.

Peacock, C. L. and Sherman, D. M. (2004). Copper (II) sorption onto goethite, hematite and lepidocrocite: A surface complexation model based on ab initio molecular geometries and EXAFS spectroscopy. **Geochemica et Cosmochimica Acta**. 68: 2623-2637.

Sadiq, M. and Alam. I. (1997). Metal concentrations in a shallow groundwater aquifer underneath petrochemical complex. **Water Research**. 31: 3089-3097.

Spring, U. O. (2010). Water resource in Maxico: scarcity, degradation, stress, conflicts, management and policy. **Hexagonal Series on Human and Environmental Security and Peace**. vol. 7. pp. 229-248.

Stumm, W., Sigg, L. and Sulzberger, B. (1992). **Chemistry of the solid-water interface: Process at the mineral-water and particle-water interface in natural system**. New York, U.S.A.: John Wiley and Sons.

Takeno, N. (2005). **Atlas of Eh-pH diagrams. Intercomparison of thermodynamic databases**. Geological surveys of Japan open file report No. 419.

Wang, W. and Fthenakis, V. (2005). Kinetics study on separation of cadmium from tellurium in acidic solution media using ion-exchange resins. **Journal of Hazardous Materials**. 125: 80-88.

Wolthoorn, A., Temminghoff, E. J. M., Weng, L. and Riemsdijk, W. H. V. (2004). Colloid formation in groundwater: effect of phosphate, manganese, silicate and dissolved organic matter on the dynamic heterogeneous oxidation of ferrous iron. **Applied Geochemistry**. 19: 611-622.

Xu, Y., Yang, L. and Yang, J. (2010). Removal of cadmium (II) from solutions by two kinds of manganese coagulants. **International Journal of Engineering, Science and Technology**. 2: 1-8.

Yadanaparthi, S. K. R., Graybill, D. and Wandruszka, R. V. (2009). Adsorbents for the removal of arsenic, cadmium, and lead from contaminated waters. **Journal of Hazardous Materials**. 171: 1-15.

Zaman, M. I., Mustafa, S., Khan, S. and Xing, B. (2009). Effects of phosphate complexation on Cd^{2+} sorption by manganese oxide (β-MnO_2). **Journal of Colloid and Interface Science**. 330: 9-19.

Zaw, M. and Chiswell, B. (1999). Iron and manganese dynamics in lake water. **Water Research**. 33: 1900-1910.

CHAPTER VI

MEMBRANE FOULING AND CLEANING IN PVDF MICROFILTRATION OF PRECIPITATES OF MANGANESE AND IRON FROM OXIDATION BY POTASSIUM PERMANGANATE

Abstract

This chapter focuses on separation of the Mn-Fe oxide precipitates by PVDF membrane with a nominal pore size of 0.30 μm. The process involved aeration and addition of $KMnO_4$ in a synthetic groundwater containing Mn^{2+}, Fe^{2+} and Cd^{2+} with the concentration of 0.50, 0.50 and 0.01 mg/L, respectively. The resulting precipitates were separated by dead-end PVDF microfiltration with pressures of 20, 35 and 50 kPa. Theoretical models were used to fit the flux obtained to propose the possible membrane fouling mechanisms. The types of membrane fouling could be a mixed blocking mechanism of the pores taken place with the predominance of cake filtration. The Mn-Fe oxide particles accumulated on the membrane were removed by several cleaning methods including backwashing, ultrasound and their combined methods. Cleaning by ultrasound for 1 min was the most effective method giving a maximum flux recovery of nearly 92% but its efficiency decreased with cleaning cycle. The combined methods did not improve the flux recovery.

6.1 Introduction

The removal of Mn^{2+}, Fe^{2+} and Cd^{2+} from synthetic groundwater by oxidation using aeration and $KMnO_4$ was reported in Chapter V. The appropriate conditions including pH, oxidant dose and stirring speed to remove Mn^{2+}, Fe^{2+} and Cd^{2+} to the level below MCL were obtained. Suspension of Mn-Fe oxide generated after the oxidation was further separated by microfiltration (MF) based on water purification process (American Water Work Association, 2002).

MF technology has recently become popular in groundwater treatment because it can effectively separate colloidal and suspended particles in the range of 0.05 to 10 µm. It closely resembles conventional coarse filtration or sieving (Nath, 2008). MF is an alternative method to solve the problems of using sand filtration in which excessive amount of precipitates tend to shorten filtration cycles. Besides, the filterability of Mn-Fe oxides is poor and process control may become difficult with raw water variations (Chae, Yamamura, Ijeda, and Watanabe, 2008).

There are two disadvantages of using MF in groundwater treatment. First, it is not able to remove dissolved inorganic species such as Mn^{2+}, Fe^{2+} and Cd^{2+} directly but it exhibits good removal of oxidized inorganic species suspended in water (American Water Work Association, 2005; Adham, Chiu, Gramith, and Oppenheimer, 2005). Second, a long operation of MF for groundwater treatment results in loss of performance of a membrane due to deposition of suspended or dissolved substances on its external surface, at pore openings, or within pores. Eventually, membrane replacement is unavoidable, resulting in an increase in production cost of drinking

water. To solve the drawbacks, a combined chemical oxidation and MF was employed.

In previous works, a bench- and pilot-scale testing for removal of Mn^{2+} and Fe^{2+} by chemical oxidation followed by MF showed promising results. Schneider, Johns, and Huehmer (2001) studied removal of Mn^{2+} and Fe^{2+} from surface water using pre-oxidation with $KMnO_4$ or $NaClO$ followed by MF. For $KMnO_4$-MF, the removal efficiency of Mn^{2+} and Fe^{2+} was 70 and 98%, respectively, while it was 29 and 98% for $NaClO$-MF. Chen et al. (2011) investigated removal of Mn^{2+} and Fe^{2+} from groundwater using aeration, chlorine oxidation and MF. The removal efficiency of Mn^{2+} was 98% in 2 weeks. However, long operation of MF results in severe membrane fouling and a decrease of permeate flux.

Several cleaning methods were investigated to reduce membrane fouling including backwashing (BW) with deionized (DI) water or air (Levesley and Hoare, 1999), sonication (Lim and Bai, 2003), chemical cleaning (Zhang and Liu, 2003) and a combination of the various cleaning methods (Lim and Bai, 2003). Among those methods, chemical cleaning gives some drawbacks such as generation of new waste solutions, high costs, operational aspects of chemical supply and handling problems. Membrane cleaning with BW of fouled Mn-Fe oxides was previously investigated (Chen et al., 2011) but there were no reports on membrane cleaning with ultrasound (US) and the combined BW and US.

The aim of this part was to study membrane fouling and cleaning efficiency of dead-end PVDF microfiltration fouled by Mn-Fe oxides which were oxidized by $KMnO_4$. The synthetic groundwater consisted of Mn^{2+}, Fe^{2+} and Cd^{2+} with a

concentration of 0.5, 0.5 and 0.01 mg/L, respectively. The possible mechanism on membrane fouling was proposed by pore block models. Several cleaning methods including BW, US and their combined methods were evaluated. Digital microscopy was employed to examine morphology of the membrane.

6.2 Preparation of water with precipitates

The chemicals and experimental methods were performed similarly to those reported in Chapter V. A 6.0-L of Mn-Fe oxide suspension was prepared in a polypropylene tank reactor with total volume of 12.75 L instead of a Jar test. The pH was fixed at 8.0 and the reaction time was 60 min. The concentrations of remaining metal ions including Mn^{2+}, Fe^{2+} and Cd^{2+}, analyzed by ICP-OES, were below the MCL (0.05, 0.30 and 0.005 mg/L, respectively).

6.3 Microfiltration experiment

A dead-end MF unit was set up as shown in Figure 6.1. This setup comprised of a water reservoir tank, a MF unit and a data acquisition system. The reservoir was obtained from the oxidation as reported in the previous sections. MF membrane module was a PVDF which was prepared as shown in Figure 6.2. The membrane has moderate hydrophobicity, excellent durability, chemical and biological resistance (Li, Fane, Winston Ho, and Matuura, 2008). The membrane nominal pore size was 0.30 µm. The data acquisition system was connected on-line to the MF unit. The weight of water per time at a particular pressure was recorded using an electronic balance which was connected to a personal computer.

Prior to operation, the membrane sheet was cut to obtain an effective area of 0.549 m^2, submerged in propanol for 30 min to remove any stain, cleaned with DI water and put on a stainless steel holder. An ultrasonic probe was connected with the membrane holder and then submerged into the reservoir.
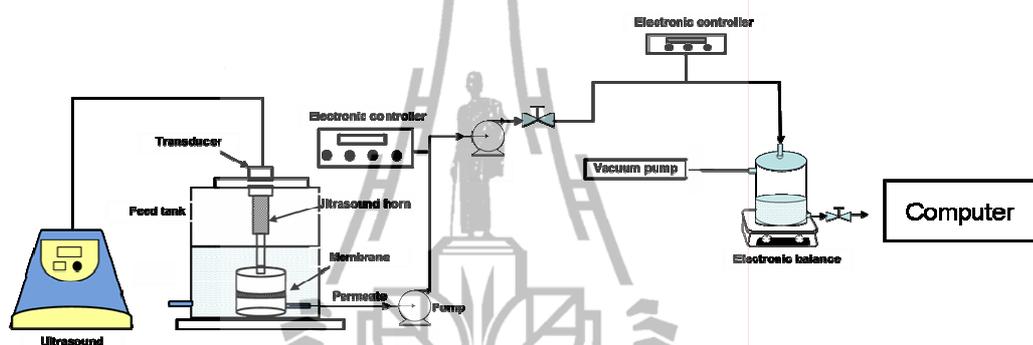

**Figure 6.1** Schematic diagram of membrane microfiltration system in a laboratory scale.
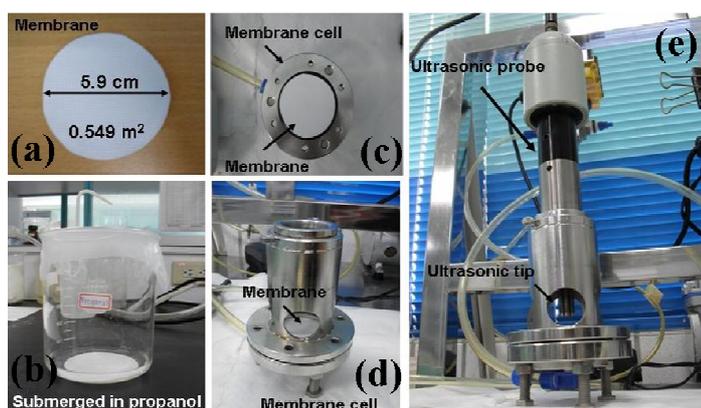
Figure 6.2 Preparation of a PVDF membrane prior to the operation; (a) effective area of the membrane (b) cleaning of the membrane using proponol, (c) and (d) membrane holder and (e) membrane holder connected with US probe.

A preliminary flux of DI water was measured to wet the membrane, determine permeability and allow the permeate flux to stabilize. Subsequently, the reservoir obtained from the oxidation was filtered under a pressure from 20 to 50 kPa. The permeate flux of the suspended solution was calculated according to Eq. 6.1 and membrane fouling was further evaluated. Permeate flux is calculated according to Eq. 6.1.

$$J = \frac{V}{A \times t} \qquad (6.1)$$

where J is permeate flux (L h^{-1} m^{-2}), V is volume of permeate (L), A is an effective area (m^2) of a membrane, and t is filtration time (h).

6.4 Membrane cleaning experiment

The MF was initially operated for 30 min where the permeate flux severely declined and then the fouled membrane was cleaned with pulse cleaning duration of 1 min and pulse interval of 20 min. The details were as follows:

6.4.1 Backwashing

BW was carried out in a flow direction opposite to MF by forcing air through the membrane at pressure higher than 20 kPa.

6.4.2 Ultrasound

A 20 kHz ultrasonic probe with a diameter tip of 12.7 mm (Misonix Sonicator, U.S.A) was used during membrane cleaning. A power output of ultrasound was 12±0.5 W for all experiments. A distance between membrane and ultrasonic probe was 20 mm. For the effect of US pulse duration, 1, 3, 5 and 7 min were applied.

6.4.3 Combined method

A combined cleaning between BW and US was investigated by different sequences, BW-US and US-BW. The pulse duration for each method was 1 min.

6.5 Analytical methods

The remaining concentration of Mn^{2+}, Fe^{2+} and Cd^{2+} was determined by ICP-OES (Perkin Elmer DV 2000). The morphology of the fresh, fouled and cleaned MF membranes was analyzed by a digital microscope (Hirox, KH-7700) with a magnification of 700x.

6.6 Theoretical background of membrane fouling mechanisms

Modeling the flux decline during MF provides a better understanding on membrane fouling and is useful to determine a proper condition for MF and membrane cleaning. Hermia (1982) proposed four empirical models to present membrane fouling mechanism in a dead-end filtration based on constant pressure: complete pore blocking (CPB), standard pore blocking (SPB), intermediate pore blocking (IPB) and cake filtration (CF). The mechanisms are shown in Figure 6.3.
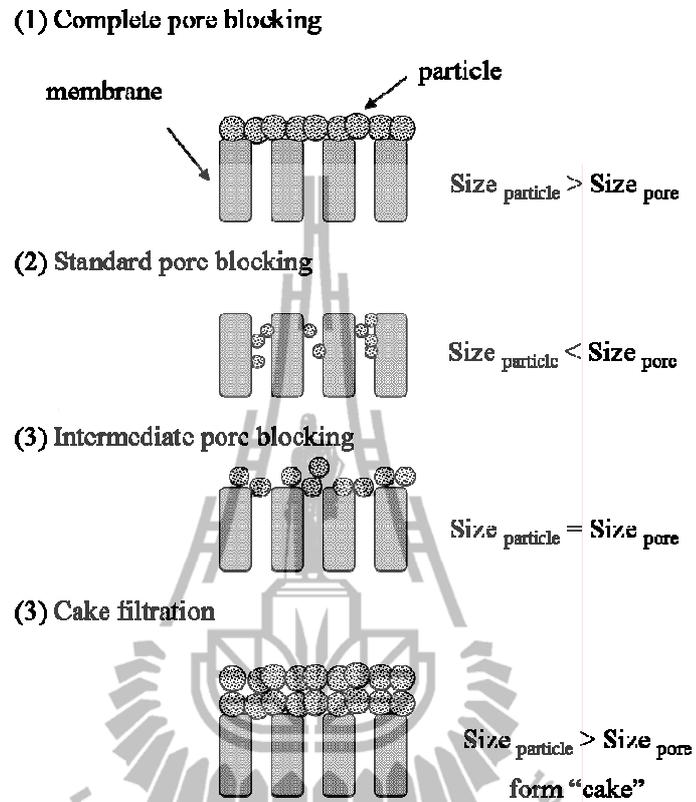
Figure 6.3 Membrane fouling mechanism.

The CPB occurs over the membrane surface and not inside the membrane pores when the sizes of the solute particles are greater than the size of membrane pores. The SPB hypothesizes that the particles enter the membrane pores and deposit over the pore walls due to the irregularity of pore passages, thereby reducing the membrane pore volume. This type of fouling is caused by particles smaller than the membrane pore size and pore blocking occurs inside the membrane pores. Therefore, the volumes of membrane pores decrease proportionally to the filtered permeate volume. IPB occurs when the solute particle size is similar to the membrane pore size. In this

model, it is assumed that a membrane pore is not necessarily blocked by the solute molecules and some particles may settle over others. Therefore, the un-blocked membrane surface area diminished with time and some molecules are expected to obstruct the membrane pore entrance without blocking the pore completely. CF corresponds to a scenario where particles larger than the average pore size accumulate on the membrane surface, thus forming a layer called "cake". The cake grows with time and it acts as an additional porous barrier to the permeating liquid. The various pore blocking models can be mathematically described using the following linearized expressions (Hermia, 1982; Nath, 2008).

$$\text{CPB: } \ln(\frac{1}{J}) = \ln(\frac{1}{J_0}) + K_b t \tag{6.2}$$

$$\text{SPB: } \frac{1}{J^{1/2}} = \frac{1}{J_0^{1/2}} + K_s t \tag{6.3}$$

$$\text{IPB: } \frac{1}{J} = \frac{1}{J_0} + K_i t \tag{6.4}$$

$$\text{CF: } \frac{1}{J^2} = \frac{1}{J_0^2} + K_c t \tag{6.5}$$

where J_0 is permeate flux of DI water though clean water, J is permeate flux of the suspended water over time and t is filtration time. Kb, Ks, Ki and Kc are system parameters relating to CPB, SPB, IPB and CF, respectively.

Eq. 6.2 to Eq. 6.5 can be employed to evaluate the effectiveness of various membrane cleaning methods in removing the different types of fouling. This can be done by fitting the laboratory experimental data collected form MF run after cleaning the membrane unit to those equations, and comparing the changes of the values in Kb,

Ks, Ki and Kc obtained from the slope of the best fitting straight lines for the MF data before and after the membrane cleaning. The change in Kb, Ks, Ki and Kc could indicate the type of membrane fouling affected by the type of cleaning method.

In order to assess the degree of membrane fouling, the total resistance at different filtration pressures is determined by Eq. 6.6 (Kang and Choo, 2003; Schafer, Fane, and Waite, 2005).

$$J = \frac{\Delta P}{\mu R_t} \qquad\qquad (6.6)$$

where J is permeate flux (m^3 m^{-2} h^{-1}), ΔP is trans-membrane pressure (Pa), μ is the fluid viscosity (Pa· s) which is assumed to be DI water at 26°C (0.8796 × 10^{-3} Pa· s) (Chin, 2006) and Rt is total resistance (m^{-1}).

6.7 Results and discussion

6.7.1 Trend of flux decline at various filtration pressures

The permeate flux variation of feed suspension at different filtration pressures is shown in Figure 6.4. Permeate flux decreases with increase of filtration time considering in all cases because of deposition of Mn-Fe oxide particles on PVDF membrane. Moreover, the flux increases with increase in filtration pressure from 20 to 50 kPa because the increase of filtration pressure enhances driving force across the membrane reducing adsorption of permeating molecules on the walls of the membrane pores. Similar results were reported by Yuan, Kocic, and Zydney (2002) in a study in which humic substance in water was separated by a polycarbonate membrane with the pore size of 0.2 µm. The initial flux increased linearly with pressure, varying from 2.1

$\times$ 10^{-4} m/s at 6.9 kPa to 16 $\times$ 10^{-4} m/s at 55 kPa. The flux remained greater at the

higher pressure throughout the filtration period, although the rate of flux decline also

increased with the increasing pressure.
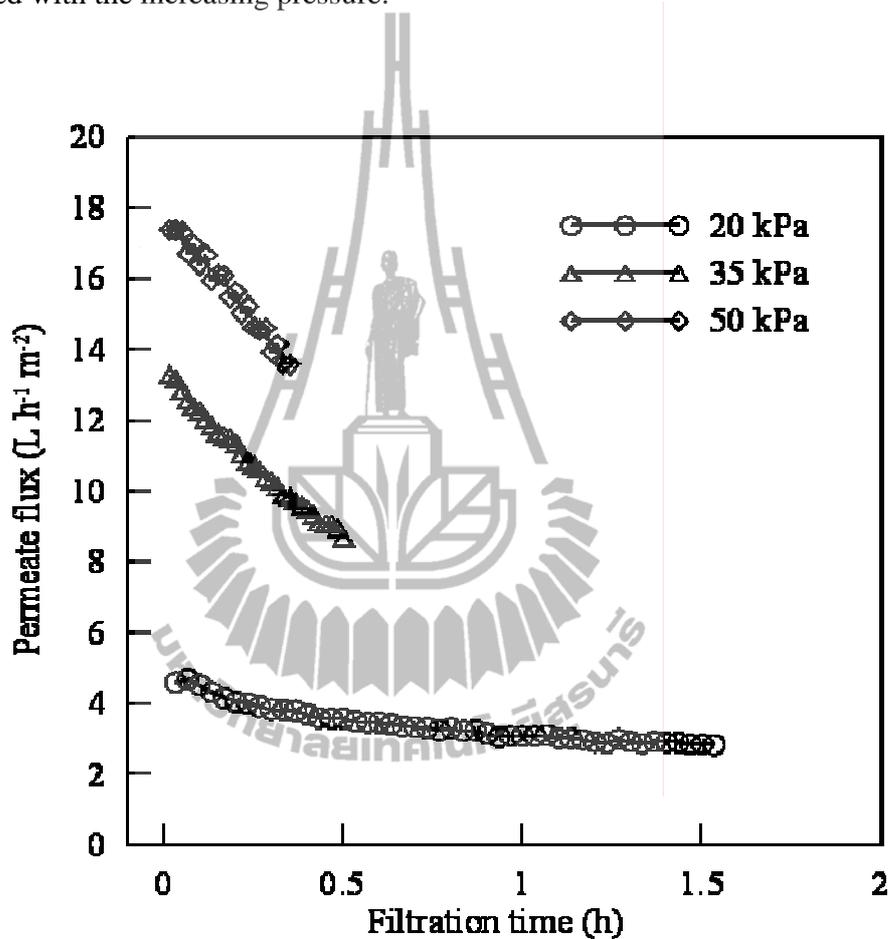
Figure 6.4 Variation of permeate flux as a function of time at different filtration

pressures.

Based on Eq. 6.6, total resistance (Rt) at different filtration pressures was

determined to judge on the degree of membrane fouling. The results are shown in

Figure 6.5. At 20 kPa, Rm increases from 17×10^{12} to 28×10^{12} m^{-1} in 90 min. When

increased the pressure to 35 and 50 kPa, Rt decreased linearly and was significantly different from that of 20 kPa. Nandi, Das, Uppaluri, and Purkait (2009) mentioned that the higher filtration pressure enables lower adsorption of the Mn-Fe oxide particles of membrane pores owing to higher liquid velocity through the pores. Besides, due to greater driving force, some of the blocked pores get cleaned by permeate liquid. As a result, the fouling behavior could not be accurately described because of the fast filtration period. Therefore, further investigation was conducted at filtration pressure of 20 kPa to follow membrane fouling during MF.
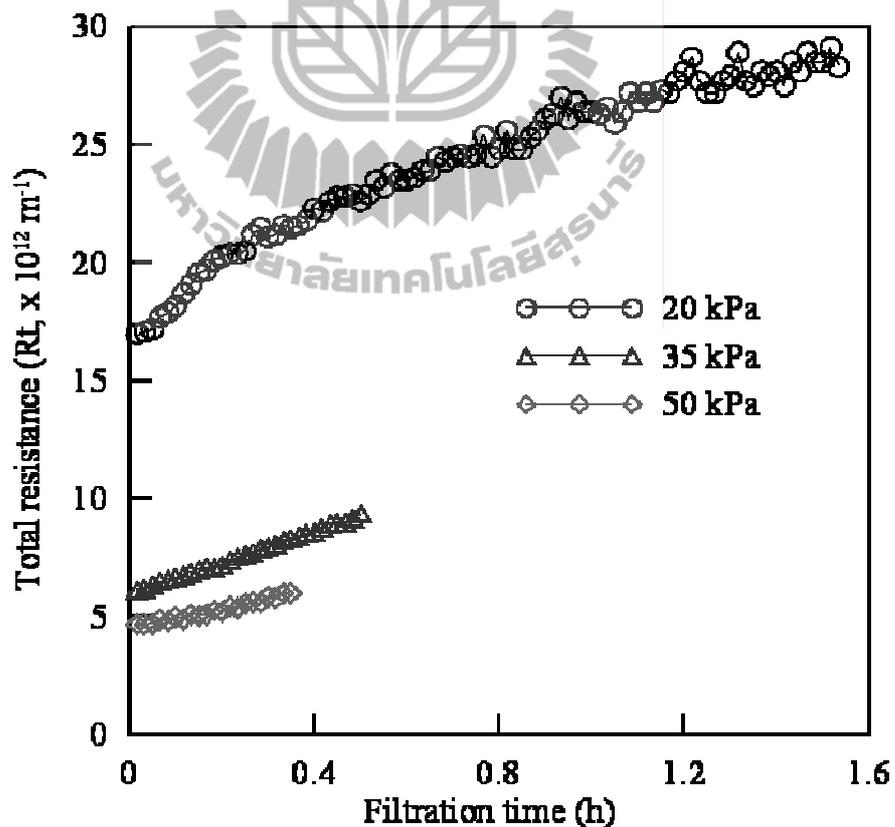

Figure 6.5 Effect of filtration pressure on total resistance (Rt).

6.7.2 Membrane fouling mechanism

To evaluate possible fouling mechanisms on the membrane surface and into its porous structure, the permeate flux obtained at filtration pressure of 20 kPa was fitted with the pore block models. The results are presented in Figure 6.6 and the parameters, K_b, K_s, K_i and K_c, calculated from the models are shown in Table 6.1.
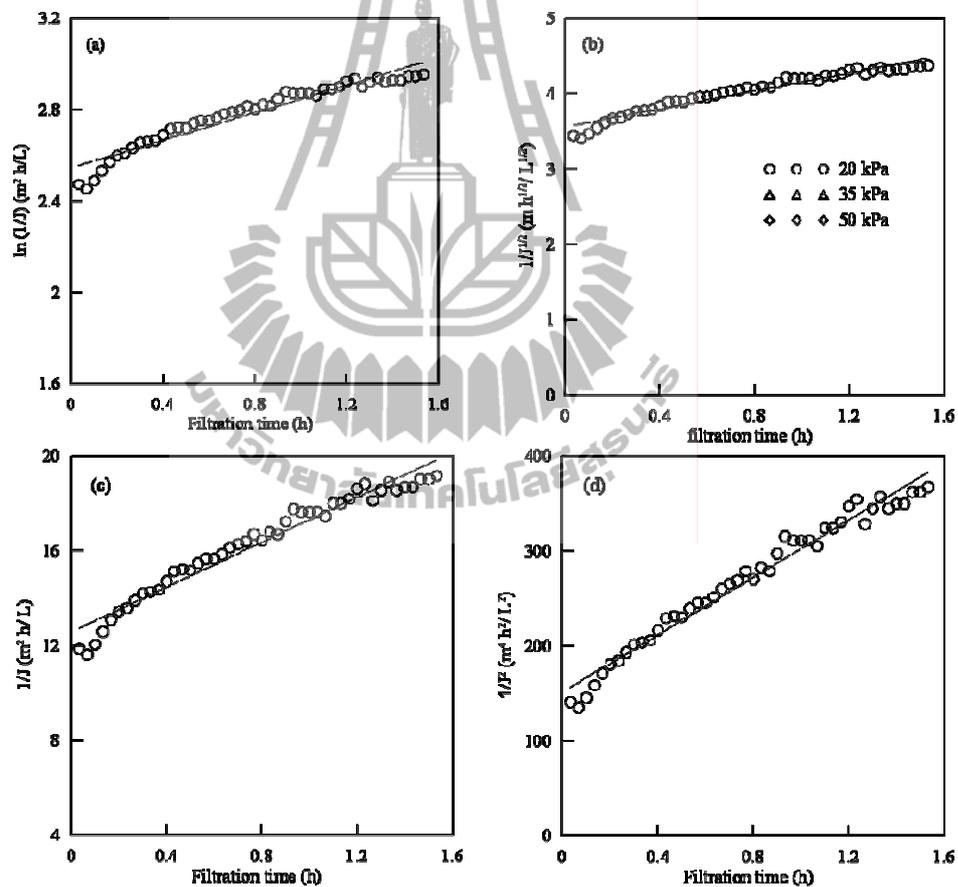

Figure 6.6 Linearized plot of permeate flux as a function of time for different pore blocking models for the MF of suspended Mn-Fe oxide at 20 kPa; (a) CPB, (b) SPB, (c) IPB and (d) CF.

The graph can be divided into two segments. The first segment was from the beginning to 0.2 h which was due to the membrane blockings, while the second one can be explained by the cake filtration model. The second stage occurred because of the accumulation of the precipitates.

Table 6.1 Summary of parameters associated to various pore blocking models at 20 kPa.

CPB		SPB		IPB		CF	
Kb	R^2	Ks	R^2	Ki	R^2	Kc	R^2
0.3009	0.9269	0.1505	0.9422	4.7337	0.9551	150.79	0.9739

As shown in Table 6.1, the highest correlation coefficient (R^2) was observed in CF suggesting that cake formation provided the best fit to represent the decline of permeate flux. However, the values of R^2 from all models were more or less similar indicating that fouling was from a mixed pore blocking mechanism with the predominance of cake filtration during the membrane filtration (Koneiczny and Rafa, 2002). This mechanism could be supported by the magnitude of Kb, Ks, Ki and Kc in which the Mn-Fe oxide particles could cause severe fouling mainly by depositing and forming cake layer.

The transition from pore blocking to cake formation observed in this study was in agreement with the observation by others (Nandi, Moparthi, Uppaluri, and Purkait, 2009; Lim and Bai, 2003). Nandi et al. (2009) studied a modeling of separation of oil-in-water emulsions using low cost ceramic membrane. They reported

that cake filtration was the best model to represent the fouling phenomena. Lim and Bai (2003) employed a hollow fiber PVDF membrane with a pore size of 0.1 µm for activated sludge wastewater treatment. The predominant fouling mechanisms were initial pore blocking followed by cake filtration. However, it was not possible to determine when one dominant fouling mechanism changed to another (Arnot, Field, and Koltuniewicz, 2000).

It should be mentioned that flux decline caused by several fouling mechanisms of suspended Mn-Fe oxide continuously took place with cake filtration as a main phenomenon. This finding is used to evaluate membrane cleaning efficiency of each type of fouling.

6.7.3 Membrane cleaning

6.7.3.1 Membrane cleaning by different methods

The variation of permeate flux with different cleaning methods is demonstrated in Figure 6.7. The average initial flux decreased from 5.238 to 3.639 L h^{-1} m^{-2} with about 30% decline. After applying cleaning methods, the flux during each filtration cycle was recovered as the reversible fouling was removed. However, the flux was not recovered completely as a result of irreversible fouling (Listiarini, Chun, Sun, and Leckie, 2009). The suitable condition for membrane cleaning is necessary.
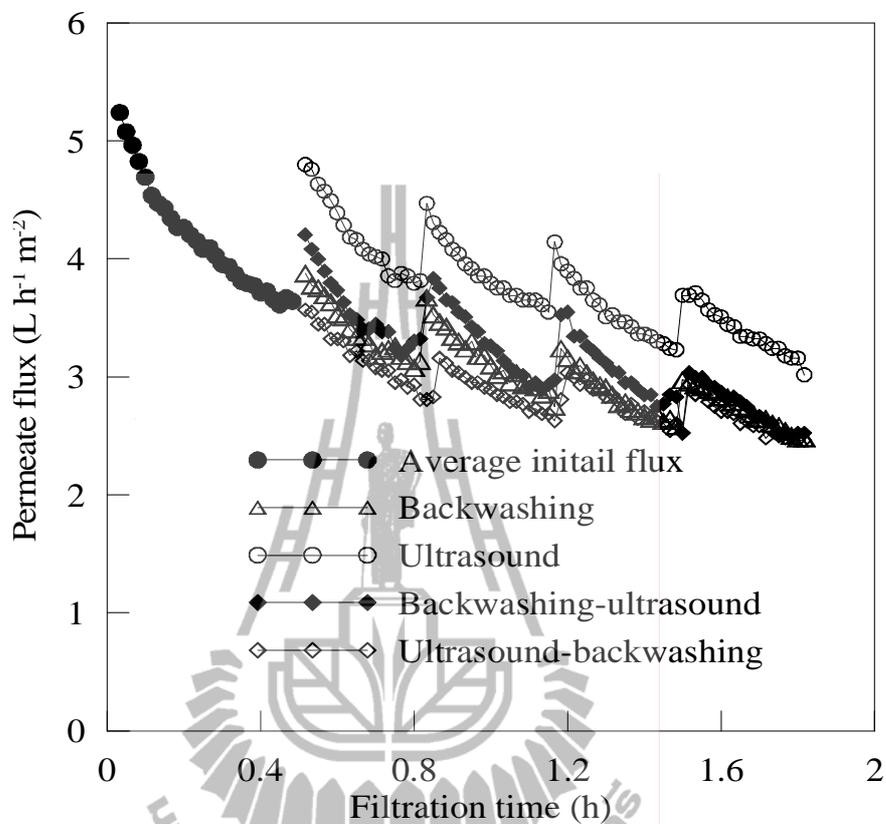
Figure 6.7 Permeate flux as a function of time at different methods; 1 min pulse

duration; 20 min pulse interval.

Table 6.2 Summary of percent flux recovery after cleaning by different methods.

US	Flux recovery (%)			
duration	1st cleaning	2nd cleaning	3rd cleaning	4th cleaning
(min)	cycle	cycle	cycle	cycle
BW	73.88	70.06	61.85	56.70
US	91.64	85.34	79.04	70.64
BW-US	80.18	70.06	67.39	57.85
US-BW	67.96	60.33	57.85	55.94

Table 6.2 shows the percentage of flux recovery after each cycle with different cleaning methods. In case of BW, flux recovery was achieved at 73.88% at the initial cycle and then continuously decreased to 56.70% at the fourth cleaning cycle. The decrease of flux recovery could be explained by the fact that Mn-Fe oxide particles generated after oxidation were responsible for pore blocking during MF (Choo, Lee, and Choi, 2005). The fouling during BW took place because of the blocking from the particles grown after passing through the pores resulting in a lower cleaning efficiency. US was the most effective method with the initial flux recovery of 91.64%. It should be mentioned that Mn-Fe particles blocked inside the PVDF pores could be removed effectively with ultrasound unlike backwashing. The effectiveness of US cleaning was reported by several researchers. Li, Sanderson, and Jacobs (2002) reported that US-associated cleaning was useful for nylon MF membranes fouled by Kraft paper mill effluent. US removed the formed layer of solute from the membrane

due to physical cleaning (Lorimer and Mason, 1990). In case of BW-US, the highest

flux recovery of 80.18% was achieved at an initial cycle and dropped to 57.85% at 4th

cleaning cycle. It was observed that the flux recovery was almost similar to that of

BW, indicating that the combination of BW followed by US was helpless in this

condition. The result was obviously observed in US-BW cleaning where the flux

recovery was the lowest with the initial recovery of 67.96%.

Based on the fouling mechanism mentioned previously, a mixed

mechanism, certain forms at least pore blocking were not effectively removed by BW,

which leads to the flux decline after each cleaning cycle. In contrast, US could remove

effectively most types of fouling. Therefore, effect of US duration was further

investigated.

6.7.3.2 Membrane cleaning by US with different US durations

To study influence of ultrasound on the membrane cleaning, the

experiments were conducted at different pulse durations. The results are presented in

Figure 6.8. In overall observations, the average initial flux decreases from 5.238 to

3.639 L h^{-1} m^{-2} in 30 min of MF. After applying US with 1, 3 and 5 min of durations,

the permeate flux was recovered with the flux of 4.800, 4.450 and 3.890 L h^{-1} m^{-2},

respectively, while exposure of US at 7 min did not recover the flux. The results can

be explained from their flux recovery.
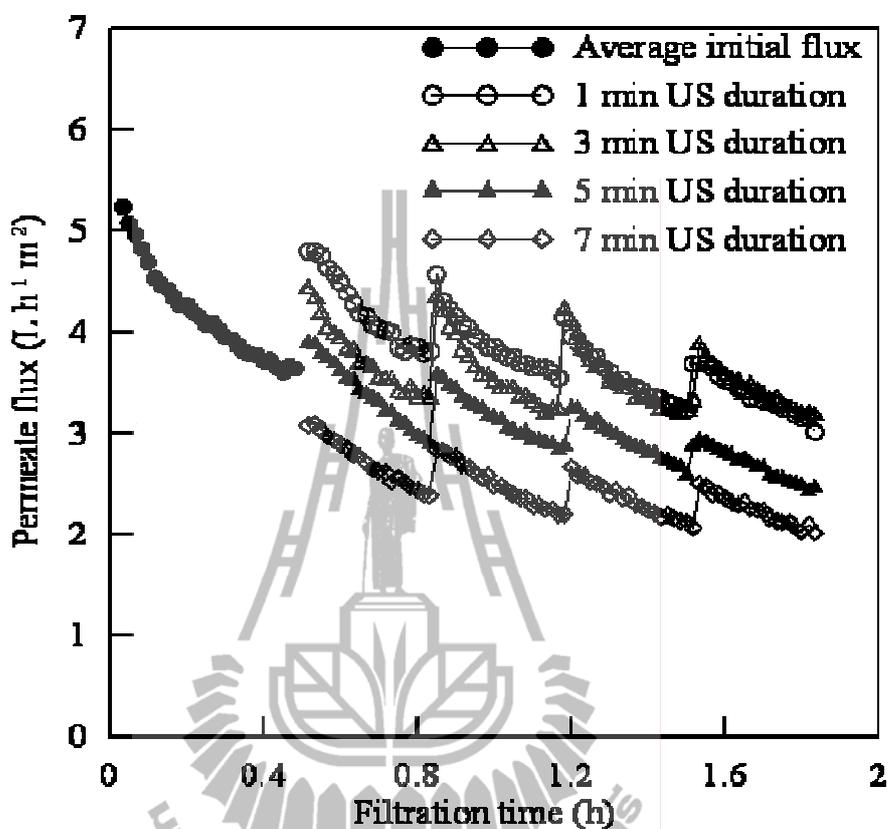
Figure 6.8 Permeate flux as a function of time at different US durations; 20 min pulse
interval.

Table 6.3 shows the percentage of flux recovery with different pulse
durations after each cleaning cycle. At 1 min, the initial flux recovery was 91.64% and
continuously dropped with the increase of cleaning cycle. Further increase in the
ultrasonic duration to 3, 5 and 7 min decreased the flux recovery. The results can be
explained according to Lim and Bai (2003) who studied membrane cleaning of PVDF
fouled by activated sludge using sonication. The experiment was performed in a
sonication bath at a frequency of 42 kHz. The highest flux recovery of 87.5% was
obtained with sonication time of 10 min. Further increase in the sonication duration to

15 and 20 min did not improve the flux recovery. The long sonication durations reduced the percentage of flux recovery, while short duration of 5 min was not efficient in cleaning the membrane. The effect of ultrasonic duration is illustrated in Figure 6.9. The long pulse duration produces small particles through the impact of the ultrasonic energy. Then, the small particles could block on the membrane pore which decreases permeate flux and flux recovery. Besides, US could increase membrane resistance and change texture of the PVDF membrane, leading to decrease of permeate flux and membrane cleaning efficiency. Muthukumaran et al. (2004) studied effect of US on the permeate flux of fouled polysulfonate ultrafiltration membrane. The results indicated that the US radiation was very effective in removal of protein foulants and increased permeate flux after fouling with the sonication time of 10 min. The short burst of US power can be used as a cost-effective method of cleaning.

Table 6.3 Summary of percent flux recovery after cleaning by ultrasound at different pulse durations.

| US duration (min)	Flux recovery (%)			
	1st cleaning cycle	2nd cleaning cycle	3rd cleaning cycle	4th cleaning cycle
1	91.64	85.34	79.04	70.64
3	84.96	83.37	81.02	74.37
5	74.26	68.11	62.24	55.97
7	58.71	54.02	50.88	47.75
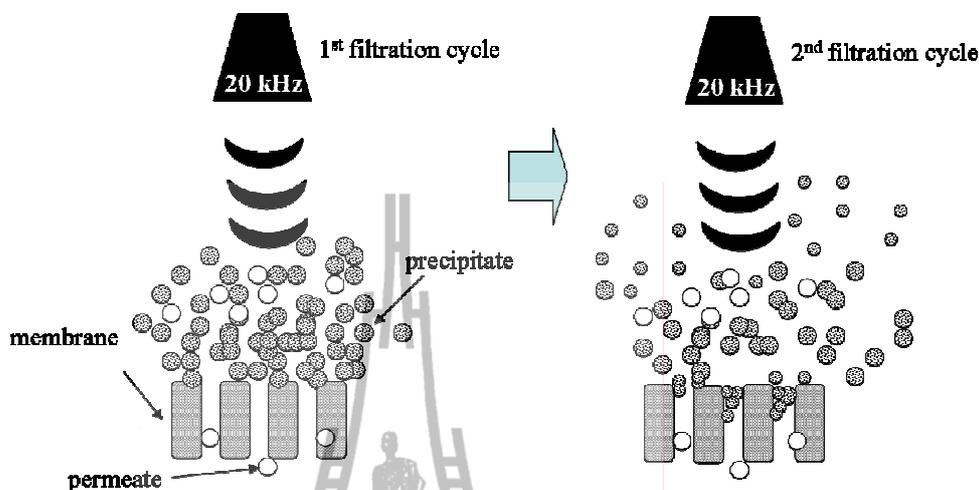
Figure 6.9 Illustration of the effect of ultrasound duration.

6.7.4 Characterization of the membrane

To study efficiency of different cleaning methods on fouling layer of PVDF membrane, the images obtained from the digital microscope of fresh, fouled and cleaned membranes were recorded. The results are shown in Figure 6.10.

The image of fresh membrane surface (Figure 6.7a) shows the typical membrane surface. After 90 min of the MF operation at 20 kPa, the brown oxide particles deposited and distributed on the membrane surface (Figure 6.7b). After cleaning by US for 1 min, the fouling particles were completely removed, resulting in an increase of flux recovery, while the brown layer particles left on the membrane surface (Figure 6.7d) after cleaning by BW for 1 min. The results agreed with the flux recovery discussed above.
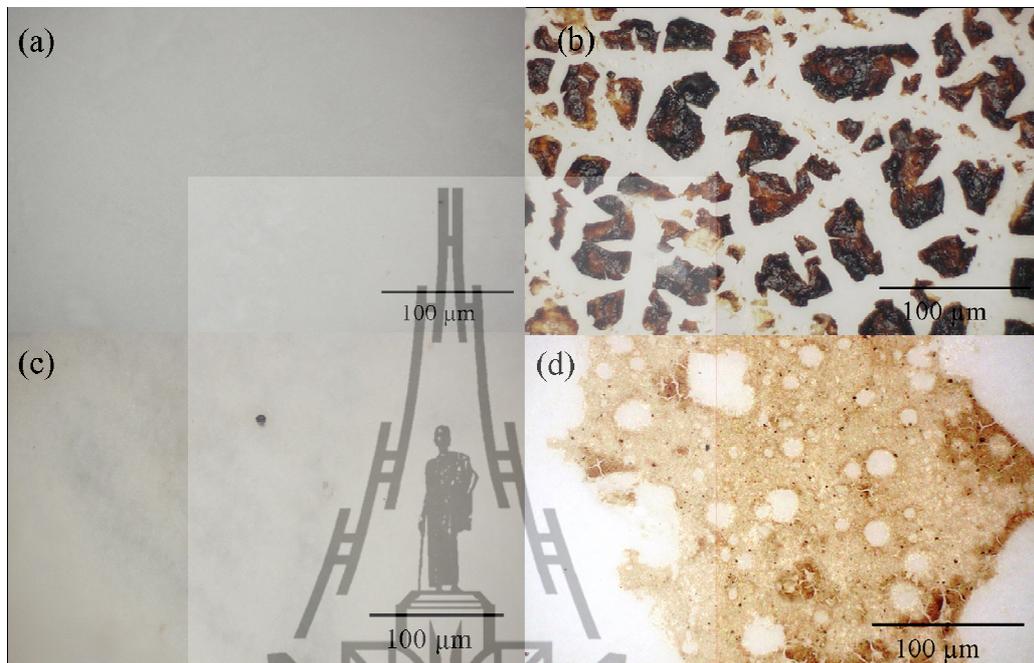
Figure 6.10 Images obtained from digital microscope showing the surfaces of (a) fresh membrane, (b) fouled membrane, (c) used membrane after cleaning by US and (d) used membrane after cleaning by BW.

6.8 Conclusions

The membrane fouling and cleaning efficiency of PVDF microfiltration fouled by manganese-iron oxides were investigated. The suspended manganese-iron oxides decreased permeate flux throughout the filtration time. The types of membrane fouling were attributed to a mixed blocking mechanism of the pores taken place with the predominance of cake filtration. Ultrasonic cleaning was the most effective with the initial flux recovery of about 92% under 1 min of US duration. Long exposure of

ultrasound caused lower effective on membrane cleaning. The combined methods did not improve flux recovery.

6.9 References

Adham, S., Chiu, K-P., Gramith, K. and Oppenheimer, J. (2005). **Development of a microfiltration and ultrafiltration knowledge base**. U.S.A.: AWWA Research Foundation. p. 27.

American Water Work Association. (2002). **Manual of Water Supply Practice-M21: Groundwater** (3rd ed.). pp. 170-171.

American Water Work Association. (2005). **Manual of Water Supply Practice-M53: Microfiltration and ultrafiltration membranes for drinking water**. p. 60.

Arnot, T. C., Field, R. W. and Koltuniewicz, A. B. (2000). Cross-flow and dead-end microfiltration of oil-water emulsions Part II. Mechanisms and modeling of flux decline. **Journal of Membrane Science**. 169: 1-15.

Chae, S-R., Yamamura, H., Ijeda, K. and Watanabe, Y. (2008). Comparison of fouling characteristics of two different poly-vinylidene fluoride microfiltration membranes in a pilot-scale drinking water treatment system using pre-coagulation/sedimentation, sand filtration and chlorination. **Water Research**. 42: 2029-2042.

Chen, W-H., Hsieh, Y-H, Wu, C-C, Wan, M. W., Futalan, C. M. and Kan, C-C. (2011). The on-site feasibility study of iron and manganese removal from groundwater by hallow-fiber microfiltration. **Journal of Water Supply: Research and Technology-AQUA**. 60: 391-401.

Chin, D. A. (2006). **Water-quality Engineering in Natural Systems**. U.S.A.: John Wiley and Sons. p. 537.

Choo, K-H., Lee, H. and Choi, S-J. (2005). Iron and manganese removal and membrane fouling during UF in conjunction with prechlorination for drinking water treatment. **Journal of Membrane Science**. 267: 18-26.

Li, N. N., Fane, A. G., Winston Ho, W. S. and Matuura, T. (2008). **Advanced Membrane Technology and Applications**, New Jersey: U.S.A.: John Wiley and Sons. p. 218.

Hermia, J. (1982). Constant pressure blocking filtration laws-application to power law non-newtonian fluid. **Transactions of the Institute of Chemical Engineers**. 60: 183-187.

Kang, S. K. and Choo, K. H. (2003). Use of MF and UF membranes for reclamation of glass industry wastewater containing colloidal clay and glass particles. **Journal of Membrane Science**. 223: 89-103.

Levesley, J. A. and Hoare, M. (1999). The effect of high frequency backflushing on the microfiltration of yeast homogenate suspensions for the recovery of solutes protein. **Journal of Membrane Science**. 158: 29-39.

Li, J., Sanderson, R. D. and Jacobs, E. P. (2002). Ultrasonic cleaning of nylon microfiltration membranes fouled by Kraft paper mill effluent. **Journal of Membrane Science**. 205: 247-257.

Lim, A. L. and Bai, R. (2003). Membrane fouling and cleaning in microfiltration of activated sludge wastewater. **Journal of Membrane Science**. 216: 279-290.

Listiarini, K., Chun, W., Sun, D. D. and Leckie, J. O. (2009). Fouling mechanism and resistance analysis of systems containing sodium alginate, calcium, alum and their combination in dead-end fouling of nanofiltration membranes. **Journal of Membrane Science**. 344: 244-251.

Lorimer, J. P. and Mason, T. J. (1990). **Sonochemistry, the uses of ultrasound in chemistry**. Royal Society of Chemistry. England. p. 18.

Muthukumaran, S., Yang, K., Seuren, A., Kentish, S., Ashokkumar, M., Stevens, G. W. and Grieser, F. (2004). The use of ultrasonic cleaning for ultrafiltration membranes in the dairy industry**. Separation and Purification Technology**. 39: 99-107.

Nandi, B. K., Das, B., Uppaluri, R. and Purkait, M. K. (2009). Microfiltration of mosambi juice using low cost ceramic membrane. **Journal of Food Engineering**. 95: 597-605.

Nandi, B. K., Moparthi, A., Uppaluri, R. and Purkait. (2009). Treatment of oil wastewater using low cost ceramic membrane: comparative assessment of pore blocking and artificial neural network models. **Chemical Engineering Research and Design**. 88: 881-892.

Nath, K. (2008). **Membrane Separation Processes**, Eastern Economy Edition, Prentice Hall of India Private Limited. New Dehli, India: PHI learning. p. 130.

Schafer, A. I., Fane, A. G. and Waite, T. D. (2005). **Nanofiltration-Principles and Applications**. Oxford, England: Elsevier.

Schneider, C., Johns, P. and Huehmer, R. P. (2001). **Removal of Manganese by Microfiltation in a Water Treatment Plant**. In proceeding of the AWWA Membrane Technology Conference. Denver, American Water Works Association. p. 19.

Yuan, W., Kocic, A. and Zydney, A. L. (2002). Analysis of humic acid fouling during microfiltration using a pore blocking-cake filtration model. **Journal of Membrane Science**. 198: 51-62.

Zhang, G. and Liu, Z. (2003). Membrane fouling and cleaning in ultrafiltration of wastewater form banknote printing works. **Journal of Membrane Science**. 211: 235-249.

CHAPTER VII

CONCLUSIONS

7.1 Conclusions

Proper conditions to remove Mn^{2+}, Fe^{2+} and Cd^{2+} from synthetic groundwater to the level below the MCL using combined aeration and $KMnO_4$ was successfully obtained. The partial removal of Mn^{2+} and Cd^{2+} and nearly complete removal of Fe^{2+} by bare aeration was observed in all systems. The aeration decreased the consumption of $KMnO_4$ needed for the oxidation.

In single system consisting of Mn^{2+} ions, pH, oxidant dose and stirring speed were important parameters. The pH of 8.0, stirring speed of 120 rpm and oxidant dose of 0.96 mg/L $KMnO_4$ were the optimum condition. The main composition of the precipitates was MnO_2. At the pH 9.0, although the $KMnO_4$ dose was insufficient, further removal of Mn^{2+} was observed because of adsorption on MnO_2 particles.

In dual system consisting of Mn^{2+} and Fe^{2+}, the minimum concentration of $KMnO_4$ of 0.603 mg/L was introduced to oxidize the Mn^{2+} to the level below the MCL. The presence of Fe^{2+} was improved the removal of Mn^{2+}. Characterization of the resulting precipitates using digital microscope and EDX proved the formation of the oxides. The presence of Ca^{2+} and Mg^{2+} as well as alum addition slightly obstructed the removal of Mn^{2+}. The possible removal mechanism of Mn^{2+} and Fe^{2+} was oxidation and sorption on the oxide precipitate.

In a triple system containing Mn^{2+}, Fe^{2+} and Cd^{2+}, the contamination of Cd^{2+} required a higher $KMnO_4$ dose than the dual system to remove all the ions to the level below MCL. The results suggested a two-step mechanism in the removal of Mn^{2+}, Fe^{2+} and Cd^{2+} by $KMnO_4$. Mn^{2+} and Fe^{2+} were mainly removed by oxidation with $KMnO_4$ whereas Cd^{2+} could be eliminated by sorption on the Mn-Fe oxides. The removal of Cd^{2+} was via sorption on Mn-Fe precipitates and the Cd^{2+} concentration of 0.025 mg/L was the maximum sorption capacity for the Mn-Fe oxide. The presence of Ca^{2+} or Mg^{2+} did not disturb the elimination of the metal ions.

In membrane microfiltration, the suspended manganese-iron oxides decreased permeate flux throughout the filtration time. The types of membrane fouling were attributed to a mixed blocking mechanism of the pores taken place with the predominance of cake filtration. Ultrasonic cleaning was the most effective and long exposure of ultrasound caused lower efficiency of membrane cleaning. Lastly, the combined methods between ultrasound and backwashing did not improve the flux recovery.

7.2 Recommendation for future work

Information from this work should be used further to remove Mn^{2+}, Fe^{2+} and Cd^{2+} in a larger scale and a continuous operation in the water treatment plant.

The effect of some interference such as nitrate, ammonia, fluoride, hydrogen sulfide and other organic compounds should be individually determined using the obtained optimum condition.

APPENDICES
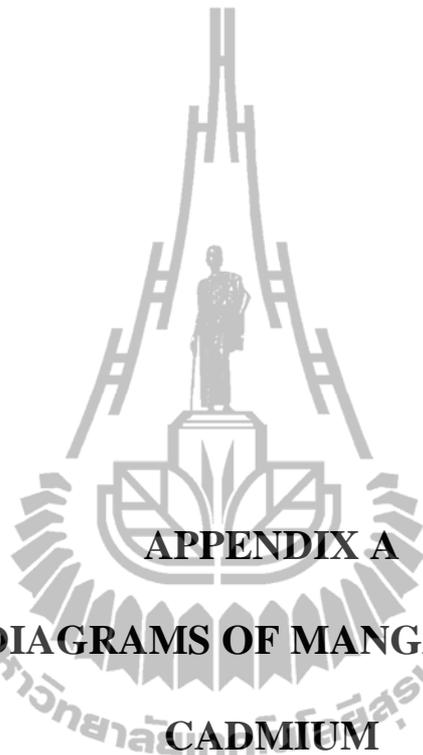
APPENDIX A

# Eh AND pH DIAGRAMS OF MANGANESE, IRON AND
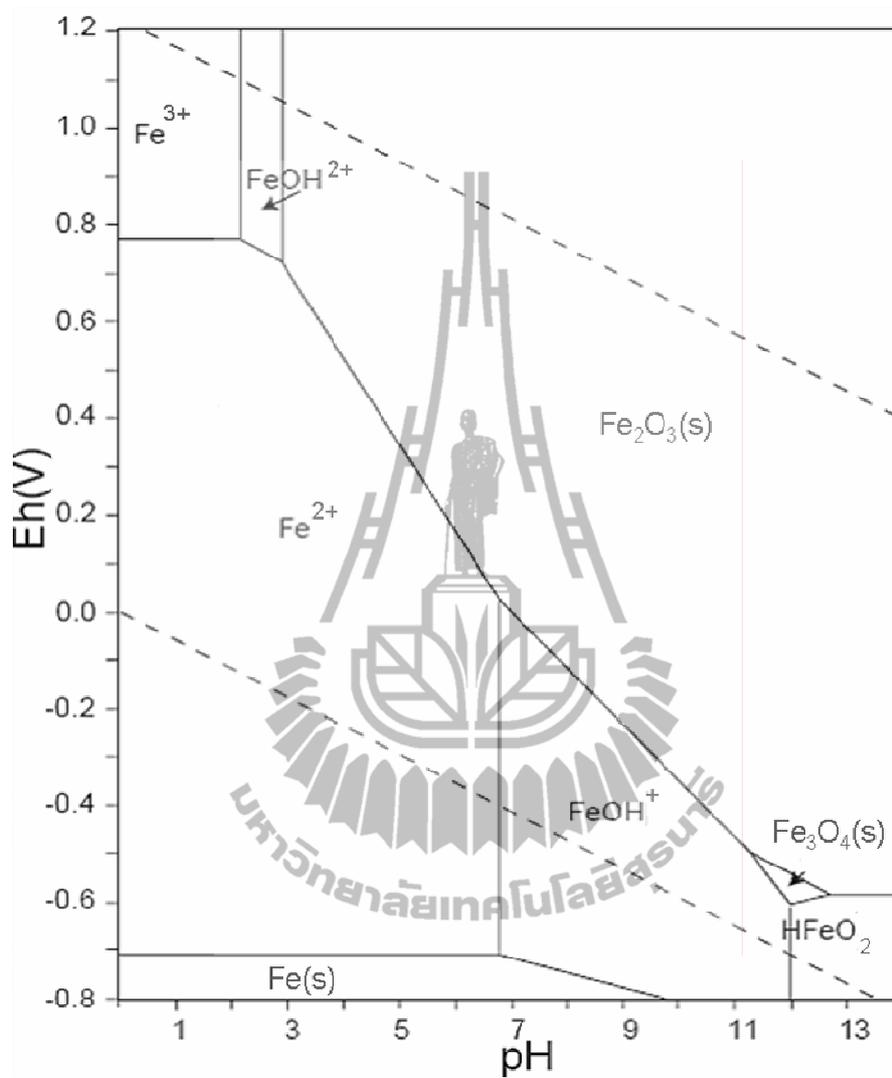
CADMIUM

**Figure A-1** The Eh-pH diagram of iron at 25°C and 0.987 atm.
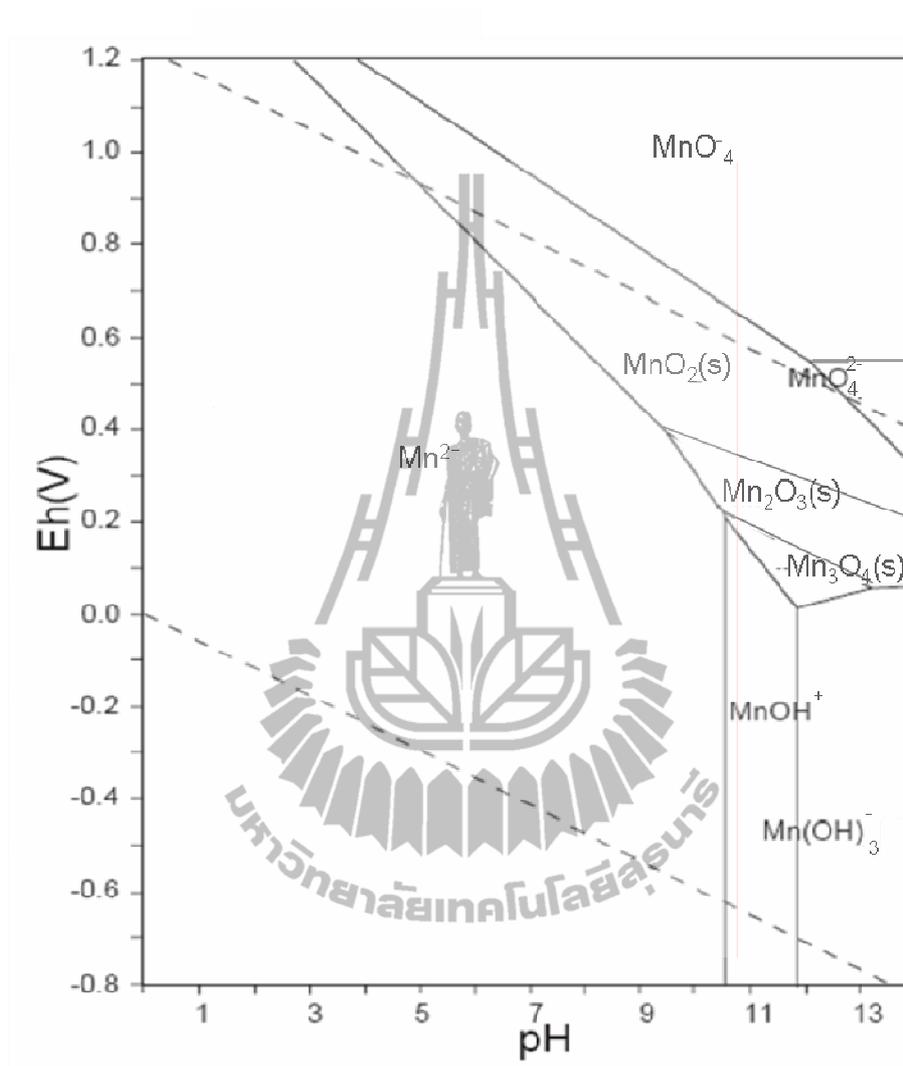
**Figure A-2** The Eh-pH diagram of manganese at 25°C and 0.987 atm.
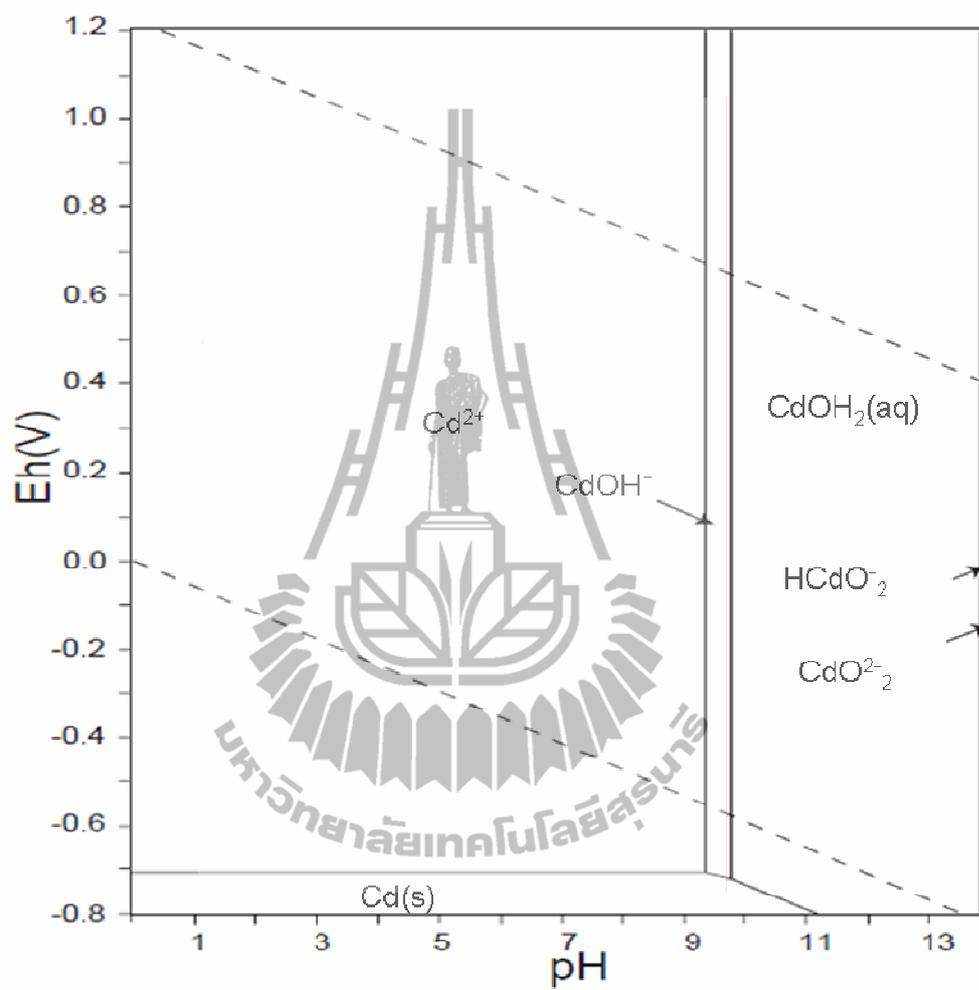
Figure A-3 The Eh-pH diagram of cadmium at 25°C and 0.987 atm.
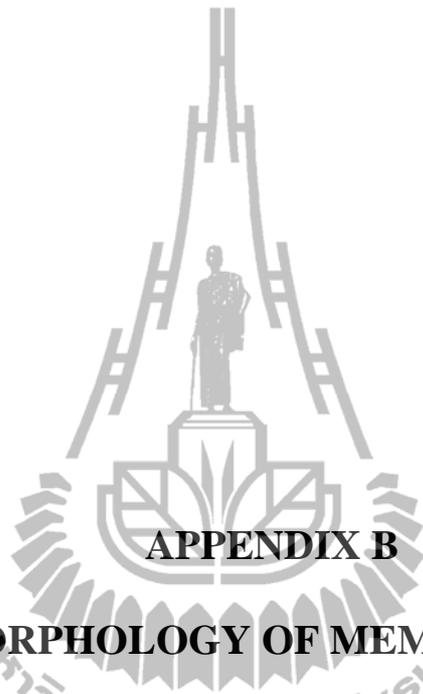
APPENDIX B

SURFACE MORPHOLOGY OF MEMBRANE OBTAINED

FROM DIGITAL MICROSCOPE
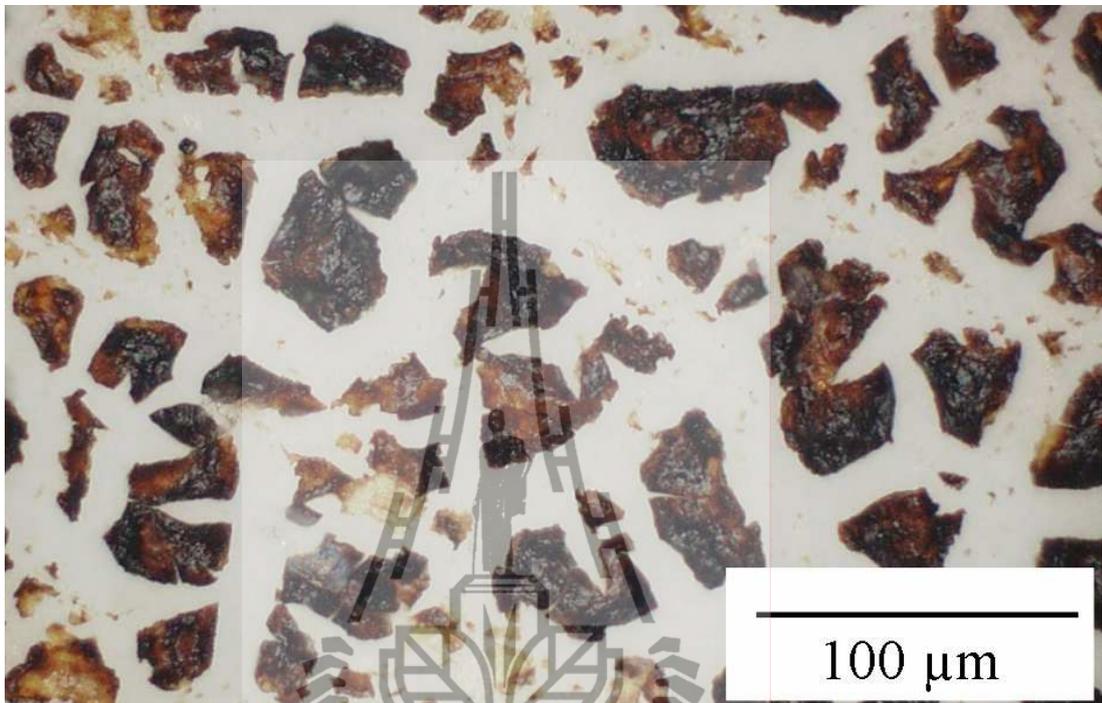
Figure B-1 Images obtained from digital microscope showing the surfaces of fouled membrane at pressure of 20 kPa.
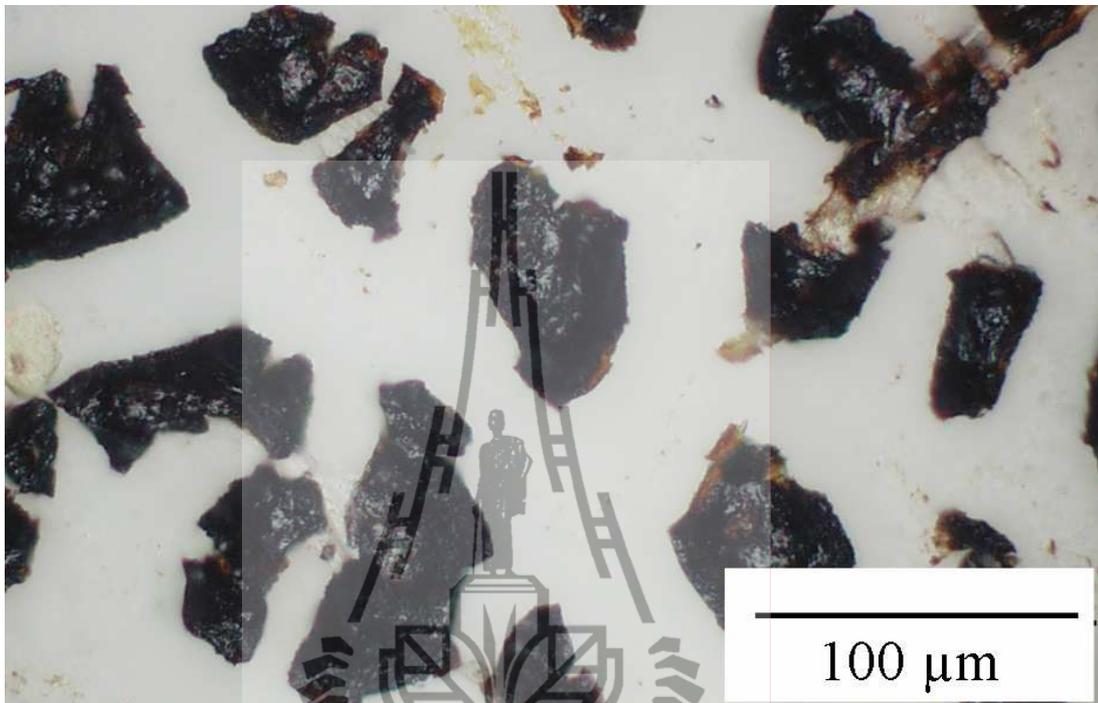
Figure B-2 Images obtained from digital microscope showing the surfaces of fouled

membrane at pressure of 35 kPa.
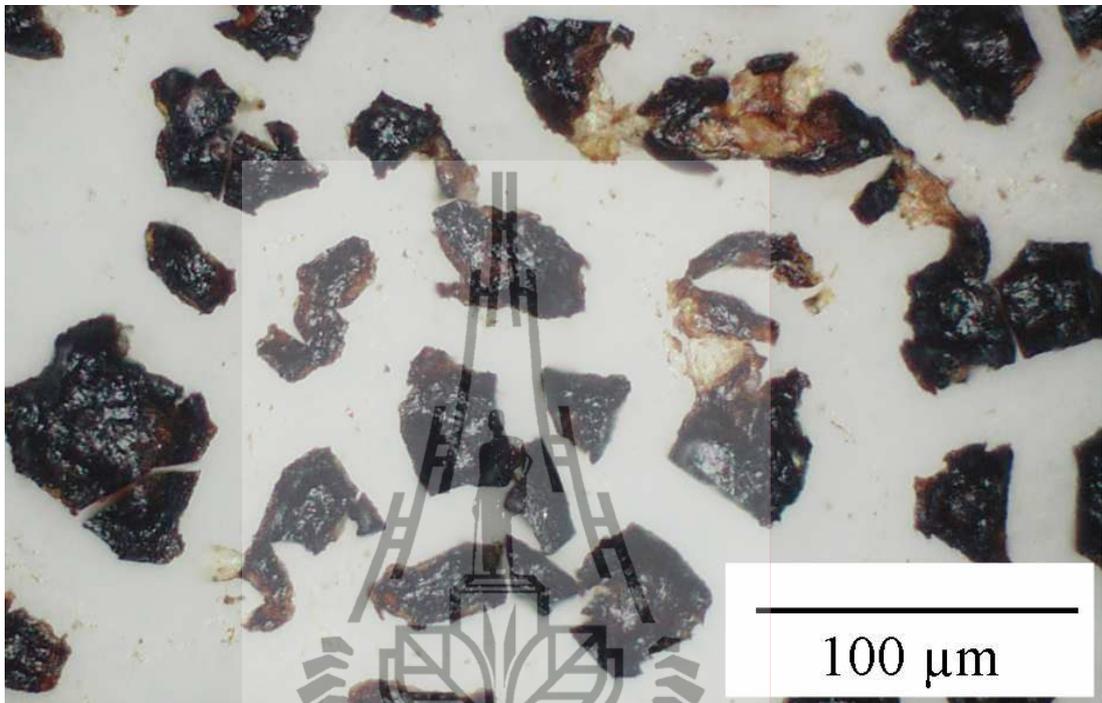
Figure B-3 Images obtained from digital microscope showing the surfaces of fouled

membrane at pressure of 50 kPa.

# APPENDIX C

MICROFILTRATION SYSTEM
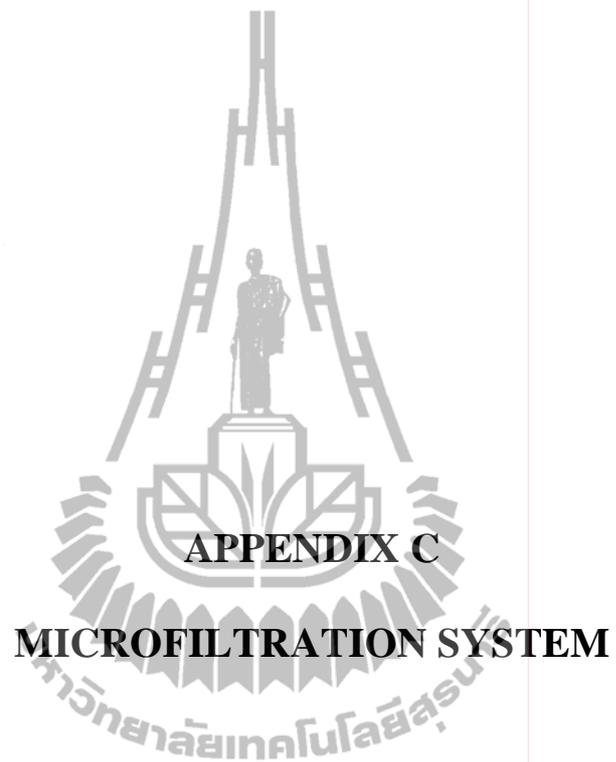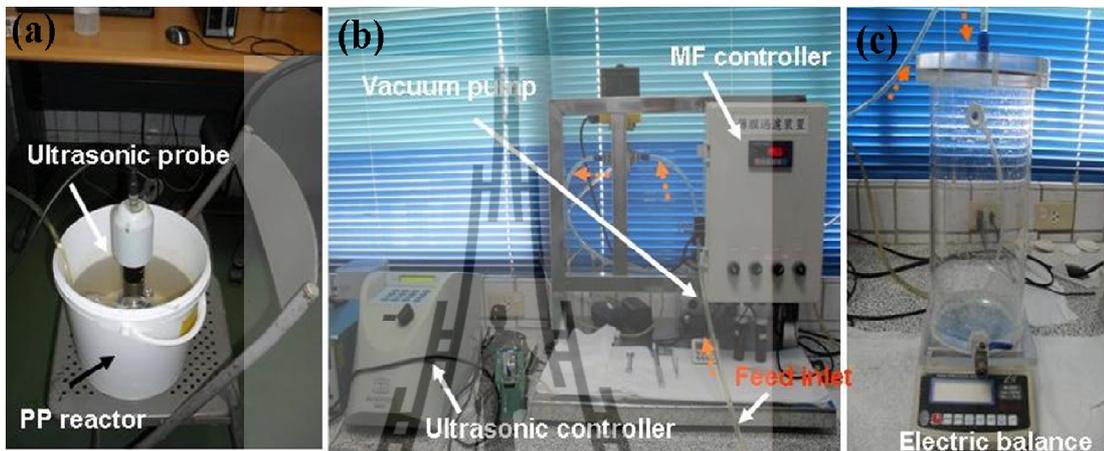
Figure C-1 Schematic diagram of laboratory scale of membrane microfiltration system

(a) water reservoir tank (b) a MF unit and (c) electric balance connected with

computer.
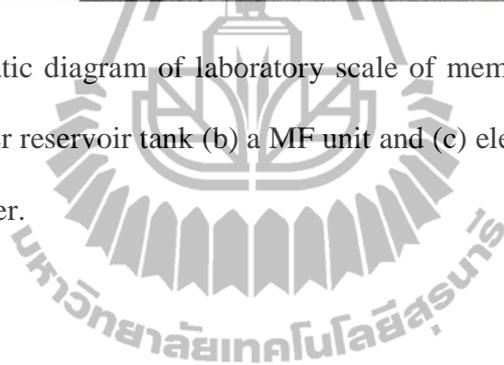
CURRICULUM VITAE

Mr. PIAW PHATAI

Date of Birth: 10 December, 1982 in Sakon Nakhon, Thailand

Education:

2001-2005   B.Sc. (Chemistry) Ubon Ratchathani University, Thailand

2005-2008   M.Eng. (Chemical Engineering) Thammasat University, Thailand

Experience:

2008-2010   Ph.D. research fellow at Department of Environmental Engineering and Science, Chia Nan University of Pharmacy and Science, Tainan, Taiwan

Publications:

Grisdanurak, N., Phatai, P. and Neramittagapong, A. (2007). Characteristics and performance of M-doped cerium zirconium mixed oxide nanosized catalysts (M = Zn, Sn) in CO oxidation, **Reaction Kinetics and Catalysis Letters**, 92: 213-221.

Phatai, P., Wittayakun, J., Grisdanurak, N., Chen, W.H., Wan, M.W., and Kan, C-C. (2010). Removal of manganese ions from synthetic groundwater by oxidation using $KMnO_4$ and the characterization of produced MnO_2 particles, **Water Science and Technology**. 62: 1719-1726.